# Josip Juraj Strossmayer University of Osijek

University of Dubrovnik

Ruđer Bošković Institute

Interdisciplinary Doctoral Studies of Molecular Biosciences

# Monika Mlinarić

# MODULATION OF OXIDATIVE STRESS AND ANTIOXIDATIVE RESPONSE BY AQUAPORINS 3 AND 5 IN BREAST CANCER CELL LINES

PhD thesis

#### **BASIC DOCUMENTATION CARD**

Josip Juraj Strossmayer University of Osijek University of Dubrovnik Ruđer Bošković Institute Doctoral Study of Molecular Biosciences PhD thesis

**Scientific Area:** Interdisciplinary area of science **Scientific Fields:** biology, basic medical sciences

#### Modulation of Oxidative Stress and Antioxidative Response by Aquaporins 3 and 5 in Breast Cancer Cell Lines

#### Monika Mlinarić

**Thesis performed at:** Laboratory for Membrane Transport and Signaling, Division of Molecular Medicine, Ruđer Bošković Institute.

Supervisor/s: Dr. Ana Čipak Gašparović

#### **Short abstract:**

Breast cancer progression is shaped by redox signaling, with hydrogen peroxide (H<sub>2</sub>O<sub>2</sub>) acting as both signal and source of damage. To preserve signaling while limiting the damage, NRF2 coordinates the antioxidant defense system, while aquaporins regulate H<sub>2</sub>O<sub>2</sub> transport. Under prolonged low-dose H<sub>2</sub>O<sub>2</sub>, increased AQP3/AQP5 and nuclear NRF2 were observed. AQP-NRF2 crosstalk and interdependent regulation of AQP isoforms indicate context-specific control with potential therapeutic value.

Number of pages: 107 Number of figures: 40 Number of tables: 4 Number of references: 253

Original in: English

Key words: Aquaporins, NRF2, oxidative stress, breast cancer

#### Date of the thesis defense:

#### **Reviewers:**

- 1.
- 3.
- 4. (substitute)

**Thesis deposited in:** National and University Library in Zagreb, Ul. Hrvatske bratske zajednice 4, Zagreb; City and University Library of Osijek, Europska avenija 24, Osijek; Josip Juraj Strossmayer University of Osijek, Trg sv. Trojstva 3, Osijek

#### TEMELJNA DOKUMENTACIJSKA KARTICA

Sveučilište Josipa Jurja Strossmayera u Osijeku Sveučilište u Dubrovniku Institut Ruđer Bošković Doktorski studij Molekularne bioznanosti Doktorski rad

**Znanstveno područje:** Interdisciplinarno područje znanosti **Znanstvena polja:** biologija, temeljne medicinske znanosti

# Akvaporini 3 i 5 kao modulatori oksidacijskog stresa i antioksidacijskog odgovora u staničnim linijama raka dojke

Monika Mlinarić

**Doktorski rad je izrađen u:** Laboratorij za membranski transport i signalizaciju, Zavod za molekularnu medicinu, Institut Ruđer Bošković

Mentor/i: dr. sc. Ana Čipak Gašparović

#### Kratki sažetak doktorskog rada:

Progresija tumora dojke pod utjecajem je redoks signalizacije, pri čemu vodikov peroksid (H<sub>2</sub>O<sub>2</sub>) djeluje kao sekundarni glasnik i izvor oksidacijskih oštećenja. Radi očuvanja homeostaze, transkripcijski faktor NRF2 osigurava antioksidacijsku zaštitu, dok akvaporini moduliraju transmembranski transport H<sub>2</sub>O<sub>2</sub>. Nakon produljenog izlaganja niskoj razini H<sub>2</sub>O<sub>2</sub>, izmjerena je povišena ekspresija AQP3/AQP5 te akumulacija NRF2 u jezgri. Uočeno je međudjelovanje AQP-NRF2 i međusobno ovisna regulacija AQP izoformi, što ukazuje na regulaciju ovisnu o biološkom kontekstu s potencijalnim terapijskim implikacijama.

Broj stranica: 107 Broj slika: 40 Broj tablica: 4

Broj literaturnih navoda: 253 Jezik izvornika: engleski

Ključne riječi: Akvaporini, NRF2, oksidacijski stres, tumor dojke

**Datum javne obrane:** 

#### Povjerenstvo za javnu obranu:

- 1.
- 2.
- 3.
- 4. (zamjena)

**Doktorski rad je pohranjen u:** Nacionalnoj i sveučilišnoj knjižnici Zagreb, Ul. Hrvatske bratske zajednice 4, Zagreb; Gradskoj i sveučilišnoj knjižnici Osijek, Europska avenija 24, Osijek; Sveučilištu Josipa Jurja Strossmayera u Osijeku, Trg sv. Trojstva 3, Osijek



This PhD thesis was performed at the Laboratory for Membrane Transport and Signaling, Division of Molecular Medicine, Ruđer Bošković Institute, under the supervision of Dr. Ana Čipak Gašparović, as part of the HRZZ research project Elucidating the role of aquaporins 3 and 5 in the development of breast cancer resistance to oxidative stress (HRZZ-IP-2020-02-3617) and Young Researchers' Career Development Project - Training New Doctoral Students (DOK-2021-02-5397).



# TABLE OF CONTENTS

1.	NTRODUCTION	1
1.1.	CANCER	1
	1.1.1. Breast Cancer	3
1.2.	CELLULAR REDOX HOMEOSTASIS	6
	1.2.1. NRF2	9
	1.2.2. Redox Regulation in Cancer Cells	. 11
1.3.	AQUAPORINS	
	1.3.1. Structure	. 14
	1.3.2. Permeability	
	1.3.3. Regulation	. 17
	1.3.4. Physiology and Disease	. 18
	1.3.4.1. Aquaporins in Breast Cancer	. 21
1.4.	AIM OF THE RESEARCH	. 23
2.	MATERIALS AND METHODS	
2.1.	CELL CULTURE	. 24
	2.1.1. Prolonged oxidative stress	
	2.1.2. Modulation of NRF2 expression and activity	. 25
	2.1.3. Modulation of Aquaporin expression	. 26
2.2.	CELL VIABILITY ASSAY	. 28
2.3.	CELL PROLIFERATION ASSAY	. 28
2.4.	WOUND HEALING ASSAY	. 29
	TOTAL LIPID EXTRACTION, GC ANALYSIS, AND MEASUREMENT OF LOO CENTRATION	
2.6.	PROTEIN ISOLATION AND WESTERN BLOT ANALYSES	. 30
2.7.	RNA ISOLATION, CDNA SYNTHESIS, AND RT-QPCR	. 32
2.8.	AQUAPORIN ACTIVITY ASSAYS	. 34
2.9.	IN SILICO PREDICTION OF NRF2 BINDING SITES	. 34
2.10	STATISTICAL ANALYSIS	35

3. RESULTS	36
3.1. EFFECT OF PROLONGED EXPOSURE TO HYDROGEN PEROXIDE	36
3.1.1. Cell Viability and Proliferation	
3.1.2. Cell Migration	
3.1.3. Fatty Acid Content and LOOH Formation	39
3.1.4. Protein Expression and Localization	40
3.1.5. Gene Expression	
3.2. EFFECT OF NRF2 MODULATION	47
3.2.1. Cell Viability	47
3.2.2. Protein Expression and Localization	49
3.2.3. Gene Expression	56
3.2.4. Aquaporin Activity	57
3.2.5. Predicted NRF2 binding in AQP3 and AQP5 regulatory regions	58
3.3. CROSS-REGULATION OF AQUAPORINS	61
3.3.1. Protein Expression	61
3.3.2. Gene Expression	
3.3.3. Aquaporin Activity	64
4. DISCUSSION	<i>(</i> =
4. DISCUSSION	05
5. CONCLUSIONS	79
6. ACKNOWLEDGEMENTS	00
6. ACKNOWLEDGEMENTS	80
7. REFERENCES.	81
8. SUMMARY	100
9. SAŽETAK	102
10. CV	104
11 PURLICATIONS:	107

#### 1. INTRODUCTION

#### 1.1. Cancer

Cancer is one of the leading causes of death worldwide, with an estimated 20 million new cases and 9.7 million deaths reported in 2022, and epidemiological projections predict a 77% increase in annual cases by 2050 [1]. This increasing burden reflects both population growth and aging, but it is also driven by exposure to different lifestyle and environmental risk factors, including tobacco use, unhealthy diet, physical inactivity, and alcohol consumption, as well as air pollution and carcinogens [2]. Despite many advances in cancer detection and treatment, millions are still diagnosed with and die of cancer each year, indicating the complexity of this disease and the existing limitations of current diagnostic technologies and treatment accessibility.

Cancer develops and progresses as cells gradually acquire capabilities that enable their malignant growth and the evasion of regulatory controls, known as the hallmarks of cancer (Figure 1) [3]. These include sustained proliferative signaling, where cancer cells continuously divide by producing their own growth factors, increasing the number of growth factor receptors to amplify signaling, or altering downstream signaling pathways, such as MAPK or PI3K, to remain constitutively active [3]. In parallel, cancer cells evade growth suppressors, including the tumor suppressor protein p53, which normally halts the cell cycle and triggers apoptosis in response to DNA damage, while also developing resistance to cell death [3]. To sustain their growth, cancer cells induce angiogenesis, the formation of new blood vessels, to secure the oxygen and nutrients necessary for cancer progression. Once established, many cancer cells acquire the ability to invade surrounding tissues and metastasize to distant organs [3]. Metabolic reprogramming is another important hallmark of cancer, allowing it to sustain the increasing bioenergetic and biosynthetic demands. Cancer cells shift toward aerobic glycolysis, a phenomenon known as the Warburg effect, which enables them to rapidly generate ATP while simultaneously producing precursors needed for cell growth and division [3]. Furthermore, accumulation of genomic instability and mutations enhances genetic diversity within the tumor, enabling adaptation to different microenvironments and therapeutic pressures [3]. Cancer cells also evade the immune system by downregulating antigen presentation, and shape the microenvironment through chronic tumor-promoting inflammation, releasing additional growth factors, cytokines, and proangiogenic signals [3]. More recently, new hallmarks of cancer were described, including cellular plasticity, which allows phenotype switches and adaptation that enables therapy resistance; nonmutational epigenetic reprogramming, which alters gene expression without changes in the DNA sequence; the presence of senescent cells, whose secretory phenotype remodels the microenvironment; and the effect of the microbiome, which modulates inflammation, immune function and therapy response [3]. These interconnected processes show the complexity and heterogeneity of cancer, in which a network of genetic, epigenetic, metabolic, and environmental factors influences its progression. Consequently, understanding the mechanisms that drive its development and progression is necessary for improving diagnosis and prognosis, as well as developing more effective treatment strategies.

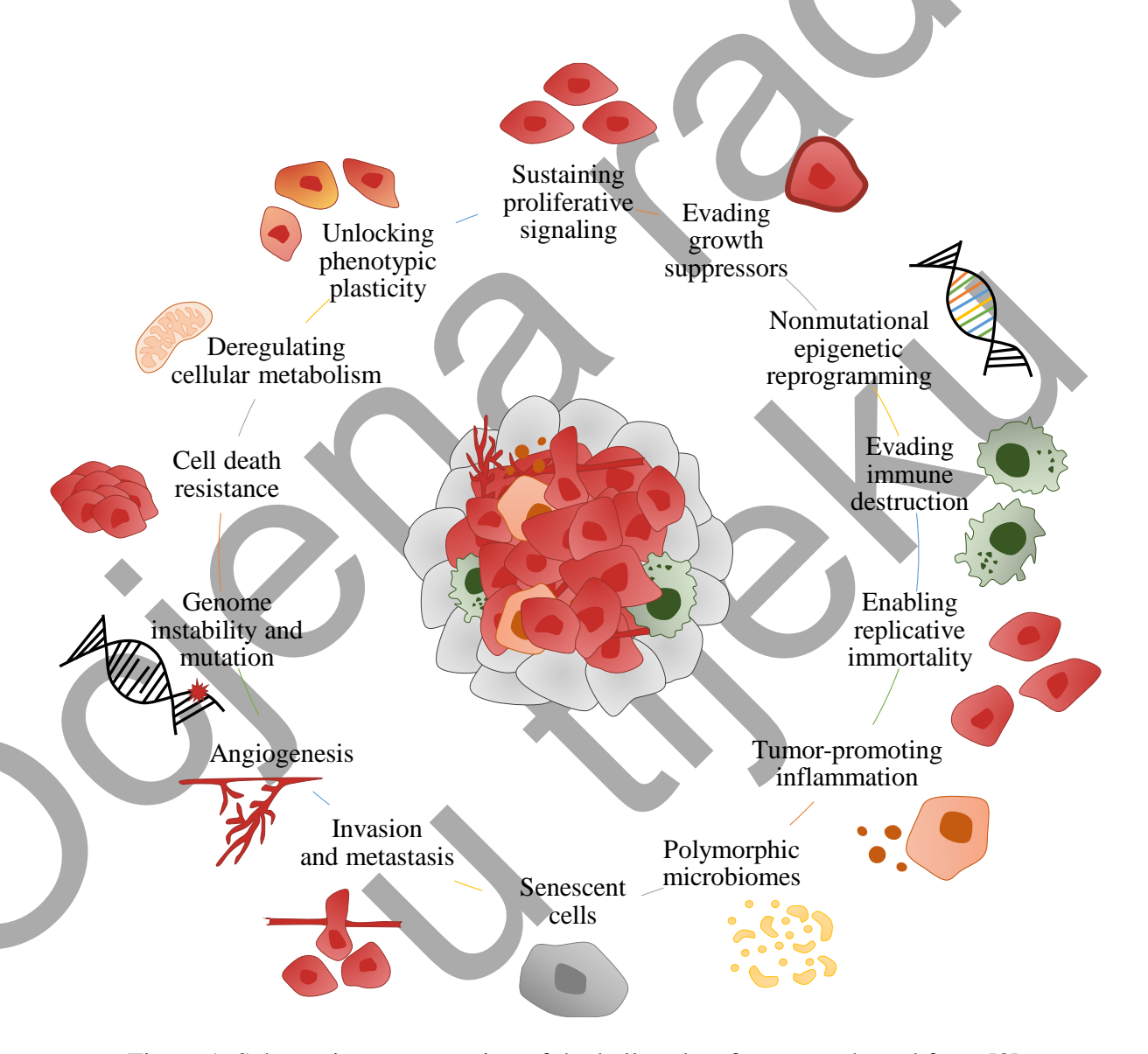


Figure 1. Schematic representation of the hallmarks of cancer, adapted from [3]

Hallmarks of cancer include sustaining proliferative signaling, evading growth suppressors, nonmutational epigenetic reprogramming, evading immune destruction, enabling replicative immortality, tumor-promoting inflammation, polymorphic microbiomes, senescent cells, invasion, metastasis, angiogenesis, genome instability and mutation, cell death resistance, deregulating cellular metabolism, and unlocking phenotypic plasticity.

#### 1.1.1. Breast Cancer

Breast cancer is the most frequently diagnosed cancer and the leading cause of cancerrelated death among women worldwide [1]. Different genetic, hormonal, reproductive, and
lifestyle-related factors influence breast cancer risk. Non-modifiable risk factors include
increasing age, reproductive and hormonal factors, for example, early menarche, late age at first
pregnancy, fewer or no pregnancies, shorter or no breastfeeding, and the use of postmenopausal
hormone replacement therapy, family history of breast cancer or *BRCA1* or *BRCA2* gene
inherited mutations, and prior therapeutic chest radiation at a young age. Beyond these, different
modifiable exposures, including obesity, excessive alcohol consumption, tobacco use, and
physical inactivity, affect breast cancer development risk [4]. However, many breast cancers
occur in women with no identifiable risk factors. Patient outcome varies widely depending on
the stage at diagnosis, tumor subtype, and access to effective therapy, ranging from surgery and
radiotherapy to systemic treatments such as chemotherapy, endocrine therapy, targeted therapy,
and immunotherapy [5].

Breast cancer is a genetically and clinically heterogeneous disease, which explains why patients experience different prognoses and responses to therapy. This heterogeneity is reflected in different molecular alterations, but also in tumor morphology and behavior. In clinical practice, the pathohistological report provides information for diagnosis, prognosis, and treatment plan; and includes parameters as tumor size, lymph node involvement, and histological grade. The first determinant of disease stage and outcome is tumor size. Small localized tumors, classified as T1 ( $\leq 2$  cm), generally have a more favorable prognosis, whereas intermediate-size tumors (T2, 2-5 cm) and larger tumors (T3, ≥ 5 cm) are associated with increasing risk of metastasis and recurrence, and tumors classified as T4 invade the chest wall or skin and correlate with poorer outcomes [8]. Lymph node involvement serves as a prognostic indicator, distinguishing node-negative cases from increasing numbers of positive axillary nodes, which indicate a higher risk of recurrence and metastasis [8]. And third, histopathological grade reflects cell differentiation and proliferation. Low-grade, welldifferentiated tumors tend to be more slow-growing and less aggressive, while high-grade, poorly differentiated tumors grow rapidly and are more aggressive, whereas intermediate tumors fall between these two categories [8].

Histologically, the majority of breast cancers are adenocarcinomas, most often invasive carcinoma of no special type (formerly known as invasive ductal carcinoma), followed by invasive lobular carcinoma [6]. Less common histological subtypes of breast cancer are tubular,

mucinous, adenoid cystic, cribriform, medullary, apocrine, micropapillary, and metaplastic carcinomas. Breast cancers are also classified as *in situ* or invasive. *In situ* carcinomas, including ductal carcinoma *in situ* and lobular carcinoma *in situ*, are confined to ducts or lobules without breaching the basement membrane. Carcinomas become invasive when tumor cells infiltrate the surrounding stroma and gain metastatic potential (Figure 2).

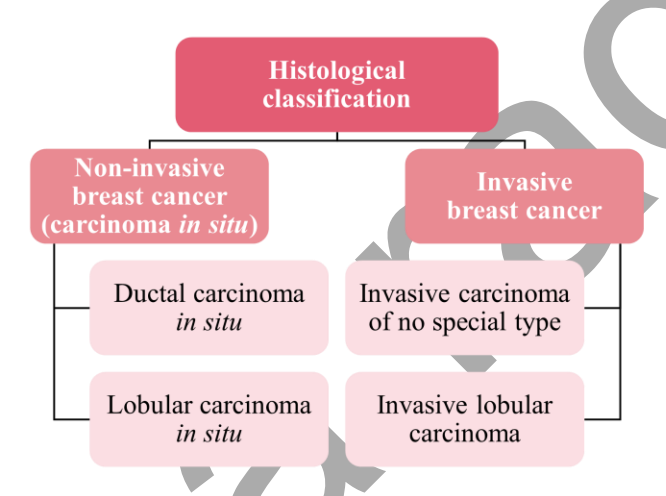


Figure 2. Histological classification of breast cancer

Breast cancers are divided into non-invasive (*in situ*) carcinomas, which remain confined to ducts or lobules and include ductal carcinoma *in situ* and lobular carcinoma *in situ*, and invasive carcinomas, which infiltrate surrounding tissues and include invasive carcinoma of no special type (formerly invasive ductal carcinoma) and invasive lobular carcinoma.

Beyond histological categories, breast cancers are most commonly classified into molecular subtypes: luminal A, luminal B, HER2-positive, and basal-like, which give prognostic and predictive information and determine treatment strategies. These are defined in clinical practice through immunohistochemical assessment of estrogen receptor (ER), progesterone receptor (PR), and human epidermal growth factor receptor 2 (HER2).

Most breast cancers are ER-positive and are divided into the luminal A and luminal B subtypes based on proliferative capacity, commonly assessed using the proliferation index Ki67. Luminal A is the most common, accounting for about 50% of breast cancer cases, and is characterized by ER and/or PR positivity, absence of HER2, and a low Ki-67 index; these tumors are usually low grade, slow growing, associated with the most favorable prognosis, and respond well to endocrine therapy [7, 8]. Luminal B, representing about 20% of breast cancer cases, is also ER positive but often PR negative, shows higher Ki-67 expression, and may be

HER2 positive or negative; these tumors are more proliferative and of higher grade, with a worse prognosis than luminal A, and typically require endocrine therapy combined with chemotherapy, with the addition of anti-HER2 therapy when amplification is present [7, 8].

Approximately 15% of breast cancers are HER2-positive and hormone receptor-negative. These tumors grow faster, are frequently of higher grade, and often have *TP53* mutations. Historically, they were associated with poor outcomes, but their prognosis has improved with HER2-targeted therapies in combination with anthracycline-based chemotherapy [7, 8].

The basal-like subtype, which represents about 15% of breast cancers, is defined by high expression of basal epithelial genes and overlaps substantially with triple-negative breast cancer (TNBC), clinically characterized by the absence of ER, PR, and HER2 [7]. These tumors typically have a high Ki-67 index, frequent *TP53* mutations, *BRCA1* and *BRCA2* dysfunction, and genomic instability [7]. TNBC is heterogeneous and can be subdivided into molecular groups, including basal-like (BL1, BL2), mesenchymal, luminal androgen receptor, and immunomodulatory; each with distinct biological features and therapeutic sensitivities [8]. Clinically, TNBCs are aggressive, more often diagnosed at advanced stages, prone to early relapse, and overall associated with the poorest prognosis, although they may respond to platinum-based chemotherapy, poly (ADP-ribose) polymerase (PARP) inhibitors, and emerging immunotherapies [7].

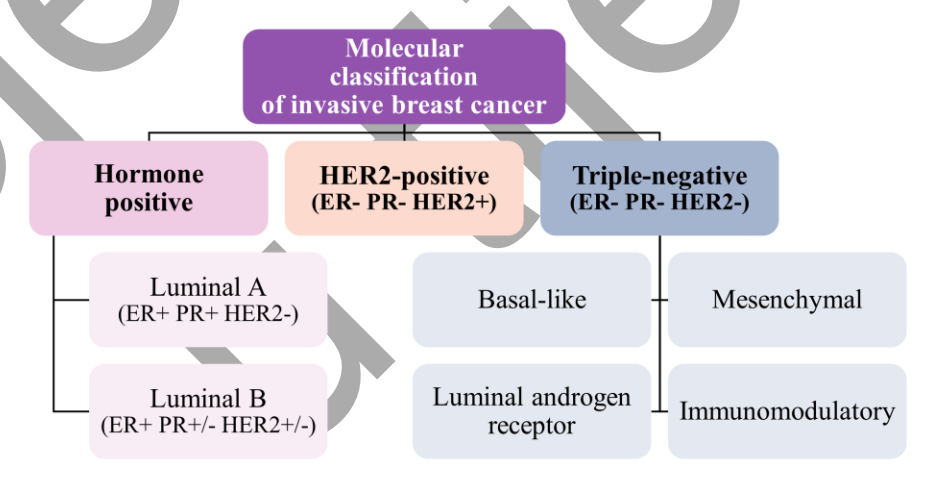


Figure 3. Molecular classification of invasive breast cancer

Invasive breast cancers are classified based on estrogen receptor (ER), progesterone receptor (PR), and human epidermal growth factor receptor 2 (HER2) status. Hormone receptor-positive cancer includes luminal A (ER+ and/or PR+, HER2-) and luminal B (ER+, PR+/-, HER2+/-). HER2-positive cancers have a high HER2 expression and are negative for ER and PR. Triple-negative breast cancers (TNBCs)

lack ER, PR, and HER2 expression and are further divided into basal-like, mesenchymal, luminal androgen receptor, and immunomodulatory subtypes.

Despite major advances in diagnostic methods, prognostic assessment, and therapeutic strategies, breast cancer remains a clinical challenge. Earlier detection and broader treatment access lead to substantially higher survival, and modeling studies suggest that scaling up imaging and treatment capacity could meaningfully improve outcomes [9]. Until then, the current high incidence and mortality rates make breast cancer a major public health challenge. Improving outcomes will require not only wider access to current therapies but also the identification of new biomarkers for earlier detection and discovery of novel therapeutic targets.

#### 1.2. Cellular Redox Homeostasis

Cellular redox homeostasis refers to the balance between continuous reducing and oxidizing reactions within the cell, including the generation of reactive oxygen species (ROS) and other reactive species, and their removal by antioxidant defense systems. This highly dynamic system, shaped by ongoing oxidative metabolism, is essential for maintaining cellular integrity, regulating signaling pathways, proliferation, and differentiation, and enabling cells to adapt to environmental and metabolic changes. Importantly, ROS are not only detrimental byproducts of cellular metabolism, as they were historically viewed. At physiological levels, ROS serve as signaling molecules rather than damaging agents, a state referred to as oxidative eustress, whereas excessive ROS disrupts signaling and damages biomolecules, resulting in oxidative distress [10]. The term oxidative stress is often used in the literature to describe redox imbalance and refers specifically to oxidative distress, highlighting the harmful effects of ROS.

ROS are constantly produced as natural byproducts of cellular metabolism, primarily in the mitochondria due to electron leakage from the respiratory chain during oxidative phosphorylation, in peroxisomes through fatty acid  $\beta$ -oxidation, and by nicotinamide adenine dinucleotide phosphate (NADPH) oxidases during immune response, wound healing, and cellular signaling. Other intracellular sources include xanthine oxidase, nitric oxide synthase, cytochrome P450 enzymes, and oxidative protein folding in the endoplasmic reticulum (ER), while cyclooxygenases and lipoxygenases contribute during lipid metabolism [11]. Moreover, immune cells such as neutrophils and macrophages generate ROS during the respiratory burst, as part of the antimicrobial response [12]. In parallel, exogenous sources, including ionizing radiation, air pollution, heavy metals, and certain drugs, further contribute to oxidative stress.

ROS include a broad range of chemically reactive molecules that can be divided into radical and non-radical forms. Radical forms include superoxide anions  $(O_2^{\bullet})$ , hydroxyl radicals ( ${}^{\bullet}OH$ ), and peroxyl radicals ( $ROO^{\bullet}$ ), whereas non-radical species, such as hydrogen peroxide ( $H_2O_2$ ), singlet oxygen ( ${}^{1}O_2$ ), and hypochlorous acid (HOCl).

Superoxide anions are generated by a one-electron reduction of molecular oxygen, primarily at complexes I and III of the mitochondrial electron transport chain [13], as well as from NADPH oxidases at the plasma membrane [14]. Although short-lived, superoxide serves as a precursor for other ROS and contributes to redox signaling, but excessive accumulation can damage proteins containing iron-sulfur clusters, impairing their enzymatic activity. To prevent this, superoxide dismutases (SODs) catalyze the dismutation of superoxide into less reactive H<sub>2</sub>O<sub>2</sub>; SOD1 is localized in the cytosol and mitochondrial intermembrane space, SOD2 in the mitochondrial matrix, and SOD3 in the extracellular space [15].

H<sub>2</sub>O<sub>2</sub> has a central role in redox biology because it is not as reactive as radical ROS species, it can diffuse across membranes, and acts as a signaling molecule. Its signaling function depends on the reversible oxidation of cysteine residues, where the cysteine thiolate anion (Cys-S<sup>-</sup>) is oxidized to a sulfenic acid form (Cys-SOH), inducing conformational changes that alter protein function [16]. Key protein targets of H<sub>2</sub>O<sub>2</sub>-mediated signaling include protein tyrosine phosphatases (PTPs), whose oxidative inactivation indirectly enhances the activity of mitogenactivated protein kinases (MAPKs) and receptor tyrosine kinases, thereby upregulating proliferative and survival pathways [17]. H<sub>2</sub>O<sub>2</sub>-mediated signaling also regulates transcription factors such as nuclear factor erythroid 2-related factor 2 (NFE2L2, often referred to as NRF2), nuclear factor kappa-light-chain-enhancer of activated B cells (NF-κB), and hypoxia-inducible factor (HIF), thereby coordinating antioxidant defenses, inflammatory pathways, and cellular response to hypoxia [18]. In the ER, H<sub>2</sub>O<sub>2</sub> is both generated and consumed during oxidative protein folding, where it modifies proteins that regulate protein folding capacity and ER stress responses [19]. Importantly, the effect of H<sub>2</sub>O<sub>2</sub> is concentration-dependent. For balanced signaling, only first-degree oxidation of cysteine residues acts as a reversible signal transduction mechanism that maintains redox homeostasis and supports adaptive responses, whereas higher levels of H<sub>2</sub>O<sub>2</sub> further oxidize thiolate anions to sulfinic (Cys-SO<sub>2</sub>H) or sulfonic (Cys-SO<sub>3</sub>H) forms, which are irreversible and cause permanent protein damage, their inactivation and disruption of cellular signaling [15]. To prevent the build-up of intracellular H<sub>2</sub>O<sub>2</sub> and limit damage, cells rely on antioxidant enzymes such as peroxiredoxins (PRX), glutathione peroxidases (GPx), and catalase (CAT), which catalyze the reduction of  $H_2O_2$  into  $H_2O$  [15].

Nevertheless, when  $H_2O_2$  accumulates excessively or antioxidant systems are overwhelmed, highly reactive hydroxyl radicals are generated through Fenton reactions in the presence of transition metals such as  $Fe^{2+}$  or  $Cu^+$ . These radicals cause irreversible damage to cellular macromolecules, including single- and double-DNA strand breaks, and base oxidations like 8-hydroxyguanine, which drive mutations and genomic instability; protein oxidation, carbonylation, and cross-linking, which lead to altered folding, aggregation, and enzymatic inactivation; and lipid peroxidation, which disrupts membrane integrity and generates toxic aldehydes like malondialdehyde and 4-hydroxynonenal that act as secondary messengers, mutagenic and proinflammatory agents and amplify oxidative stress [20].

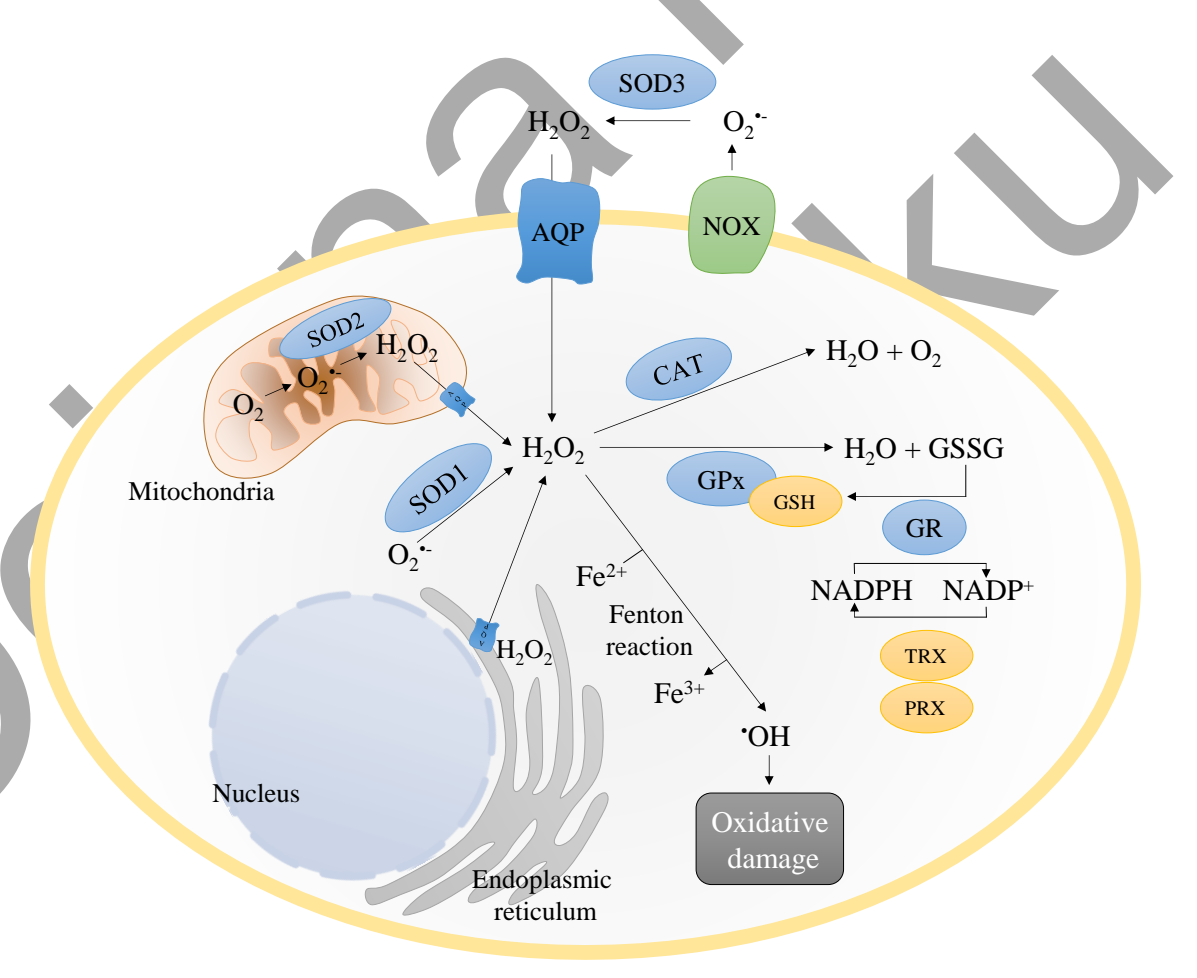


Figure 4. Redox regulation

Reactive oxygen species (ROS) are generated by mitochondrial respiration, NADPH oxidases (NOX) at the plasma membrane, and within the endoplasmic reticulum (ER) through protein-folding oxidoreductases. Superoxide ( $O_2$ ) is converted into hydrogen peroxide ( $H_2O_2$ ) by superoxide dismutases (SOD1 in the cytosol, SOD2 in mitochondria, and extracellular SOD3).  $H_2O_2$  can diffuse

through membranes via aquaporins.  $H_2O_2$  is detoxified by catalase (CAT) or glutathione peroxidase (GPx), with glutathione (GSH) oxidized to glutathione disulfide (GSSG) and recycled by glutathione reductase (GR) using NADPH. The thioredoxin (TRX) and peroxiredoxin (PRX) systems also contribute to redox regulation. In the presence of  $Fe^{2+}$ ,  $H_2O_2$  undergoes the Fenton reaction to generate hydroxyl radicals (OH), which cause oxidative damage to biomolecules.

ROS are not only metabolic byproducts but key mediators of redox signaling, supporting processes such as angiogenesis, stem cell renewal and differentiation, circadian rhythm regulation, immune responses, and cellular adaptation to stress, thereby contributing to the maintenance of cellular and tissue homeostasis. However, when present at damaging levels, oxidative stress disrupts signaling pathways and damages macromolecules, contributing to various pathologies, including atherosclerosis, diabetes, neurodegeneration, chronic inflammation, and cancer [18]. To maintain redox homeostasis, cells have a network of signaling pathways and transcription factors that coordinate the cellular response to oxidative stress in a concentration- and/or time-dependent manner.

#### 1.2.1. NRF2

NRF2 is a redox-sensitive transcription factor that acts as the major regulator of the antioxidant and cytoprotective response. It induces over 200 different genes, including those involved in glutathione (GSH) metabolism, NADPH regeneration, and thioredoxin (TRX) systems, thereby buffering high ROS levels and maintaining redox homeostasis [21]. Beyond redox control, NRF2 also reprograms cancer metabolism, drug transport, upregulates the pentose phosphate pathway, and glutaminolysis [22].

Under basal conditions, NRF2 activity is suppressed to prevent unnecessary activation of stress-response pathways. This is achieved through continuous ubiquitination and proteasomal degradation mediated by its repressor Kelch-like ECH-associated protein 1 (Keap1), which acts as a substrate adaptor for the Cullin 3 (CUL3)-based E3 ubiquitin ligase [23]. Keap1 is a redox sensor; its highly reactive cysteine residues undergo covalent modifications under oxidative or electrophilic stress, inducing conformational changes that impair NRF2 partial release and degradation. As a result, newly synthesized NRF2 accumulates in the cytoplasm and translocates to the nucleus, where it heterodimerizes with small Maf proteins and binds to antioxidant-responsive elements (AREs, 5'-TGACNNNGC-3') within the regulatory regions of its target genes [24–26]. NRF2 controls the transcription of a wide array of cytoprotective genes, including the ones involved in antioxidant defense (e.g., heme oxygenase-1, HO-1) [27], detoxification (e.g., NAD(P)H quinone oxidoreductase 1, NQO1) [28], and metabolic

adaptation (e.g., aldo-keto reductase family 1 member B10, AKR1B10) [29]. NRF2 activity is also modulated by additional regulators, such as glycogen synthase kinase 3β (GSK-3β), which phosphorylates NRF2, promoting its nuclear export and degradation [30], Bach1, a transcriptional repressor that competes with NRF2 for ARE binding [31], and p62/SQSTM1, which can sequester Keap1 into autophagosomes and lead to non-canonical NRF2 activation [32]. Crosstalk with other signaling pathways further shapes NRF2 activity; for example, oncogenes such as *KRAS*, *BRAF*, and *MYC* upregulate NRF2 transcription, while PI3K-Akt signaling suppresses GSK-3β and thereby stabilizes NRF2 [21].

NRF2 plays a central role in redox regulation in both physiological and pathological conditions. Dysregulation of NRF2 activity has been linked to neurodegenerative diseases, chronic inflammation, metabolic dysfunction, and cancer. Consequently, it has emerged as a therapeutic target, with both NRF2 activators, intended for diseases driven by oxidative stress, and inhibitors, designed to counteract cancer-promoting NRF2 signaling, currently under investigation [33].

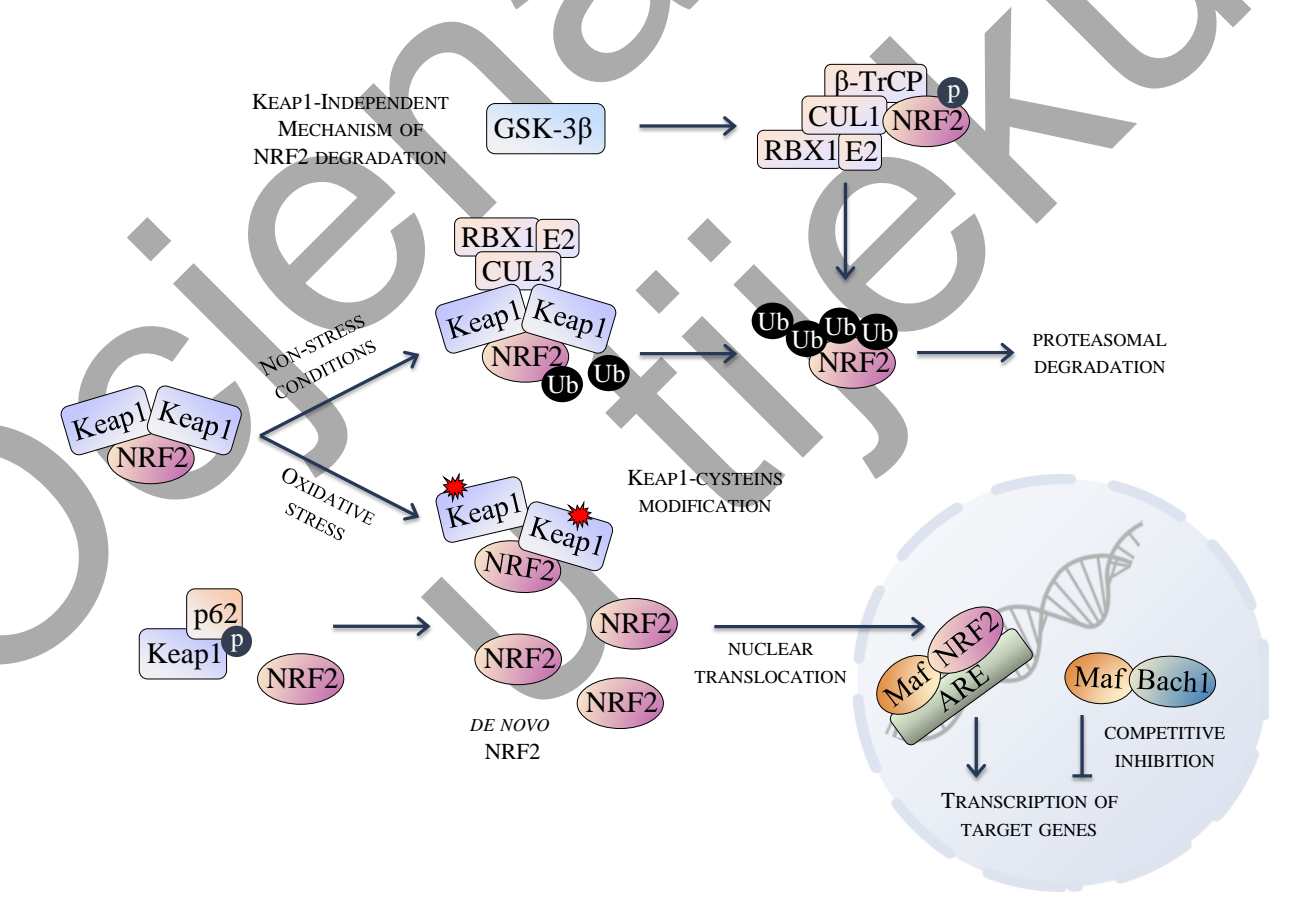


Figure 5. Regulation of NRF2

The transcription factor NRF2 is regulated through ubiquitination and proteasomal degradation under non-stress conditions, but it can be activated in response to oxidative stress. In the canonical pathway,

NRF2 binds to its repressor, Keap1, which acts as a substrate adaptor for the E3 ubiquitin ligase complex composed of Cullin 3 (CUL3), RING-box protein (RBX1), and an E2 ubiquitin-conjugating enzyme. This complex mediates the NRF2 ubiquitination and subsequent proteasomal degradation. Under oxidative stress, redox-reactive cysteine residues in Keap1 are modified, impairing its ability to release NRF2, thereby disrupting its degradation. Newly synthesized NRF2 accumulates in the cytoplasm, then translocates to the nucleus, where it heterodimerizes with small Maf proteins and binds to antioxidant response elements (ARE), activating the transcription of target genes. Alternatively, phosphorylation of Keap1 by p62 disrupts the Keap1-NRF2 interaction, leading to NRF2 stabilization. A non-canonical pathway of NRF2 degradation involves GSK-3 $\beta$ -mediated phosphorylation of NRF2, which enables its recognition by  $\beta$ -TrCP and recruitment of the CUL1-RBX1-E2 ligase complex for ubiquitination and proteasomal degradation. In the nucleus, Bach1 competes with NRF2 for binding to ARE sequences, thereby inhibiting NRF2-dependent gene transcription.

#### 1.2.2. Redox Regulation in Cancer Cells

Cancer cells are characterized by chronically elevated ROS levels [34], which arise from increased metabolic activity, mitochondrial dysfunction, peroxisomal activity, the activity of enzymes such as oxidases, cyclooxygenases, and lipoxygenases, as well as interactions with infiltrating immune cells within the tumor microenvironment [35]. Cancer cells persist in a hypermetabolic state that sustains not only the increased energy and biosynthetic demands but also contributes to the regulation of redox balance, thereby promoting tumor growth, progression, and therapy resistance, while further enhancing ROS production [36].

ROS have a dual role in cancer, where they regulate cancer initiation and progression by acting both as signaling molecules and as sources of molecular damage, thereby contributing to multiple hallmarks of cancer (Figure 6). ROS act as second messengers in signaling cascades, such as PI3K/Akt, MAPK/ERK, and NF-κB, and stabilize transcription factors like HIF-1α, which cancer cells exploit to sustain proliferation, reprogram metabolism, and stimulate angiogenesis [15, 37, 38]. Through induction of epithelial-mesenchymal transition (EMT) and activation of matrix metalloproteinases (MMPs), ROS enhance invasion and metastasis [42]. They also inactivate tumor suppressors, such as p53, facilitating uncontrolled growth and survival [43]. ROS also shape the tumor microenvironment and mediate interactions with the immune system. They impair the function of cytotoxic T cells, contribute to immune evasion, and promote the recruitment of immunosuppressive populations such as regulatory T cells and myeloid-derived suppressor cells [44], and promote inflammation through interactions with the microbiome [45]. At the genomic level, ROS contribute to telomere dysfunction and modulate telomerase activity, thereby supporting replicative immortality [46], while also inducing cellular senescence, and senescent cells additionally modulate the tumor microenvironment

through senescence-associated secretory phenotype (SASP) [47]. While moderate ROS levels promote tumorigenesis, excessive ROS cause oxidative damage to DNA, proteins, and lipids. Oxidative DNA lesions, such as 8-hydroxyguanine, and lipid peroxidation products like malondialdehyde and 4-hydroxynonenal, further drive genomic instability and malignant transformation [39, 40], but also induce non-mutational epigenetic reprogramming and increase cellular plasticity, further promoting cancer progression. Nevertheless, even in cancer cells, uncontrolled ROS accumulation can ultimately trigger apoptosis, necrosis, or autophagy. This is why many chemotherapeutics and radiotherapy rely on ROS generation to induce cytotoxicity [38].

To survive in this pro-oxidant environment and resist therapy-induced oxidative stress, cancer cells upregulate antioxidant systems, including GSH, GPx, TRX, and PRX. This adaptation is often reinforced by constitutive NRF2 activation, driven by mutations or epigenetic modifications in *Keap1*, *NFE2L2*, or *CUL3*, or through oncogenic signaling cascades that stabilize NRF2 activity, resulting in enhanced antioxidant capacity of cancer cells [50]. In addition, NRF2 regulates the expression of ATP-binding cassette (ABC) transporters, including ABCB1 (multidrug resistance protein 1, MDR1, or P-glycoprotein, P-gp), and ABCG2 (breast cancer resistance protein, BCRP), which contribute to drug efflux and chemoresistance [41]. In this context, NRF2 is considered a double-edged sword: in normal cells, it protects against oxidative and electrophilic stress, yet in cancer cells, NRF2 activation promotes survival, metabolic reprogramming, invasion, metastasis, and resistance to chemotherapy and radiotherapy, often correlating with more aggressive phenotypes and poor prognosis [42].

Ultimately, this finely tuned balance between ROS generation and antioxidant defense enables cancer cells to use ROS as drivers of proliferation, migration, invasion, angiogenesis, and drug resistance, while simultaneously protecting cells from oxidative cytotoxicity [43]. This highlights the importance of redox homeostasis in cancer and explains why targeting ROS and redox-regulatory pathways has emerged as a promising therapeutic strategy.

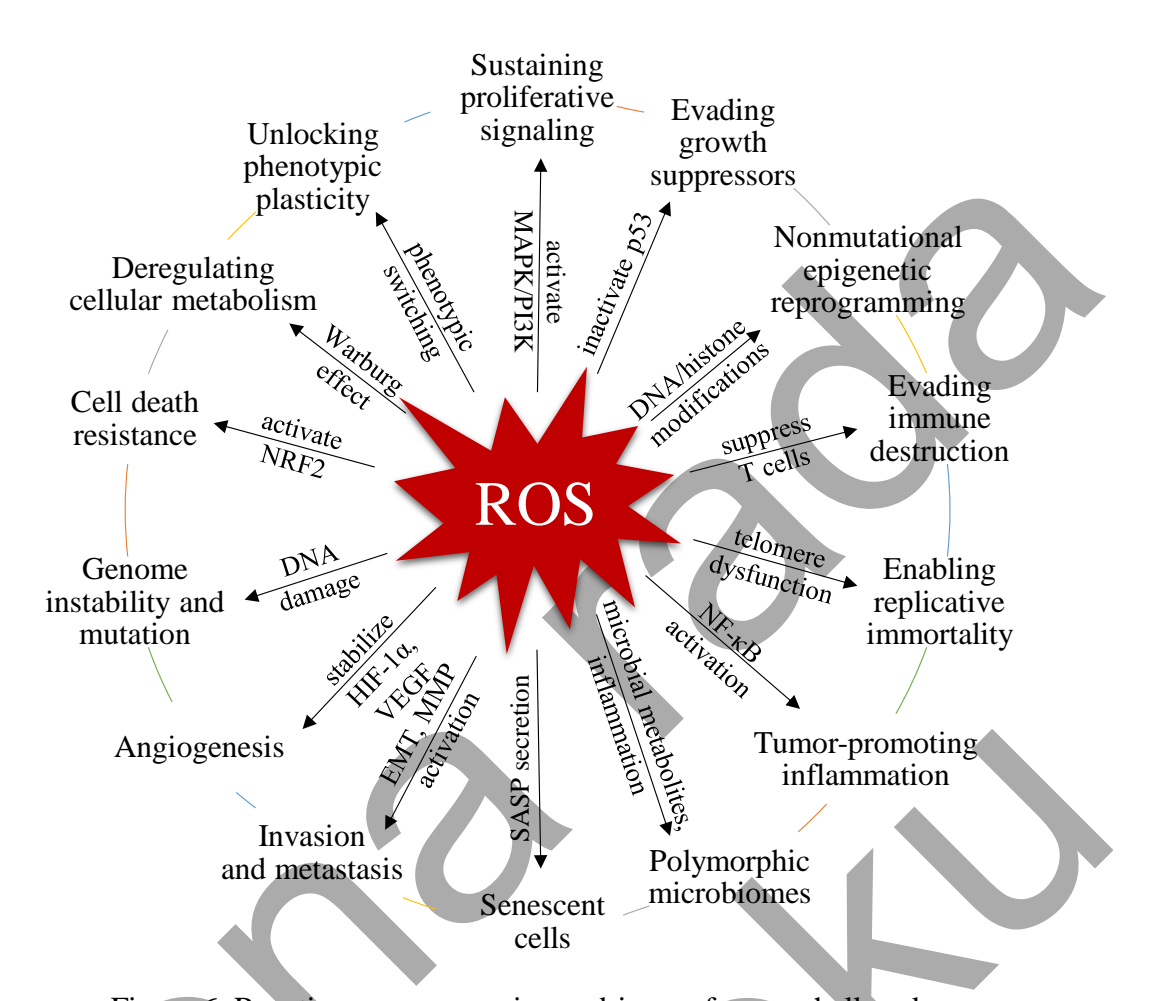


Figure 6. Reactive oxygen species as drivers of cancer hallmarks

ROS promote proliferative signaling, help evade growth control, contribute to resistance to cell death, and reprogram metabolism toward aerobic glycolysis. They also enable invasion and metastasis and drive angiogenesis. High ROS levels impair the immune system and sustain tumor-promoting inflammation, in part through interactions with the microbiome. In addition, ROS promote genome instability, replicative immortality, cellular plasticity, drive non-mutational epigenetic reprogramming, and induce senescence with its senescence-associated secretory phenotype (SASP).

#### 1.3. Aquaporins

Aquaporins are a family of small, highly conserved transmembrane proteins that function as channels facilitating the selective transport of water across cell membranes. This transport is passive and driven by a concentration gradient. The first aquaporin (AQP1) was discovered in 1992 by Peter Agre and colleagues, who isolated a 28-kDa membrane protein, referred to as channel-forming integral protein of 28 kDa (CHIP28) [44]. This discovery provided the first evidence for the existence of dedicated water channels and fundamentally changed our understanding of cellular water transport. This contribution was recognized with the 2003 Nobel Prize in Chemistry [45]. Since then, 13 aquaporin isoforms (AQP0–AQP12) have been identified in humans, each with distinct tissue distribution, permeability characteristics, and physiological roles.

Aquaporins are ubiquitously expressed in most tissues and participate in a wide array of physiological processes. They are essential for maintaining systemic water homeostasis, particularly through their roles in urinary concentration in the kidney, brain water regulation, cerebrospinal fluid circulation, and edema formation in the central nervous system, secretory functions in exocrine and endocrine glands, regulation of skin hydration, maintenance of lens transparency in the eye, and contributions to male fertility and sperm maturation [46]. Collectively, these functions underscore the importance of aquaporins in physiology and highlight why their dysregulation has been implicated in a variety of pathological conditions, from cataract and nephrogenic diabetes insipidus to neurological disorders and cancer.

#### 1.3.1. Structure

Aquaporin monomers are composed of approximately 250-300 amino acids, which fold into six transmembrane alpha helices connected by five interhelical loops (A-E), with both N- and C-termini located in the cytoplasm (Figure 7A) [47]. Each monomer forms a barrel-like conformation surrounding the water-conducting pore. Two highly conserved NPA (asparagine, proline, alanine) motifs, located in loop B (cytoplasmic side) and loop E (extracellular side), are oppositely oriented and meet in the center of the pore, forming the characteristic hourglass-shaped constriction that ensures water selectivity and prevents proton leakage (Figure 7B) [48, 49]. In addition, aquaporin selectivity is determined by the aromatic/arginine (ar/R) filter, a conserved cluster of residues that narrows the pore to approximately 3 Å in diameter (Figure 7C), thereby creating an electrostatic barrier that excludes ions and other solutes, while permitting the rapid, single-file passage of water molecules [49, 50]. Subtle variations in the

ar/R residues across the aquaporin isoforms alter pore size and hydrophobicity, explaining differences in substrate specificity [51]. In the membrane, aquaporins assemble as tetramers, with each monomer functioning as an independent water channel (Figure 7D, Figure 7E), while the central pore formed in the tetramer may have additional functions, such as gas or ion transport [52].

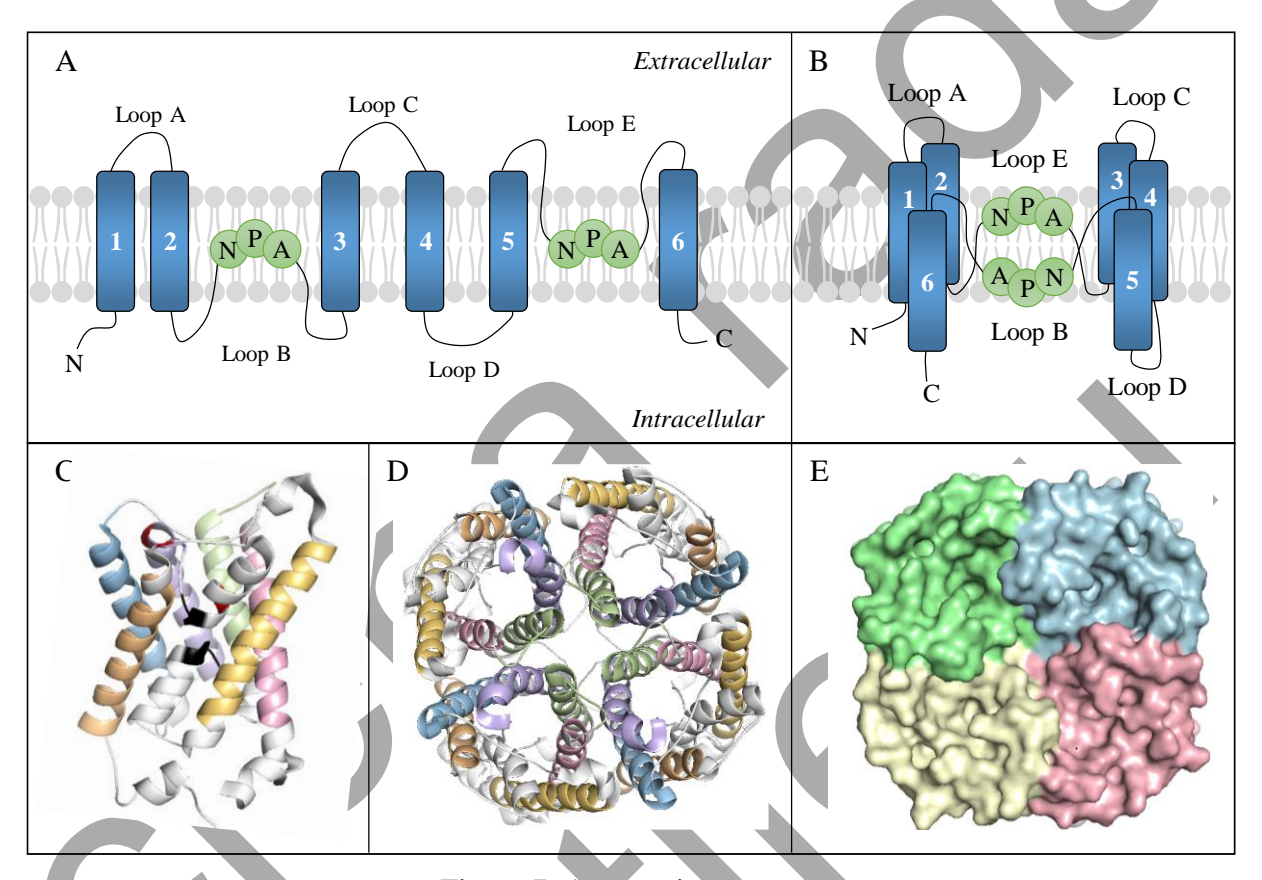


Figure 7. Aquaporin structure

Secondary structure of aquaporin showing six transmembrane domains (1-6) connected by five loops (A-E), with two conserved NPA motifs and both terminal ends located in the cytoplasm (A). Secondary structure highlighting the NPA motifs forming the selective channel in the membrane (B). Tertiary protein structure of an AQP monomer with transmembrane domains in different colors, NPA motifs in black, and ar/R filter in red (C). Quaternary tetramer structure viewed from the extracellular side in cartoon representation, with each transmembrane domain in a different color (D). Quaternary tetramer structure viewed from the cytoplasmic side in surface representation, with each monomer shown in a different color (E). Panels C-E were generated in PyMOL (The PyMOL Molecular Graphics System, Version 3.1, Schrödinger, LLC) using the human AQP5 structure (PDB ID: 3D9S).

#### 1.3.2. Permeability

Aquaporins were first described as water channels, but it is now recognized that they can also transport other small molecules. Based on their permeability, they are classified into three groups: orthodox or classical aquaporins (AQP0, AQP1, AQP2, AQP4, AQP5, AQP6, AQP8), which are primarily selective for water; aquaglyceroporins (AQP3, AQP7, AQP9, AQP10), which have slightly larger pores that permit the passage of small neutral solutes like glycerol and urea in addition to water; and unorthodox aquaporins or superaquaporins (S-aquaporins; AQP11, AQP12), which are atypical in sequence and structure, and localized intracellularly (Figure 8) [49, 53]. Other aquaporins are localized on the cell membrane or in the intracellular vesicles until stimulation.

The physiological role of aquaporins is closely linked to their permeability. Classical aquaporins primarily regulate osmotic balance and water homeostasis, aquaglyceroporins participate in metabolic regulation and energy homeostasis, and S-aquaporins maintain ER homeostasis and intracellular vesicle function.

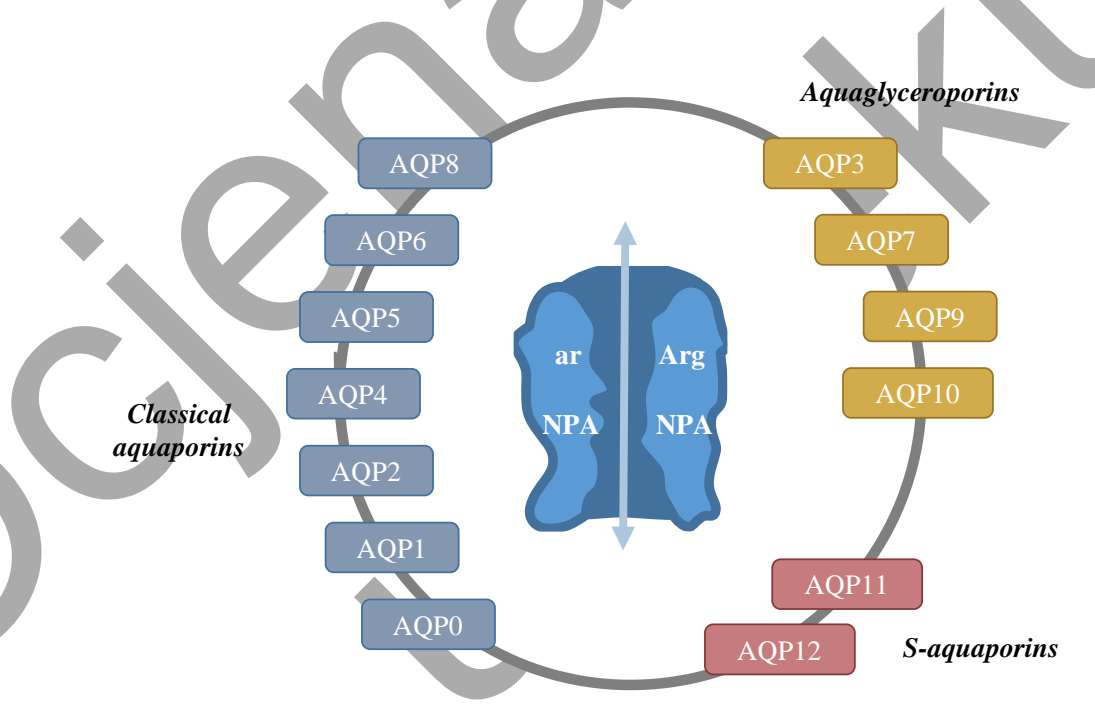


Figure 8. Aquaporin classification

Human aquaporins are divided into three groups based on their selectivity. Classical aquaporins (AQP0, AQP1, AQP2, AQP4, AQP5, AQP6, and AQP8; shown in blue) are primarily selective for water, aquaglyceroporins (AQP3, AQP7, AQP9, and AQP10; shown in yellow) transport glycerol as well, and S-aquaporins (AQP11 and AQP12, shown in red) are less characterized and localized intracellularly. The central scheme highlights the NPA motifs and the ar/R filter that form a selective channel.

Beyond water and glycerol, aquaporins can transport other small molecules. For example, AQP1 also acts as a cGMP-gated ion channel and conducts CO<sub>2</sub> and NO [54–56], while AQP6 functions as a gated chloride channel that opens at low pH [57], and AQP7 and AQP9 participate in arsenite intake [58].

Importantly, several aquaporins function as peroxiporins, channels that facilitate H<sub>2</sub>O<sub>2</sub> transport across membranes. AQP8 was the first experimentally confirmed peroxiporin, with studies in yeast demonstrating increased intracellular ROS accumulation upon H<sub>2</sub>O<sub>2</sub> exposure [59]. AQP1 was later confirmed to conduct H<sub>2</sub>O<sub>2</sub>, with studies showing that mutations in its selectivity filter altered H<sub>2</sub>O<sub>2</sub> flux [60]. AQP3 facilitates H<sub>2</sub>O<sub>2</sub> intake that is required for downstream redox signaling, including the NADPH oxidase-dependent pathways activated by growth factor stimulation [61]. AQP5 expression increases H<sub>2</sub>O<sub>2</sub> intake in yeast and pancreatic cancer cell models, and this effect is reversed by aquaporin inhibitors or mutagenesis [62, 63]. AQP6 has been linked to oxidative stress resistance and contributes to chemotherapy resistance in mesothelioma cells [64]. H<sub>2</sub>O<sub>2</sub> intake was increased in AQP9-overexpressing hamster ovary cells and reduced after knockdown with small interfering RNA (siRNA) in human hepatoma cells [65]. More recently, AQP11 was shown to transport H<sub>2</sub>O<sub>2</sub> into the ER lumen, thereby regulating ER redox homeostasis [66], Collectively, these studies demonstrate that AQP1, AQP3, AQP5, AQP6, AQP8, AQP9, and AQP11 function as peroxiporins and shape intracellular ROS dynamics and redox signaling.

#### 1.3.3. Regulation

To ensure controlled transport, aquaporins are regulated at transcriptional, translational, and post-translational levels.

At the transcriptional level, hormones and growth factors influence aquaporin expression. For example, vasopressin upregulates AQP2 transcription in renal collecting duct cells [67], while estrogen regulates AQP1, AQP3, and AQP5 in reproductive tissues by directly activating the estrogen response element in the promoter of the gene [68–70]. Cytokines and growth factors such as TNF- $\alpha$ , EGF, and TGF- $\beta$  can also alter aquaporin gene expression, linking them to inflammation and cancer progression [71–73].

Post-translational modifications, especially phosphorylation, control aquaporin trafficking and gating. In renal collecting duct cells, phosphorylation of AQP2 at Ser256 by protein kinase A (PKA) promotes its translocation from intracellular vesicles to the apical plasma membrane when body fluid osmolality rises and vasopressin is released, resulting in

increased water reabsorption [67, 74]. In contrast, phosphorylation of AQP4 at Ser180 by protein kinase C (PKC) reduces water permeability and cell migration in glioma models [75].

Trafficking also regulates aquaporin activity: for example, AQP5 relocates to the apical surface of salivary gland cells during parasympathetic stimulation to facilitate saliva secretion [76]. Aquaporins are shuttled to and from the cell membrane in response to different stimuli, and factors such as pH and calcium can modulate aquaporin activity. Besides the already mentioned chloride transport by AQP6 at low pH, acidification inhibits the water/glycerol permeability of AQP3 and AQP7 [77, 78], while AQP10 shows low permeability at physiological pH but high activity under acidic conditions [79]. Regulation of aquaporins is often complex, as in AQP0, where site-specific phosphorylation modulates Ca<sup>2+</sup>/calmodulin-mediated gating [80].

Complex regulatory mechanisms, including transcriptional induction, post-translational modifications, and environmental modulation, allow aquaporins to modulate their activity to physiological demands, thereby maintaining cellular and systemic homeostasis.

## 1.3.4. Physiology and Disease

Aquaporin isoforms are expressed in a tissue-specific manner that aligns with their physiological roles. They maintain water homeostasis, regulate glycerol metabolism, secretion, and other organ-specific functions, as summarized in Table 1, which also lists associated pathologies and cancers in which specific aquaporin isoforms were shown to have a potential diagnostic or prognostic significance.

Table 1. Tissue distribution, physiological roles, and associated pathologies of aquaporin isoforms

	Tissue distribution	Physiological Roles	Associated Pathology	Reference
AQP0	Lens fiber cells in the eye	Functions as a water channel and adhesion molecule, essential for maintaining lens transparency and optical accommodation	Autosomal dominant congenital cataracts, presbyopia	[81–84]
AQP1	Red blood cells; renal proximal tubule epithelium; descending vasa recta endothelium; choroid plexus epithelium; microvascular endothelia	Mediates water permeability and reabsorption, urine concentration, cerebrospinal fluid secretion, and transendothelial water exchange	Shortened red blood cell lifespan, nephrogenic diabetes insipidus–like phenotype, polyuria, impaired urine concentration; brain, lung, colorectal, breast, ovarian, and endometrial cancer, multiple myeloma	[85–100]
AQP2	Collecting duct principal cells (apical membrane and intracellular vesicles)	Vasopressin-regulated water reabsorption, urine concentration	Nephrogenic diabetes insipidus (hereditary and acquired), inability to concentrate urine; lung and endometrial cancer	[67, 101– 103]
AQP3	Basolateral membranes of renal collecting duct cells; epidermis (basal keratinocytes); epithelia of lung, urinary bladder, gastrointestinal tract	Water and glycerol transport; involved in skin hydration, wound healing, renal water reabsorption, and glycerol metabolism; colorectal cancer	Nephrogenic diabetes insipidus (in mice), dry skin, impaired wound healing; pituitary, salivary gland, lung, thymic, esophageal, pancreatic, colorectal, breast, ovarian, prostate, testicular, urothelial, and skin cancer	[91, 96, 97, 104– 115]
AQP4	Astrocytes at the blood-brain barrier; ependymal cells; renal inner medulla; skeletal muscle; stomach parietal cells; lung epithelium	Regulates brain water homeostasis, glial migration, neural signaling, and urine concentration	Neuromyelitis optica (autoimmune AQP4-IgG disease), brain edema; brain, thyroid, and colorectal cancer	[116–122]

AQP5	Apical membranes of salivary, lacrimal, submucosal, and sweat glands; alveolar type I cells in the lung; lens fiber cells	Important in saliva, tears, and sweat secretion; pulmonary fluid balance, and lens transparency	Sjögren's syndrome, dry mouth, dry eye, sweat disorders, cataracts; lung, gastric, pancreatic, colorectal, breast, ovarian, and cervical cancer	[84, 91, 96, 97, 99, 114, 123– 134]
AQP6	Intracellular vesicles of acid-secreting intercalated cell s in renal collecting ducts	Functions as a gated anion channel under acidic pH, may assist in urine acidification	Ovarian cancer	[135, 136]
AQP7	Adipocyte plasma membranes; renal proximal tubules; pancreatic β-cells	Glycerol efflux during lipolysis; glycerol and water reabsorption in the kidney; links fat metabolism to gluconeogenesis	Adult-onset obesity with insulin resistance, glyceroluria; breast cancer	[137–139]
AQP8	Small intestine and colon epithelial cells; hepatocytes; cholangiocytes; pancreatic acinar cells	Mediates water absorption and ammonia transport; contributes to bile secretion and ammonia detoxification	Altered pregnancy outcomes in mice; implicated in liver injury and colon disorders; leukemia, ovarian cancer	[136, 140–144]
AQP9	Hepatocyte basolateral membranes; male reproductive tract (epididymis, vas deferens); epidermis; leukocytes	Transports glycerol, urea, lactate, water; crucial for hepatic gluconeogenesis and sperm maturation	Diabetes (via altered gluconeogenesis), lipid metabolism disorders; lung, and prostate cancer	[102, 145, 146]
AQP10	Enterocytes in the duodenum and jejunum; adipocytes	Intestinal water and glycerol absorption; adipocyte glycerol efflux	Breast cancer	[147–149]
AQP11	Intracellular, mainly the endoplasmic reticulum of proximal tubule cells; testis, liver, and brain	Maintains endoplasmic reticulum homeostasis	Polycystic kidney disease (in knockout mice)	[150–153]
AQP12	Pancreatic acinar cells (intracellular compartments, zymogen granules)	Supports digestive enzyme secretion by regulating vesicular water flux	Unknown	[154]

#### 1.3.4.1. Aquaporins in Breast Cancer

Aquaporins are increasingly being recognized as contributors to breast cancer progression and therapy outcomes. Numerous studies have shown correlations between aquaporin expression and cancer type, histological grade, prognosis, and the development of chemoresistance, but it is still unclear if they could be considered as biomarkers or therapeutic targets [155–157]. In breast cancer, AQP1, AQP3, and AQP5 are most frequently mentioned as overexpressed and associated with prognostic and therapeutic potential [158–161]. All correlate with larger tumor size, positive lymph node status, relapse, and distant metastasis in TNBC patients, and are associated with worse five-year disease-free and overall survival rates [107, 169].

AQP1 is widely expressed in epithelial and endothelial cells and is frequently upregulated in breast cancer. It correlates with high grade, poor prognosis, and characterizes an aggressive basal-like subgroup, highlighting its potential as a prognostic marker [107]. In TNBC, AQP1 is aberrantly localized in the cytoplasm and was shown to promote breast cancer progression [171]. Functionally, AQP1 promoted TNBC progression by binding and suppressing RIPK1-mediated necroptosis/apoptosis [172], and contributed to local invasion [173], highlighting AQP1 as a therapeutic target. *In vivo*, AQP1 was implicated in angiogenesis, and AQP1-deficiency reduced breast cancer growth and lung metastasis in mice, further supporting its therapeutic relevance [174]. Despite its association with poor prognosis, in anthracycline-treated breast cancer patients, high AQP1 expression predicted better outcomes, where AQP1 inhibited  $\beta$ -catenin degradation, allowing nuclear  $\beta$ -catenin to activate topoisomerase II $\alpha$  and thereby increasing anthracycline sensitivity [175].

AQP3 is normally expressed in mammary epithelium but is significantly upregulated in breast cancer, where it correlates with poor prognosis and larger tumor size [162]. The regulation of AQP3 expression is closely linked to hormonal signaling, and its transcription is directly regulated by estrogen through binding to ERE in the gene promoter, which explains why ER-positive cancers often show poor differentiation and are more likely to metastasize to lymph nodes [69]. In addition, ER-positive breast cancer tissue from premenopausal patients shows higher AQP3 expression compared to that from postmenopausal patients [69]. AQP3 has prognostic value in HER2-positive early breast cancer, associating with poorer recurrence-free survival [170], and in TNBC, where higher expression correlates with worse survival and suggests potential therapeutic relevance [169]. Functionally, AQP3 facilitates water and glycerol transport, enhancing cell motility, glycolysis, and lipid biosynthesis. It also acts as a

peroxiporin that activates EGFR/ERK/p38/MAPK, and NF-κB signaling pathways through H<sub>2</sub>O<sub>2</sub> signaling, thereby promoting proliferation, migration, invasion, and EMT [78, 165, 177], and was shown to colocalize with NADPH oxidase 2, suggesting a spatially coordinated mechanism for localized ROS signaling [113, 163]. Silencing AQP3 reduced cell proliferation, migration, and invasion, and sensitized breast cancer cells to 5-fluorouracil [164], suggesting its therapeutic potential as well.

In contrast to AQP3, AQP5 is minimally expressed in normal breast epithelium, but becomes upregulated in breast cancer, where its levels increase with tumor stage and correlate with lymph node metastasis, higher histological grade, and poorer overall survival [180]. This suggests the potential role of AQP5 as a marker of breast cancer aggressiveness, but also a potential contributor to cancer progression. AQP5 expression predicts poorer survival in early breast cancer [168, 181], and is associated with worse survival in TNBC [169]. Like AQP3, AQP5 functions as a peroxiporin and shapes intracellular ROS signaling to sustain oncogenic pathways while preventing oxidative damage. In cancer cell models, overexpression of AQP5 enhances proliferation and migration through activation of EGFR/ERK/p38/MAPK signaling cascade [139, 177], while silencing reduces both [166]. AQP5 also contributes to EMT through activation of the Wnt/β-catenin pathway in TNBC [183]. Beyond its role in cancer progression, elevated AQP5 expression has also been linked to chemotherapy resistance, and its silencing restored chemosensitivity by downregulating P-gp [167].

Beyond these, other aquaporin isoforms were implicated in breast cancer. For example, AQP4 downregulation inhibited breast cancer cell proliferation, migration, and invasion [185]. Furthermore, AQP7 was identified as a novel regulator of breast cancer and a key mediator of metabolic and signaling responses to environmental stress [148].

AQP1, AQP3, and AQP5, along with other isoforms, influence breast cancer progression and therapeutic response, and their dysregulated expression highlights their potential as new prognostic biomarkers and potential therapeutic targets for overcoming chemoresistance. This study focuses on AQP3 and AQP5, the most consistently overexpressed isoforms with strong clinicopathologic associations and defined roles in invasion, EMT, and therapy resistance.

#### 1.4. Aim of the research

Considering aquaporins' overexpression in breast cancer and their association with poor prognosis and chemoresistance, understanding their regulation and function is essential for clarifying their potential as biomarkers or therapeutic targets.

While it is known that they transport  $H_2O_2$ , it remains unclear how they respond to oxidative stress within the cell. Therefore, the first aim is to investigate the role of AQP3 and AQP5 in the cellular response to oxidative stress and determine whether this response differs between breast cancer cell lines of different molecular subtypes and a non-tumorigenic breast epithelial cell line.

Although NRF2 is well established as a master regulator of cellular redox balance and stress responses, it is not clear whether it can directly or indirectly regulate aquaporin expression and activity. Thus, the second aim is to examine the influence of the transcription factor NRF2 on both the expression and activity of aquaporins.

Finally, humans have 13 aquaporin isoforms expressed in a tissue-specific manner, and it is hypothesized that cells may regulate their expression to modulate substrate transport. Accordingly, the third aim is to explore the potential interdependence of aquaporin expression.

#### 2. MATERIALS AND METHODS

#### 2.1. Cell Culture

This study was conducted on three human breast cancer cell lines (MCF7, SkBr3, and SUM159PT) and one human non-tumorigenic breast epithelial cell line (MCF10A), purchased from the European Collection of Authenticated Cell Cultures (ECACC, Porton Down, UK) or Elabscience (Vienna, Austria). The MCF7 cell line, derived from human breast adenocarcinoma, represents the luminal A subtype and is ER and PR positive, and HER2 negative. SkBr3, also originating from breast adenocarcinoma, belongs to the HER2-positive subtype and is ER and PR negative. SUM159PT, derived from a breast carcinoma, is classified as a basal-like/triple-negative subtype with ER, PR, and HER2 negative status. MCF10A is a non-tumorigenic human mammary epithelial cell line with a normal-like basal phenotype and lacks expression of ER, PR, and HER2.

All cell culture procedures, including cell maintenance, handling, seeding, and treatments, were conducted under sterile conditions in a biosafety cabinet located in a sterile room. The methods applied were identical for all cell lines. Cells were stored in cryotubes in liquid nitrogen at -196 °C and thawed when needed for experiments. The cancer cell lines were cultivated in Dulbecco's Modified Eagle Medium (DMEM, Sigma Aldrich, St. Louis, MO, USA) supplemented with 10% fetal bovine serum (FBS, Sigma Aldrich), while the non-tumorigenic cell line was cultured in DMEM:F12 1:1 (Sigma Aldrich) containing 10% FBS, 10 µg/mL insulin (Sigma Aldrich), 20 ng/mL epidermal growth factor (EGF, PeproTech, London, UK), and 100 ng/mL cholera toxin (Sigma Aldrich). Cells were grown in a humidified atmosphere with 5% CO<sub>2</sub> at 37 °C. Upon reaching semiconfluency, cells were trypsinized, counted, and seeded for treatments.

#### 2.1.1. Prolonged oxidative stress

To evaluate the effects of prolonged oxidative stress,  $3 \times 10^5$  cells were seeded into T25 flasks (Techno Plastic Products (TPP), Trasadingen, Switzerland) and exposed to  $H_2O_2$  (Gram-Mol, Zagreb, Croatia) at concentrations of 10 or 20  $\mu$ M for 14 days. The culture medium with or without  $H_2O_2$  was replaced every two days, and cells were trypsinized between treatments before they reached full confluence. Control cells were maintained under the same conditions, including seeding density and medium changes, but without  $H_2O_2$  treatment. Following 14 days of  $H_2O_2$  exposure, cell viability, proliferation, and migration were assessed. To examine whether prolonged exposure to low  $H_2O_2$  concentrations induced an adaptive cellular response,

cells were challenged with  $H_2O_2$  at concentrations ranging from 0 to 100  $\mu$ M, covering physiological to pathological levels, and assessed after 24 hours using commercially available kits, following the manufacturer's instructions. Cell migration was assessed using a wound healing assay over a 48-hour period, under both  $H_2O_2$ -treated and untreated conditions. Cells were then collected for downstream analyses, including protein and mRNA expression profiling, as well as the preparation of dry cell pellets for lipid and lipid hydroperoxide quantification.

#### 2.1.2. Modulation of NRF2 expression and activity

To investigate the role of the transcription factor NRF2 in regulating aquaporin expression and activity, NRF2 protein levels and function were modulated using genetic and pharmacological approaches.

Stable overexpression of NRF2 was achieved by transfecting cells with a plasmid encoding the NFE2L2 gene (RC204140, OriGene, Herford, Germany) using Lipofectamine 3000 reagent (Thermo Fisher Scientific, Waltham, MA, USA). Cells transfected with the empty vector plasmid pCMV6-Entry (PS100001, OriGene) served as controls. Cells were seeded in 6-well plates (TPP) and, after 24 hours, the culture medium was replaced with serum-free medium containing the transfection mixture composed of 1 µg plasmid DNA complexed with Lipofectamine 3000 according to the manufacturer's protocol. After 24 hours, the medium was replaced with fresh growth medium. Following an additional 24 hours of recovery, cells were subjected to selection with 500 µg/mL G418 (Roche, Basel, Switzerland) to establish stable NRF2- or empty vector-expressing cell lines. The optimal G418 concentration was selected after a cytotoxicity assay with increasing concentrations of G418 over 10 days, followed by cell viability assessment. Successful transfection was confirmed by the survival of transfected cells and the death of untransfected control cells during antibiotic selection. Transient knockdown of NRF2 was achieved using a specific siRNA targeting human NFE2L2 (s9491, Thermo Fisher Scientific), with an On-Target Plus Non-targeting Control siRNA (Horizon Discovery, Waterbeach, UK) serving as a negative control. Cells were seeded in 12-well plates (TPP), and 24 hours later, transfections were performed using 10 pmol of siRNA complexed with Lipofectamine RNAiMAX (Thermo Fisher Scientific) diluted in Opti-MEM reduced serum medium (Thermo Fisher Scientific). The complexes were added to cells in serum-free medium with a final volume of 500 µL per well, achieving a final siRNA concentration of 20 nM. Cells were incubated for 24 or 48 hours before harvesting for downstream analyses.

In addition to genetic modulation, NRF2 activity was pharmacologically regulated using the well-established NRF2 activator sulforaphane (S4441, Sigma Aldrich), a naturally occurring isothiocyanate that induces NRF2 by modifying its negative regulator Keap1 [168]. To inhibit NRF2, the selective inhibitor ML385 (HY-100523, MedChemExpress, Monmouth Junction, NJ, USA), which suppresses its activity by interfering with the DNA-binding capability, was used. For further analysis, a non-toxic sulforaphane and ML385 concentrations were selected after cell viability assays with tested concentrations ranging from 0 to 10  $\mu$ M. Dimethyl sulfoxide (DMSO, Carl Roth, Karlsruhe, Germany) was included as the vehicle control.

NRF2 activity was estimated by measuring the protein levels in the nuclear fraction two hours post-treatment with sulforaphane and ML385, representing its transcriptional activation. Additionally, the expression of the downstream target protein HO-1 was quantified 6 and 24 hours after treatment to confirm its transcriptional activity. The efficiency of NRF2 genetic modulation was confirmed by Western blot analysis, performed either after stable transfection or 48 hours post-siRNA knockdown, by measuring the protein levels of NRF2 and its downstream target. Upon confirming successful NRF2 modulation, further analyses were performed to measure aquaporin gene and protein expression, as well as aquaporin-mediated H<sub>2</sub>O<sub>2</sub> transport.

### 2.1.3. Modulation of Aquaporin expression

To study the functional roles of AQP3 and AQP5 in the cell, overexpression and knockdown of AQP3 and AQP5 were performed using plasmid-based transfection and shRNA-mediated silencing, respectively.

Stable overexpression of AQP3 and AQP5 was achieved using plasmids encoding human AQP3 (RC201856, OriGene) and AQP5 (RC206069, OriGene), respectively. The transfection protocol, selection procedure using G418, and use of the empty vector pCMV6-Entry as a control were identical to those described in the previous paragraph for NRF2 overexpression (2.1.2).

For gene silencing, short hairpin RNA (shRNA) constructs targeting AQP3 and AQP5 were designed using the VectorBuilder shRNA design tool (https://en.vectorbuilder.com), and oligonucleotides were synthesized accordingly and shown in Table 2.

Table 2. Oligo sequences used for AQP3 and AQP5 silencing

AQP3	5'-GATCCCCGAACCGGAATTTGGGTCAATATTCAAGAGATATTGACCCAAATTCCGGTTCTTTTTA-3'
AQP5	5'-GATCCCCACGCGCTCAACAACACAACACAATTCAAGAGATTGTTGTTGTTCAGCGCGTTTTTA-3'

The shRNA oligos were designed with a BgIII overhang (purple) at the 5' end, followed by the sense target sequence (green), a hairpin loop (orange), the antisense sequence (green), and a HindIII overhang (blue) at the 3' end to enable directional cloning into the pSUPER vector.

Oligos were annealed in a buffer containing 100 mM NaCl (Gram-Mol) and 50 mM HEPES (pH 7.5, Carl Roth) by heating to 90 °C for 4 min, followed by gradual cooling in 5 °C increments from 70 °C to 37 °C to ensure duplex formation. Annealed oligos were then ligated into the pSUPER vector with a puromycin resistance gene (VEC-PBS-0007/0008, OligoEngine, Seattle, WA, USA), which was previously linearized using HindIII (FD0505) and BglII (FD0084) FastDigest restriction enzymes (Thermo Fisher Scientific). The linearized plasmid was gel-extracted and purified using the QIAquick Gel Extraction Kit (Qiagen, Hilden, Germany). Ligation reactions were performed using T4 DNA ligase (EL0011, Thermo Fisher Scientific) at a 1:1 oligo:plasmid ratio. Plasmids were transformed into electrocompetent Escherichia coli DH5α by electroporation using the Gene Pulser Xcell<sup>TM</sup> (Bio-Rad Laboratories, Hercules, CA, USA) at 2.5 kV. Following a 1-hour recovery in Super Optimal broth with Catabolite repression medium (Thermo Fisher Scientific) at 37 °C, E. coli was plated on LB-agar (Carl Roth) containing ampicillin (100 µg/mL, Thermo Fisher Scientific) and incubated overnight. Colonies were picked into LB broth containing ampicillin and grown overnight at 37 °C. Plasmid DNA was purified using a QIAprep® Spin Miniprep Kit (Qiagen), and positive clones were identified by restriction enzyme digestion with FastDigest EcoRI (FD0274, Thermo Fisher Scientific) and HindIII. Successful integration of shRNA inserts was confirmed after agarose (Sigma Aldrich) gel electrophoresis, and the expected fragment sizes of positive clones (Figure 9).

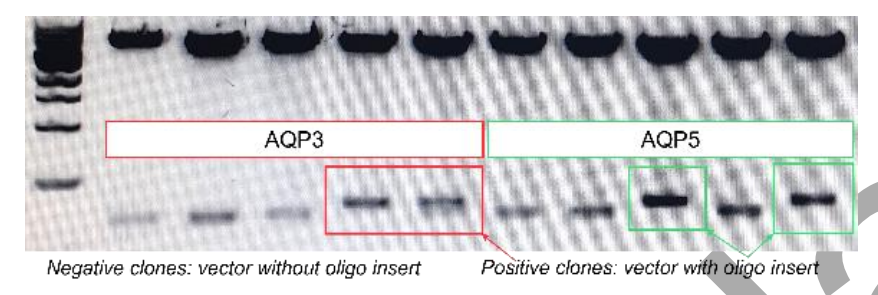


Figure 9. Confirmation of AQP3 and AQP5 shRNA oligo insert successful integration

Successful integration of AQP3 (red box) and AQP5 (green box) shRNA inserts was confirmed by agarose gel electrophoresis, showing DNA fragments of larger sizes in positive clones. The DNA ladder on the left was used as a molecular size reference.

shRNA plasmids and empty pSUPER as a control were transfected into breast cancer cell lines following the same protocol as for overexpression. Selection of stably transfected clones was carried out using 1  $\mu$ g/mL puromycin (Carl Roth), following determination of the optimal concentration by a cytotoxicity assay. Upon confirming successful AQP3 or AQP5 overexpression or knockdown on mRNA and protein levels, further analyses were performed to measure all aquaporin isoforms gene expression and aquaporin-mediated  $H_2O_2$  transport.

#### 2.2. Cell Viability Assay

Cell viability was measured using the EZ4U Cell Proliferation Assay and Cytotoxicity Test (Biomedica, Vienna, Austria), which measures metabolic activity through the reduction of a tetrazolium salt into a water-soluble yellow formazan dye.  $1 \times 10^4$  cells per well were seeded into 96-well plates (TPP) and allowed to attach for 24 hours, followed by treatment according to the experimental setup. After 24 hours, the culture medium was replaced with colorless medium and the assay dye. Absorbance was measured at 450 nm with a reference wavelength of 620 nm using a microplate reader (EZ Read 2000, Biochrom, Cambridge, UK).

#### 2.3. Cell Proliferation Assay

Cell proliferation was measured using the BrdU Cell Proliferation ELISA Kit (Roche), which quantifies the incorporation of 5-bromo-2'-deoxyuridine (BrdU) into newly synthesized DNA. As with the viability assay,  $1 \times 10^4$  cells per well were seeded into 96-well plates (TPP) and allowed to attach for 24 hours before treatment. After an additional 24-hour incubation with treatments, BrdU was added and incubated for 1 hour. Cells were then fixed, and DNA was denatured to permit binding of an anti-BrdU-POD antibody. Colorimetric detection was performed using a substrate solution, and the reaction was terminated with a stop solution.

Absorbance, corresponding to DNA synthesis and cell proliferation, was measured at 450 nm using the same microplate reader as in the viability assay.

#### 2.4. Wound Healing Assay

Cell migration was evaluated using a wound healing assay over 48 hours.  $3 \times 10^4$  cells were seeded per well in a 96-well plate (TPP) and cultured until a confluent monolayer was achieved. Cells were then treated with 5 µg/mL mitomycin C (Roche) for 2 hours to inhibit proliferation [187]. A scratch was made in the monolayer using a sterile pipette tip, and the medium was replaced with either fresh control medium or medium containing a treatment. Images of the scratch area were taken immediately after scratching (0 h), and at 24- and 48-hours post-scratch. Wound closure was quantified using ImageJ software (version 1.53t) by measuring the remaining scratch area over time.

#### 2.5. Total Lipid Extraction, GC Analysis, and Measurement of LOOH Concentration

Total lipids were extracted from dry cell pellets using a modified Folch method [169]. Briefly, 5 mL of chloroform (Gram-Mol) was added to each sample and thoroughly mixed, followed by the addition of 1.5 mL of an aqueous MgCl<sub>2</sub> solution (0.034%, w/v, Carl Roth). After vortexing and centrifugation, the upper aqueous layer was removed, and 2.5 mL of 2 M KCl (Gram-Mol) in methanol (4:1, v/v, Gram-Mol) was added to the remaining organic phase. The mixture was then vortexed and centrifuged again, after which the aqueous layer was discarded. Subsequently, 2.5 mL of a chloroform/methanol mixture (2:1, v/v) was added to further purify the lipid fraction. The hydrophobic phase was transferred to a new glass tube and evaporated under a nitrogen stream. For fatty acid methyl ester (FAME) preparation, the dried lipid extracts were treated with 0.5 M KOH (Gram-Mol) in methanol for 10 minutes at room temperature. FAMEs were then extracted with n-hexane and analyzed by gas chromatography (GC) using a Varian 450-GC system equipped with a flame ionization detector and a Stabilwax capillary column (60 m × 0.25 mm, polyethylene glycol stationary phase, Restek Corporation, Bellefonte, PA, USA). Helium was used as the carrier gas. The temperature program was set from 150 °C to 250 °C with an increment of 5 °C/min. FAMEs were identified by comparison of retention times with those of a standard mixture (marine oil FAME mix, Restek Corporation), and their relative abundance was determined by measuring the area under each chromatographic peak and expressing it as a percentage of the total fatty acid content. For lipid hydroperoxide (LOOH) quantification, the extracted lipid layer was transferred to glass tubes, evaporated, weighed, and stored at -20 °C until analysis. LOOH concentration was determined by a spectrophotometric ferric thiocyanate assay. Lipids were diluted in a deaerated CH<sub>2</sub>Cl<sub>2</sub>/MeOH solvent mixture (2:1, v/v, Gram-Mol), and the absorbance of the resulting [FeNCS]<sup>2+</sup> complex was measured at 500 nm. The concentration of LOOH was calculated using a molar absorptivity of 58,440 dm<sup>3</sup>mol<sup>-1</sup>cm<sup>-1</sup> [170].

### 2.6. Protein Isolation and Western Blot Analyses

Total cellular proteins were extracted using RIPA buffer (Sigma Aldrich) supplemented with protease and phosphatase inhibitors (Thermo Fisher Scientific). Following cell lysis on ice and centrifugation at 13,400 rpm for 10 minutes, supernatants containing proteins were collected. Subcellular fractionation was performed in parallel to isolate cytoplasmic and nuclear proteins. For a subset of samples, fractionation was carried out using the NE-PER<sup>TM</sup> Nuclear and Cytoplasmic Extraction Reagents (Thermo Fisher Scientific), according to the manufacturer's instructions. Briefly, cells were harvested and centrifuged, then incubated with Cytoplasmic Extraction Reagent I with protease and phosphatase inhibitors, followed by Cytoplasmic Extraction Reagent II to selectively lyse the cytoplasmic membrane and release cytoplasmic proteins. After centrifugation, the supernatant was collected as the cytoplasmic fraction, and the resulting pellet was treated with Nuclear Extraction Reagent with protease and phosphatase inhibitors to lyse the nuclear membrane and extract nuclear proteins. In parallel, an in-house method was applied to another subset of samples to isolate cytoplasmic and nuclear proteins. Trypsinized cells were washed with phosphate-buffered saline (PBS, 137 mM NaCl, 2.7 mM KCl, 10 mM Na<sub>2</sub>HPO<sub>4</sub> (Gram-Mol), and 1.8 mM KH<sub>2</sub>PO<sub>4</sub> (Gram-Mol), pH 7.4) and incubated on ice for 5 minutes in a hypotonic buffer (10 mM HEPES, pH 7.5; 10 mM NaCl; 1 mM dithiothreitol (DTT, Carl Roth), 1 mM ethylenediaminetetraacetic acid (EDTA, Gram-Mol), 2 mM MgCl<sub>2</sub> x 6H<sub>2</sub>O (Carl Roth)) supplemented with protease and phosphatase inhibitors. NP-40 (MilliporeSigma, Burlington, MA, USA) was added to a final concentration of 0.7%, followed by an additional 10-minute incubation on ice with intermittent vortexing. The lysates were centrifuged at  $13,400 \times g$  for 10 minutes to pellet the nuclei. The supernatant (cytoplasmic fraction) was collected and kept on ice. The nuclear pellet was washed once with hypotonic buffer without detergent, centrifuged again, and then lysed in RIPA buffer containing protease and phosphatase inhibitors for subsequent protein analysis. Protein concentrations were determined using the Bradford assay [171], using bovine serum albumin (BSA, Sigma Aldrich) standards prepared either in 20% RIPA buffer or PBS, depending on the lysate type. Samples and standards were appropriately diluted, incubated with Bio-Rad protein dye reagent (Bio-Rad Laboratories) for 5 minutes, and absorbance was measured at 595 nm. Equal amounts of protein (10-20 µg per sample) were mixed with loading buffer (125 mM Tris (Gram-Mol), 4% sodium dodecyl sulfate (SDS, Carl Roth), 150 mM DTT, 20% glycerol (Carl Roth), 0.01% bromophenol blue (Michrome, London, UK)) to a final volume of 20 µL, vortexed, and denatured at 95 °C for 5 minutes. Proteins were separated by sodium dodecyl sulfate polyacrylamide gel electrophoresis (SDS-PAGE) using a discontinuous gel system consisting of a stacking gel (125 mM Tris (Carl Roth), 0.1 % SDS, pH 6.8; 5 % acrylamide/bisacrylamide (Carl Roth), 0.1 % ammonium persulfate (APS, Bio-Rad Laboratories), 0.13 % tetramethylethylenediamine (TEMED, Carl Roth) and a resolving gel (375 mM Tris, 0.1 % SDS, pH 8.8; 8% acrylamide/bisacrylamide, 0.1% APS, 0.13% TEMED), with running buffer (25 mM Tris, 192 mM glycine (Carl Roth), 0.1% SDS). Electrophoresis was performed initially at 90 V and then increased to 105 V until completion. Proteins were transferred onto nitrocellulose membranes (Roti-NC 0.2 µm; Carl Roth) by wet transfer in transfer buffer (25 mM Tris, 192 mM glycine, 20% methanol) at 300 mA for 65 minutes on ice. Transfer efficiency was confirmed by Ponceau S staining (Sigma Aldrich). Membranes were blocked in 5% nonfat dry milk (Carl Roth) in TBST (50 mM Tris, 150 mM NaCl, 0.1% Tween 20 (Carl Roth)) for 1 hour at room temperature, followed by overnight incubation at 4 °C with primary antibodies diluted in blocking buffer. Primary antibodies used included: anti-Nrf2 (D1Z9C), anti-HO-1 (E3F4S), anti-NQO1 (D6H3A), anti-GSK-3β (D5C5Z), anti-Keap1 (D6B12), anti-ABCB1 (E1Y7B), anti-ABCG2 (D5V2K), anti-PI3K (C73F8), anti-PTEN (D4.3), anti-pAkt (D9E), anti-Akt (C67E7), anti-Ras (27H5), anti-phospho-mTOR (D9C2), anti-Raptor (24C12), anti-Rictor (53A2), anti-β-Actin (D6A8), anti-GAPDH (D16H11) and anti-LSD1 (2139) (1:1000, Cell Signaling Technology, CST, Danvers, MA, USA); anti-AQP3 (sc-518001) and anti-AQP5 (sc-514022) (1:200, Santa Cruz Biotechnology, Dallas, TX, USA); and anti-AKR1B10 (ab96417) (1:10,000, Abcam, Cambridge, UK). After washing, membranes were incubated for 1 hour at room temperature with the appropriate secondary antibodies: anti-rabbit IgG HRP-linked (1:2000, CST, 7074) or anti-mouse IgG HRP-linked (1:4000, CST, 96714). Protein bands were visualized using the SuperSignal<sup>TM</sup> West Pico PLUS Chemiluminescent Substrate (Thermo Fisher Scientific) and imaged on the Alliance 4.7 Digital Imaging System (Uvitec, Cambridge, UK). Band intensities were quantified using Nine Alliance software Q9 (Uvitec), and protein expression levels were normalized to housekeeping proteins (β-Actin, GAPDH, or LSD1) and further validated by Ponceau S staining.

## 2.7. RNA Isolation, cDNA Synthesis, and RT-qPCR

Total RNA was extracted using TRIzol reagent (Thermo Fisher Scientific) according to the manufacturer's instructions. Briefly, cells were lysed in TRIzol reagent, followed by the addition of chloroform and centrifugation to separate phases. The aqueous phase was collected, and RNA was precipitated with isopropanol (Gram-Mol). The RNA pellet was washed with 75% ethanol (Gram-Mol), air-dried, and resuspended in RNase-free water. RNA purity and concentration were measured spectrophotometrically using a NanoPhotometer® N60 (Implen GmbH, München, Germany). RNA quality was additionally assessed by agarose gel electrophoresis to verify the integrity of ribosomal RNA bands. One microgram of RNA from each sample was reverse-transcribed into cDNA using the High-Capacity cDNA Reverse Transcription Kit (Thermo Fisher Scientific), following the manufacturer's protocol, on an Eppendorf 5331 MasterCycler Gradient Thermal Cycler (Eppendorf, Hamburg, Germany). The reaction mix was incubated at 25 °C for 10 minutes, followed by 37 °C for 120 minutes, and then 85 °C for 5 minutes to inactivate the enzyme. Quantitative real-time polymerase chain reaction (RT-qPCR) was performed using 2 µL of cDNA per reaction on a CFX Opus 96 Real-Time PCR System (Bio-Rad Laboratories) with TaqMan Universal PCR Master Mix (Thermo Fisher Scientific) and predesigned TagMan gene expression assays for (Hs01105469\_g1), AQP5 (Hs00387048\_m1), NFE2L2 (Hs00975961\_g1), and ACTB (Hs01060665\_g1) (Thermo Fisher Scientific). Cycling conditions were as follows: initial activation at 95 °C for 10 minutes, followed by 40 cycles of 95 °C for 15 seconds and 60 °C for 1 minute. For the quantification of AQP1, AQP2, AQP3, AQP4, AQP5, AQP6, AQP7, AQP8, AQP9, AQP10, AQP11, AQP12 and housekeeping genes B2M, and HPRT-1, SYBR Green chemistry was employed. Primer sequences are listed in Table 3. Each reaction contained 10 μL SsoAdvanced Universal SYBR Green Supermix (Bio-Rad Laboratories), 8 μL nucleasefree water, 0.5 µL of mixed forward and reverse primers (5 µM each), and 1.5 µL of cDNA template. Amplification was carried out on a CFX Opus 96 Real-Time PCR System (Bio-Rad Laboratories) with the following cycling conditions: initial denaturation at 95 °C for 2 minutes, followed by 40 cycles of 95 °C for 15 seconds and 62 °C for 30 seconds. A melting curve analysis was conducted to verify PCR product specificity. Relative gene expression was calculated using the  $2^{-4}$  method [172] and expressed as fold change relative to control conditions.

Table 3. Primer sequences used for quantitative reverse transcription PCR analysis

A OD1	Forward	AATGACCTGGCTGATGGTGT			
AQP1 —	Reverse	CAGGAGGTGTCCAAGGGCTA			
AQP2 —	Forward	TGGCTGTCAATGCTCTCAGC			
	Reverse	GCCACAGAGAAGCCTATGGA			
AQP3 -	Forward	GGGCTGTATTATGATGCAATCTC			
	Reverse	GTCCAGAGGGTAGGTAGCA			
Endogenous	Forward	AGACAGCCCCTTCAGGATTT			
AQP3	Reverse	TCCCTTGCCCTGAATATCTG			
1074	Forward	CTTCTACATCGCAGCCCAGT			
AQP4 —	Reverse	TGAACCATGGTGACTCCCAG			
1 O D #	Forward	CCCGCTCACTGGGTTTTCT			
AQP5 —	Reverse	GTCCTCGTCAGGCTCATACG			
AQP6 —	Forward	TTGGGATCCACTTCACTGGC			
	Reverse	CGGGGAACAGGACGAAGTTG			
	Forward	GAACGCAGCTGTGACCTTTG			
AQP7	Reverse	AAAGTGGAGAATGGCCGTGT			
1070	Forward	CGCTGGGGAATATCAGTGGT			
AQP8 —	Reverse	GAGACCCAGTACGGGAGGAG			
None -	Forward	TCTCAGTCGAGGACGTTTTGG			
AQP9 —	Reverse	GTGACCACCAGAGACACCG			
lonus.	Forward	TGGGTGGTAACGTCTCAGGG			
AQP10 —	Reverse	TGTAAATGGGGAGCTTGACCC			
	Forward	TGCAGGAGGAAGTCTAACAGG			
AQP11 —	Reverse	AGCCATGGAAGGAAAAAGCTG			
	Forward	GAGGCGATGAGGACGCTG			
AQP12 —	Reverse	GAAGAGCAGGAAGAGCAGGG			
	Forward	TGTCTTTCAGCAAGGACTGGT			
B2M —	Reverse	ACATGTCTCGATCCCACTTAAC			
	Forward	CCCTGGCGTCGTGATTAGTG			
HPRT-1 -	Reverse	TCGAGCAAGACGTTCAGTCC			

#### 2.8. Aquaporin Activity Assays

Aquaporin activity was assessed by measuring H<sub>2</sub>O<sub>2</sub> transport into cells using the chemical probe H<sub>2</sub>-DCFDA (Sigma Aldrich), which detects a broad range of intracellular ROS, including H<sub>2</sub>O<sub>2</sub>. To evaluate aquaporin-mediated H<sub>2</sub>O<sub>2</sub> permeability, 3 × 10<sup>4</sup> cells were seeded onto 22 mm glass coverslips (Carl Roth) in 200 μL of medium and allowed to adhere for 24 hours, after which they were treated according to the experimental plan. Cells were incubated with 10 μM H<sub>2</sub>-DCFDA for 30 minutes at 37 °C in a humidified atmosphere with 5% CO<sub>2</sub>. Before imaging, cells were washed with 25 mM HEPES buffer and mounted in a chamber on an inverted Eclipse Ti2 microscope (Nikon Europe B.V., Amstelveen, Netherlands) combined with a Dragonfly high-speed confocal platform (Andor Technology Ltd, Belfast, UK). After a 1-minute equilibration in HEPES buffer, 100 μM H<sub>2</sub>O<sub>2</sub> was added, and fluorescence images were recorded every 5 seconds with excitation at 495/10 nm with a Sona sCMOS camera (Andor Technology Ltd). Changes in fluorescence intensity over time were used to determine H<sub>2</sub>O<sub>2</sub> transport, and H<sub>2</sub>O<sub>2</sub> permeability was calculated from the slope of the fluorescence intensity over time using a custom Microsoft Excel Visual Basic script (available at https://github.com/nijelic/slope-residualsfor-multivariate-time-series).

## 2.9. In silico prediction of NRF2 binding sites

UCSC Genome Browser (https://genome.ucsc.edu/) [192] was used to analyze the regulatory regions of AQP3 and AQP5 on the hg38 human genome assembly. Predicted regulatory elements, including promoters and enhancers, were obtained from the GeneHancer database (https://www.genecards.org/Guide/GeneHancer) [193] integrated into the UCSC Genome Browser. Experimental transcription factor binding data were obtained from ChIP-seq targeting NRF2 (experiments ENCSR197WGI, ENCSR488EES, ENCSR707IUN, produced by the Snyder lab, Stanford) from the ENCODE4 Project (https://www.encodeproject.org/) [194], and visualized as part of the transcription factor representative peak clusters. Additional binding data were obtained from the ReMap 2022 atlas of regulatory regions [195] in the UCSC Genome Browser. Predicted NRF2 binding motifs were obtained from the JASPAR 2024 CORE collection [196], and visualized in the UCSC Genome Browser transcription factor binding sites track using a minimum motif score threshold of 400 (corresponding to p  $\leq$  0.0001). Additionally, promoter and enhancer sequences defined by GeneHancer were extracted and analyzed using FIMO (Find Individual Motif Occurrences, MEME Suite v5.5.8, https://memesuite.org/meme/tools/fimo) [197] with the JASPAR MA0150.2 NFE2L2 position weight

matrix. A threshold of  $p \le 0.0001$  was applied, and predicted motif events were uploaded as UCSC custom tracks for visualization.

# 2.10. Statistical Analysis

All experiments were performed in both biological and technical triplicates. Data is presented as mean  $\pm$  standard error of the mean (SEM). Statistical analyses were carried out using Microsoft Excel and GraphPad Prism version 8.0 (GraphPad Software, La Jolla, CA, USA). Depending on the experimental design, statistical significance was evaluated using unpaired Student's t-test, one-way ANOVA, or two-way ANOVA, followed by a post hoc test where appropriate. A p-value of less than 0.05 was considered statistically significant.



#### 3. RESULTS

#### 3.1. Effect of Prolonged Exposure to Hydrogen Peroxide

Aquaporins are known to facilitate the transport of  $H_2O_2$  across cellular membranes, implying a role in regulating oxidative stress within the cell. Since they are overexpressed in breast cancer, and cancer is characterized by elevated oxidative stress, we investigated whether prolonged exposure to  $H_2O_2$  affects their expression and related cellular responses.

## 3.1.1. Cell Viability and Proliferation

To evaluate the effect of prolonged oxidative stress, cells were pretreated with low concentrations of H<sub>2</sub>O<sub>2</sub> (10 or 20 µM) every two days for 14 days and subsequently acutely challenged with a range of H<sub>2</sub>O<sub>2</sub> concentrations. Cell viability was assessed with the EZ4U assay, and proliferation with BrdU incorporation 24 h post-treatment. Prolonged exposure influenced breast cancer and non-tumorigenic breast epithelial cells in a cell-type-specific manner. In SUM159PT cells, pretreatment with 10 or 20 µM H<sub>2</sub>O<sub>2</sub> for 14 days resulted in significantly higher viability upon acute 100 µM H<sub>2</sub>O<sub>2</sub> compared to untreated controls (p ≤ 0.0001 and  $p \le 0.001$ ), while no significant differences were detected at lower concentrations (Figure 10a). Pretreatment with 20 µM H<sub>2</sub>O<sub>2</sub> also resulted in significantly higher proliferation upon acute exposure to 5, 10, and 25  $\mu$ M H<sub>2</sub>O<sub>2</sub> (p = 0.0138, p = 0.0113, and p = 0.0118) (Figure 10e). In SkBr3 cells, increased viability was observed at 25 µM H<sub>2</sub>O<sub>2</sub>, where pretreatment with  $10 \mu M$  (p  $\leq 0.001$ ) and  $20 \mu M$  (p = 0.0485) H<sub>2</sub>O<sub>2</sub> had a protective effect (Figure 10b), whereas proliferation remained unchanged (Figure 10f). In MCF7 cells, pretreatment enhanced survival following acute exposure to 50  $\mu$ M (both p  $\leq$  0.0001) and 75  $\mu$ M (p = 0.0073 and p  $\leq$  0.0001) H<sub>2</sub>O<sub>2</sub> in cells pretreated with 10 and 20 μM H<sub>2</sub>O<sub>2</sub> (Figure 10c). Proliferation was also increased, but only in a 20 µM pretreatment group, with significant differences detected at 5 and 10 µM  $H_2O_2$  (p = 0.0016, p  $\leq$  0.001) (Figure 10g). In contrast, the non-tumorigenic MCF10A cells showed no evidence of adaptation in viability, which was even reduced at 75 µM H<sub>2</sub>O<sub>2</sub> following pretreatment with 20  $\mu$ M H<sub>2</sub>O<sub>2</sub> (p = 0.0071) (Figure 10d). However, they showed an increased proliferation at 100 µM H<sub>2</sub>O<sub>2</sub> following pretreatment with either 10 or 20 µM H<sub>2</sub>O<sub>2</sub> (p = 0.018, p = 0.0266) (Figure 10h). Because prolonged exposure to  $20 \mu M H_2O_2$  altered both cell viability and proliferation, this concentration was selected for all subsequent assays.

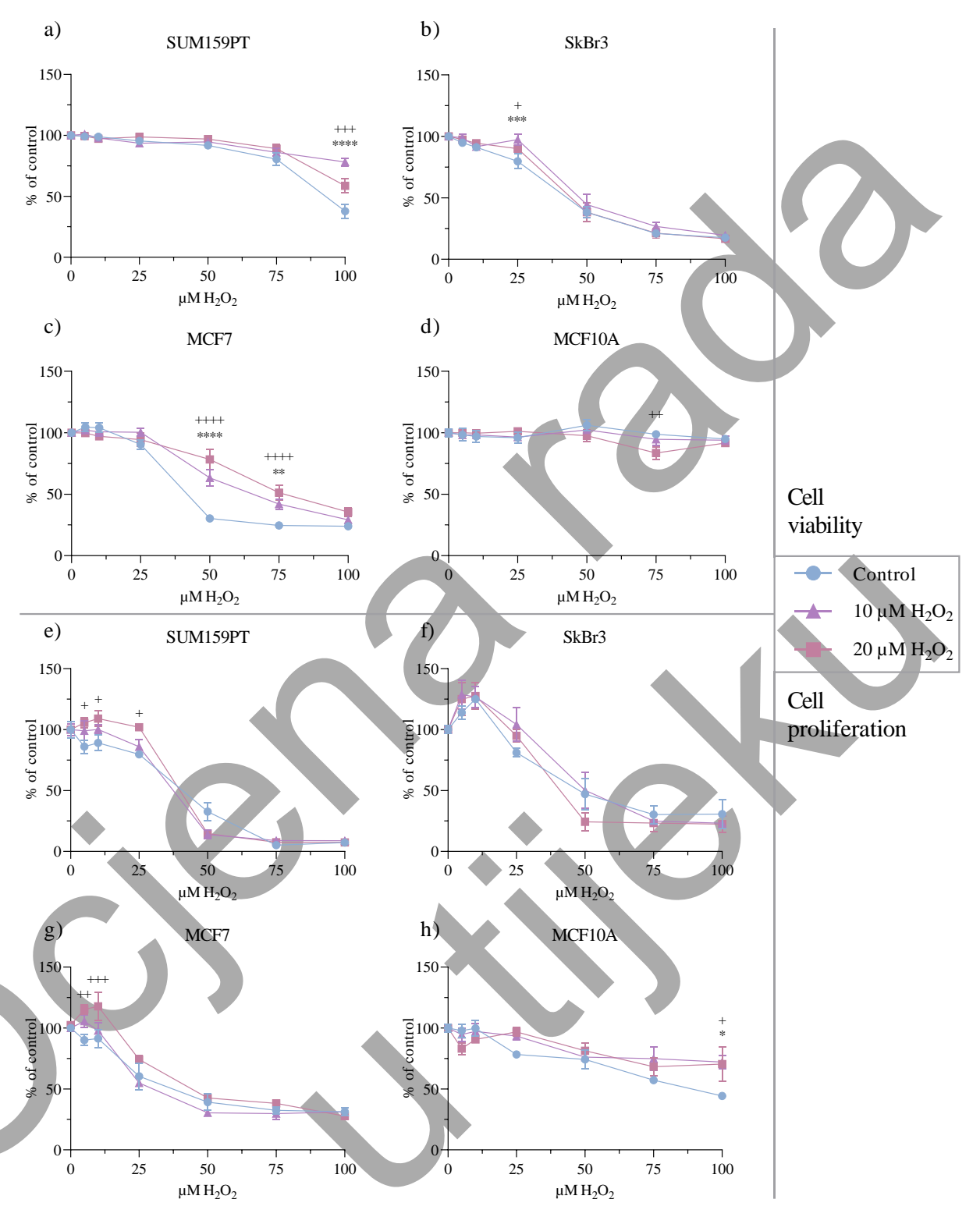


Figure 10. Effect of prolonged exposure to hydrogen peroxide on cell viability and proliferation

SUM159PT (a, e), SkBr3 (b, f), MCF7 (c, g), and MCF10A (d, h) cells were treated with 10 or  $20 \,\mu\text{M}$  H<sub>2</sub>O<sub>2</sub> every two days for 14 days, after which they were treated with a range of H<sub>2</sub>O<sub>2</sub> concentrations. Cell viability was assessed by EZ4U assay (a-d) and cell proliferation by BrdU incorporation (e-h) 24 h post-treatment. Experiments were performed in biological and technical triplicates. Cell viability and proliferation were calculated as the ratio between the treated cells and the untreated control, and are

shown as a percentage of the control. Statistical analysis was performed using two-way ANOVA followed by Sidak's multiple comparisons test. The results are presented as mean  $\pm$  SEM. Significance is indicated as follows: \*/+ p  $\leq$  0.05, \*\*/++ p  $\leq$  0.01, \*\*\*/+++ p  $\leq$  0.001, \*\*\*\*/+++++ p  $\leq$  0.0001. The asterisk (\*) indicates the p-value for the 10  $\mu$ M-treated cells compared to the control, and the plus (+) indicates the p-value for the 20  $\mu$ M H<sub>2</sub>O<sub>2</sub>-treated cells compared to the control.

### 3.1.2. Cell Migration

To investigate whether prolonged oxidative stress affected cell migration, a wound-healing assay was performed with the addition of mitomycin C to inhibit proliferation. Prolonged exposure did not significantly affect cell migration in any of the tested cell lines. In SUM159PT and MCF10A cells, wound closure occurred faster compared to the other cell lines, but remained unaffected by either acute or prolonged  $H_2O_2$  treatment (Figure 11a, d). In contrast, SkBr3 cells showed improved migration after acute 20  $\mu$ M  $H_2O_2$  exposure, with significant differences at 24 h (p = 0.0406) and 48 h (p = 0.0110) in untreated cells (Figure 11b). In MCF7 cells, acute treatment with 20  $\mu$ M  $H_2O_2$  enhanced wound closure at 48 h in both untreated (p = 0.0205) and pretreated cells (p ≤ 0.001) (Figure 11c).

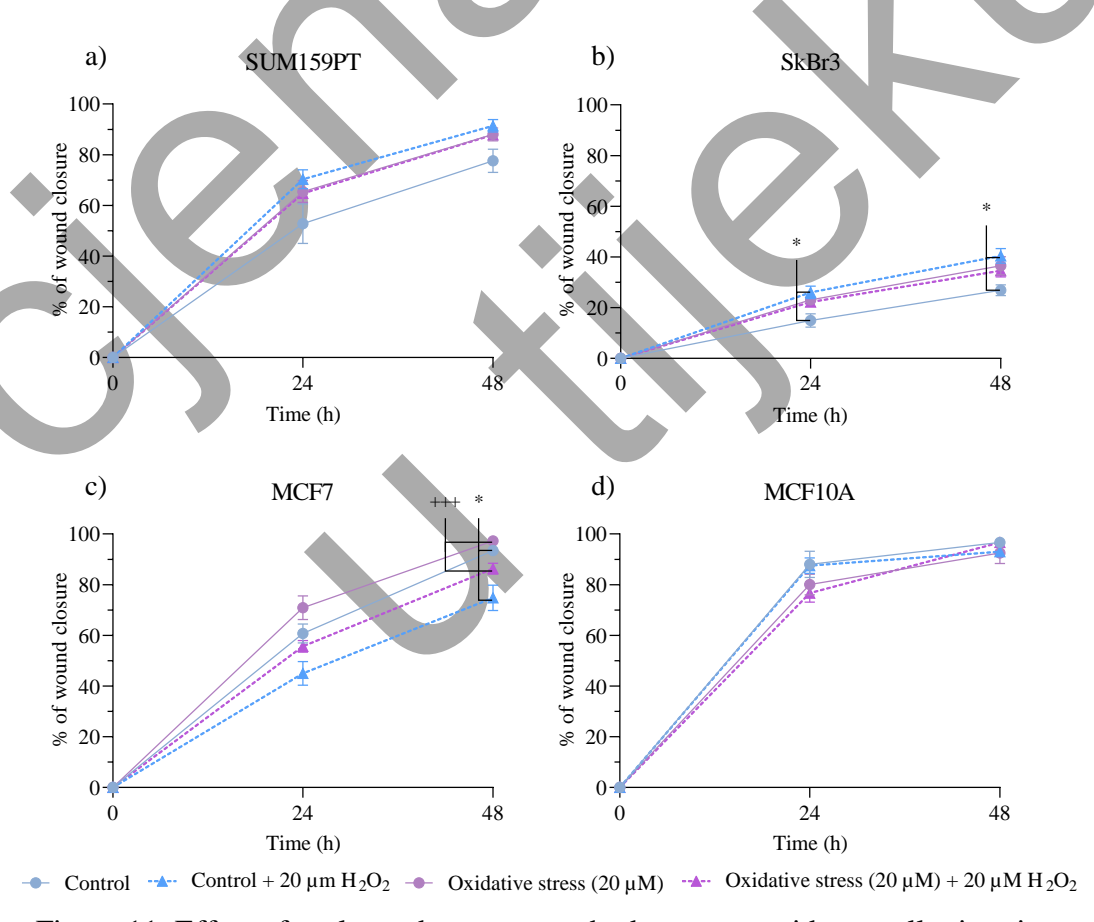


Figure 11. Effect of prolonged exposure to hydrogen peroxide on cell migration

SUM159PT (a), SkBr3 (b), MCF7 (c), and MCF10A (d) cells were treated with 20  $\mu$ M H<sub>2</sub>O<sub>2</sub> every two days for 14 days, after which they were scratched and treated with 20  $\mu$ M H<sub>2</sub>O<sub>2</sub>. Cell migration was observed by photographing the scratch area at 0, 24, and 48 hours. Cell migration was calculated as the reduction in wound area over time, shown as a percentage of the initial wound area. Experiments were performed in biological and technical triplicates, and results are presented as mean  $\pm$  SEM. Statistical analysis was performed using two-way ANOVA followed by Tukey's multiple comparisons test. Significance is indicated as follows: \* p  $\leq$  0.05 compared to untreated control; +++ p  $\leq$  0.001 compared to 20  $\mu$ M H<sub>2</sub>O<sub>2</sub>-treated cells.

## 3.1.3. Fatty Acid Content and LOOH Formation

To determine whether prolonged oxidative stress influenced lipid metabolism, the fatty acid content was determined in cells pretreated with  $20 \,\mu\text{M}\,\text{H}_2\text{O}_2$  for 14 days, and no significant differences were observed (Figure 12). To assess whether prolonged oxidative stress induced lipid peroxidation, LOOH formation was measured. LOOH formation was unaffected by prolonged oxidative stress (Figure 13).

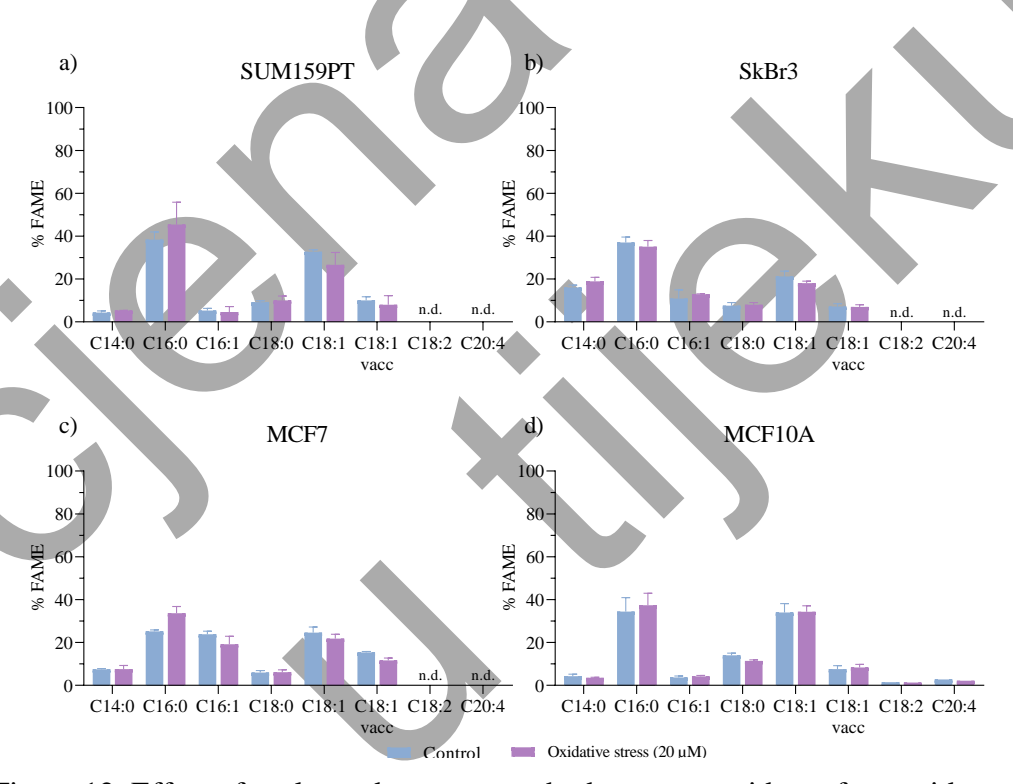


Figure 12. Effect of prolonged exposure to hydrogen peroxide on fatty acid content

SUM159PT (a), SkBr3 (b), MCF7 (c), and MCF10A (d) cells were treated with 20  $\mu$ M H<sub>2</sub>O<sub>2</sub> every two days for 14 days, after which they were collected for the analysis of fatty acid content. Experiments were performed in biological and technical triplicates, and results are presented as mean  $\pm$  SEM. Statistical analysis was performed using two-way ANOVA followed by Sidak's multiple comparisons test. Significance is indicated as follows: \*/+ p  $\leq$  0.05, +++ p  $\leq$  0.01, +++ p  $\leq$  0.001.

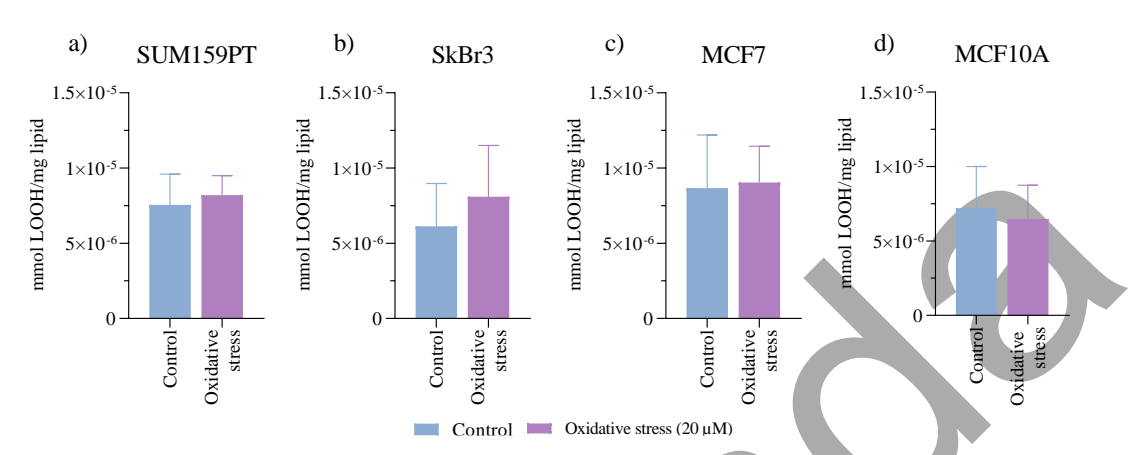


Figure 13. Effect of prolonged exposure to hydrogen peroxide on LOOH formation

SUM159PT (a), SkBr3 (b), MCF7 (c), and MCF10A (d) cells were treated with 20  $\mu$ M H<sub>2</sub>O<sub>2</sub> for 14 days, after which they were collected for the analysis of lipid hydroperoxide formation. Experiments were performed in biological and technical triplicates, and results are presented as mean  $\pm$  SEM. Statistical analysis was performed using an unpaired two-tailed Student's t-test. A p-value  $\leq$  0.05 was considered statistically significant.

### 3.1.4. Protein Expression and Localization

The effect of prolonged exposure to oxidative stress on the protein expression was evaluated by Western blotting after 14 days of treatment with  $20 \,\mu M \, H_2O_2$ .

In SUM159PT cells, both AQP3 (p = 0.0330) and AQP5 (p = 0.0370) expression increased compared to untreated controls (Figure 14a). In SkBr3 cells, expression was also elevated for AQP3 (p = 0.0053) and AQP5 (p = 0.0343) (Figure 14b). In MCF7 cells, only AQP3 expression was significantly increased (p = 0.0130), while AQP5 levels remained unchanged (Figure 14c). In contrast, the non-tumorigenic MCF10A cells showed decreased expression of AQP3 (p = 0.0015), with no significant change in AQP5 (Figure 14d).

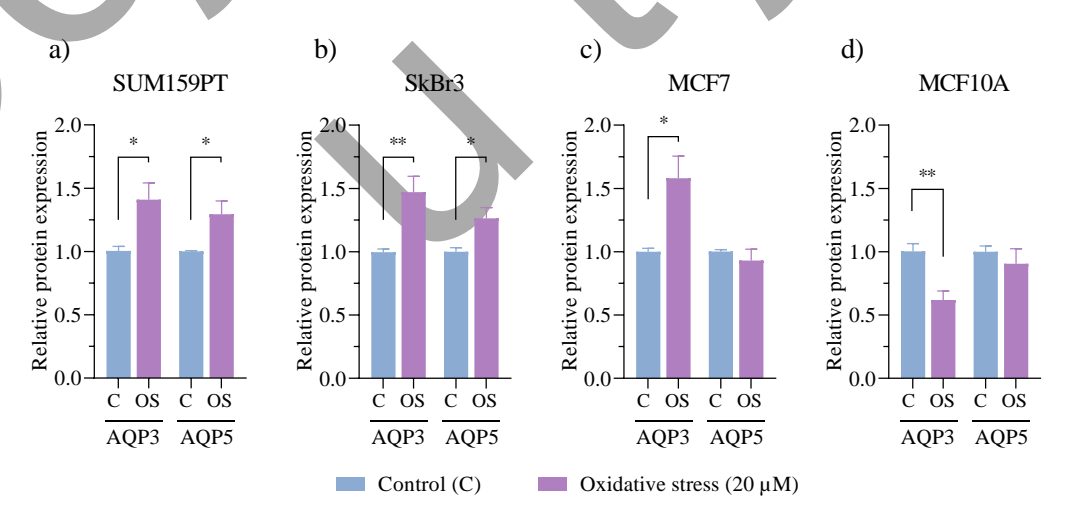


Figure 14. Effect of prolonged exposure to hydrogen peroxide on AQP3 and AQP5 protein expression

SUM159PT (a), SkBr3 (b), MCF7 (c), and MCF10A (d) cells were treated with 20  $\mu$ M H<sub>2</sub>O<sub>2</sub> every two days for 14 days, after which the proteins were harvested and assayed by Western blot for AQP3 and AQP5 protein expression. Experiments were performed in biological and technical triplicates. The protein level is shown as a relative value compared to the untreated control, and results are presented as mean  $\pm$  SEM. Statistical analysis was performed using an unpaired two-tailed Student's t-test. Significance is indicated as follows: \* p  $\leq$  0.05 and \*\* p  $\leq$  0.01.

To further assess the effect of prolonged oxidative stress on therapy resistance, the expression of the ATP-binding cassette transporters ABCB1 and ABCG2 was examined. In SkBr3 cells, both ABCB1 (p = 0.0281) and ABCG2 (p = 0.0450) were significantly reduced compared to untreated controls (Figure 15b), while no significant differences were observed in SUM159PT, MCF7, or MCF10A cells.

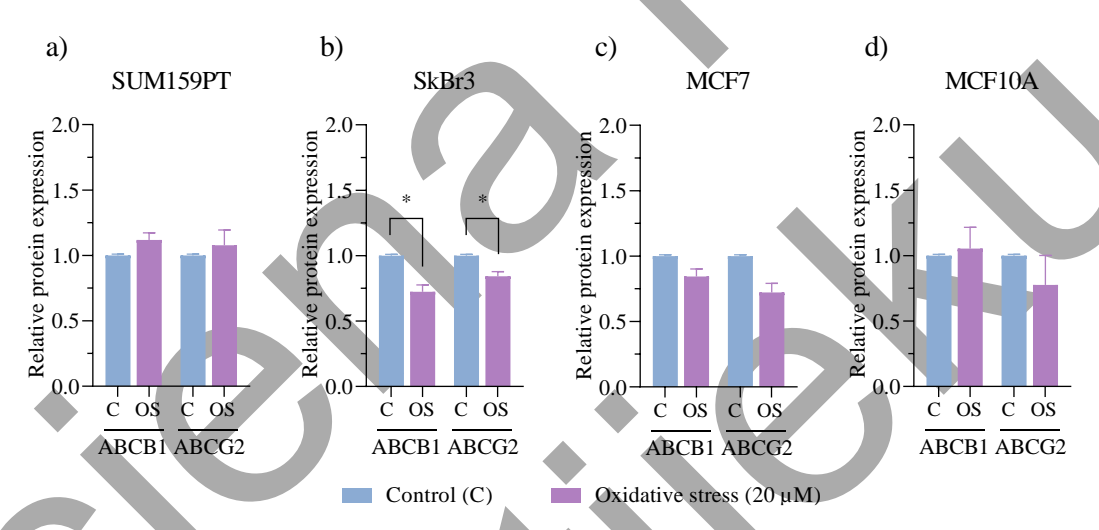


Figure 15. Effect of prolonged exposure to hydrogen peroxide on drug efflux transporters ABCB1 and ABCG2 protein expression

SUM159PT (a), SkBr3 (b), MCF7 (c), and MCF10A (d) cells were treated with 20  $\mu$ M H<sub>2</sub>O<sub>2</sub> every two days for 14 days, after which the proteins were harvested and assayed by Western blot for ABCB1 and ABCG2 protein expression. Experiments were performed in biological and technical triplicates. The protein level is shown as a relative value compared to the untreated control, and results are presented as mean  $\pm$  SEM. Statistical analysis was performed using an unpaired two-tailed Student's t-test. Significance is indicated as follows: \* p  $\leq$  0.05.

Oxidative stress can impact different signaling pathways, and the PI3K/Akt/mTOR pathway is a possible regulator of aquaporin expression. Therefore, the involvement of the PI3K/Akt/mTOR signaling pathway was investigated. Prolonged treatment with 20  $\mu$ M H<sub>2</sub>O<sub>2</sub> did not affect the expression of PI3K, PTEN, or Akt activity, expressed as the pAkt/Akt ratio. Similarly, no significant differences were detected in the expression of mTORC1 and mTORC2

subunits (Raptor and Rictor, respectively) or in phosphorylated mTOR. The only significant change observed was in SkBr3 cells, where Ras expression was increased (p = 0.0431) (Figure 16b).

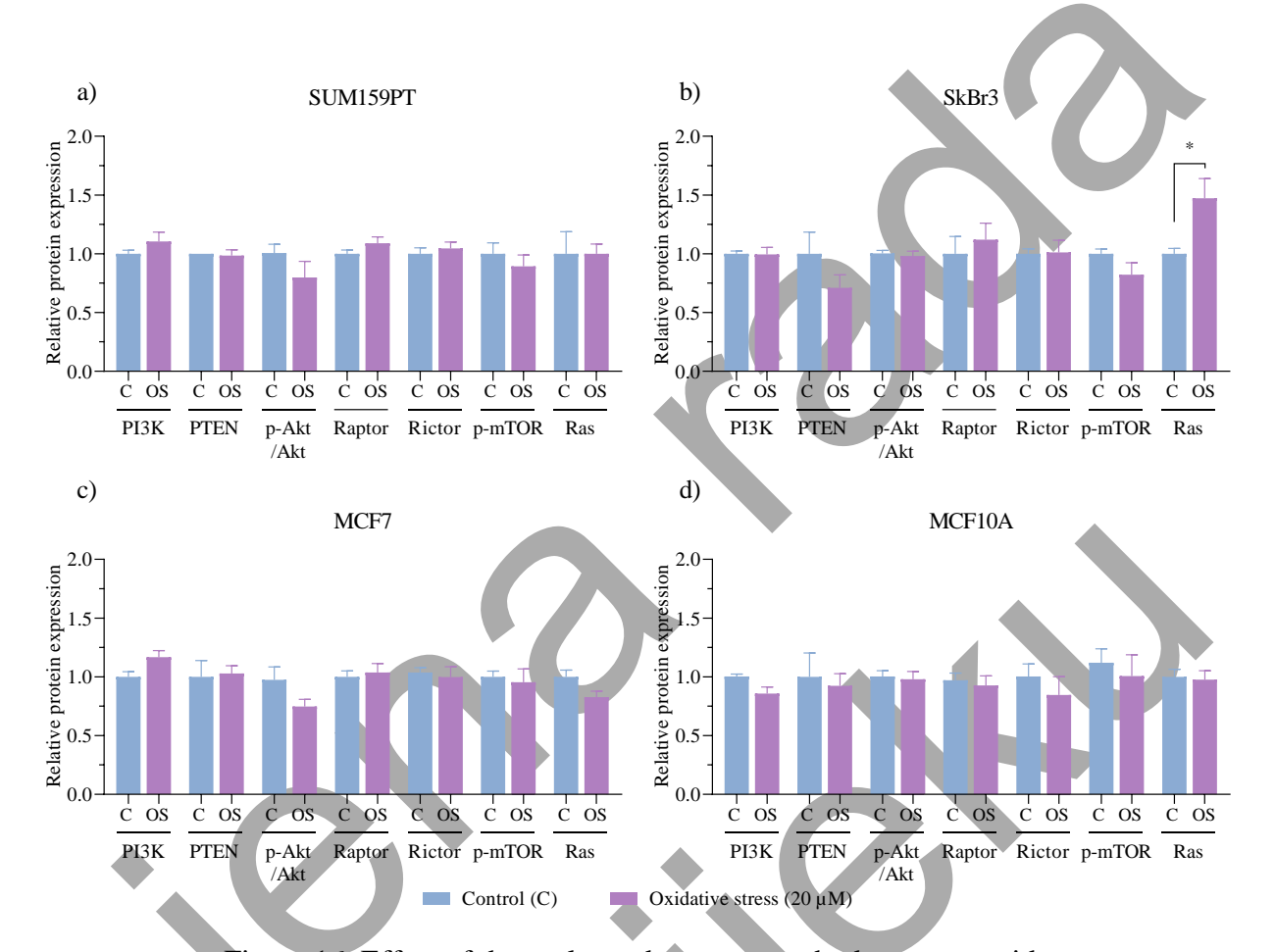


Figure 16. Effect of the prolonged exposure to hydrogen peroxide on the protein expression of members of the PI3K/Akt signaling pathway

SUM159PT (a), SkBr3 (b), MCF7 (c), and MCF10A (d) cells were treated with 20  $\mu$ M H<sub>2</sub>O<sub>2</sub> every two days for 14 days, after which the proteins were harvested and assayed by Western blot for PI3K, PTEN, pAkt, Akt, Raptor, Rictor, p-mTOR, and Ras protein expression. The protein level is shown as a relative value compared to the untreated control, and pAkt/Akt is shown as a ratio. Experiments were performed in biological and technical triplicates, and results are presented as mean  $\pm$  SEM. Statistical analysis was performed using an unpaired two-tailed Student's t-test. Significance is indicated as follows: \* p  $\leq$  0.05.

In addition, the NRF2 signaling pathway was examined under the same prolonged oxidative stress conditions. In SUM159PT cells, NRF2 expression was significantly reduced (p = 0.0489), accompanied by a decrease in its regulator Keap1 (p = 0.0027) (Figure 17a). In SkBr3 cells, Keap1 expression was also reduced (p = 0.0436), while NRF2 remained unchanged (Figure 17b). In contrast, in MCF7 cells, Keap1 levels were increased (p = 0.0359), while NRF2 expression remained unchanged (Figure 17c). In the non-tumorigenic MCF10A cells, neither

NRF2 nor Keap1 expression was affected (Figure 17d). GSK3β, another regulator of NRF2 activity, as well as the NRF2 downstream targets HO-1, NQO1, and AKR1B10, showed no significant differences in any of the tested cell lines.

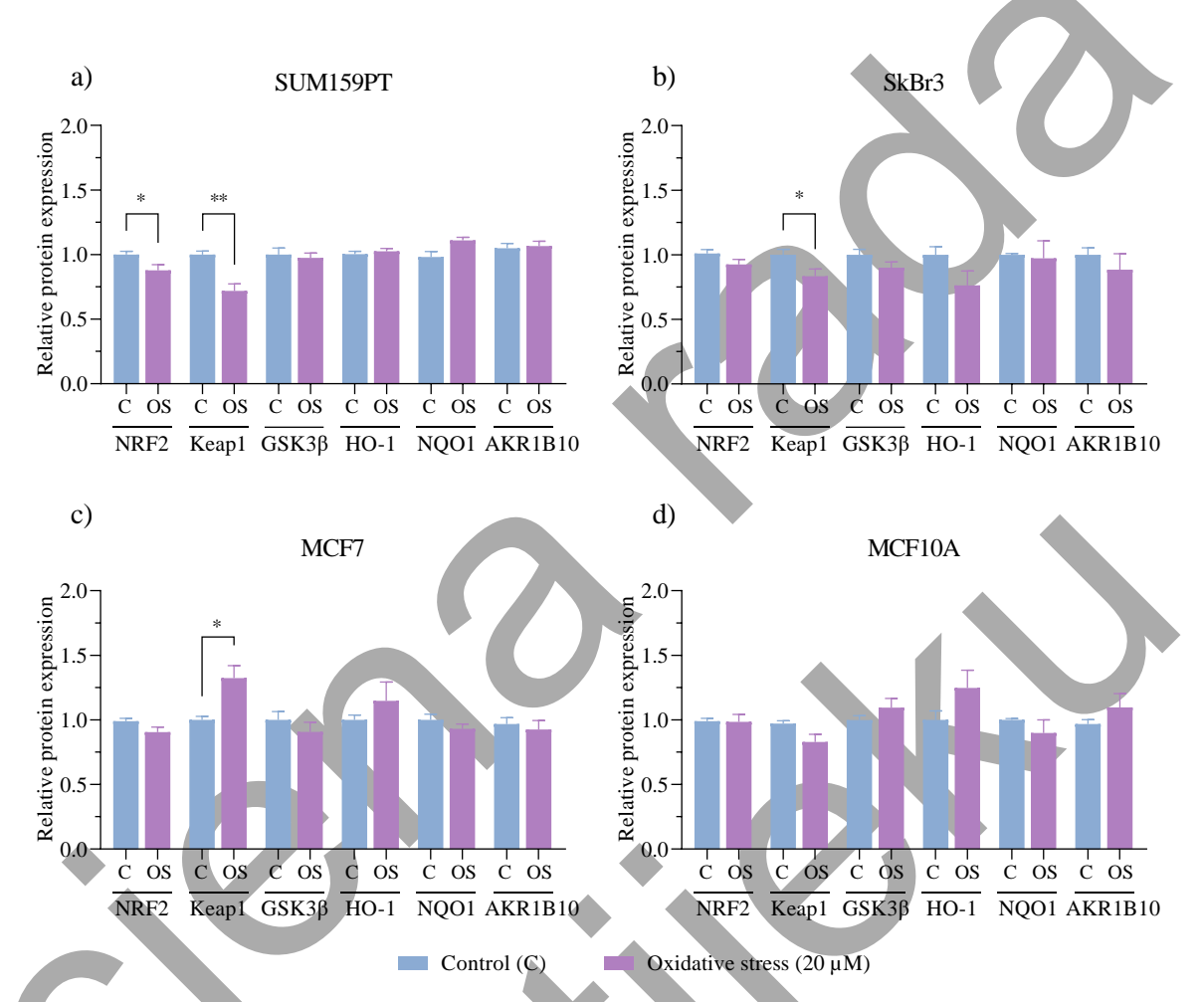


Figure 17. Effect of the prolonged exposure to hydrogen peroxide on the protein expression of members of the NRF2 signaling pathway

SUM159PT (a), SkBr3 (b), MCF7 (c), and MCF10A (d) cells were treated with 20  $\mu$ M H<sub>2</sub>O<sub>2</sub> for 14 days, after which the proteins were harvested and assayed by Western blot for NRF2, Keap1, GSK3 $\beta$ , HO-1, NQO1, and AKR1B10 protein expression. Experiments were performed in biological and technical triplicates. The protein level is shown as a relative value compared to the untreated control, and results are presented as mean  $\pm$  SEM. Statistical analysis was performed using an unpaired two-tailed Student's t-test. Significance is indicated as follows: \* p  $\leq$  0.05 and \*\* p  $\leq$  0.01.

Since whole-cell NRF2 protein levels may not fully reflect its activity due to rapid turnover, NRF2 localization was examined in cytoplasmic and nuclear fractions. In SUM159PT (p = 0.0233), SkBr3 (p = 0.0357), and MCF7 (p = 0.0261) cells, prolonged oxidative stress led to a significant increase in nuclear NRF2 compared to untreated controls (Figure 18). NRF2 localization was unchanged in the non-tumorigenic MCF10A cells. Fractionation quality was

verified using LSD1 as a nuclear marker and  $\beta$ -Actin as a cytoplasmic marker, and representative immunoreactive bands are shown in Figure 19.

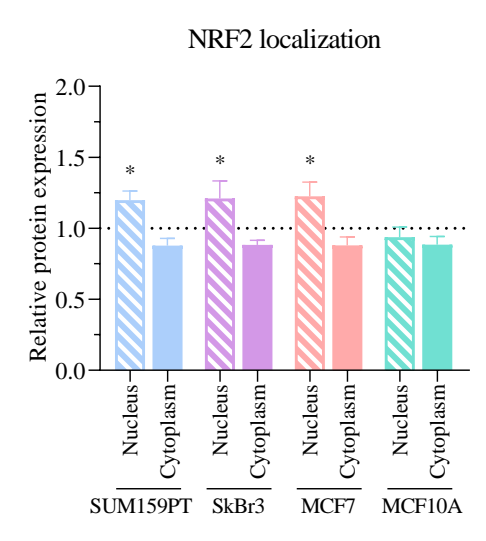


Figure 18. Effect of the prolonged exposure to hydrogen peroxide on the NRF2 protein localization

SUM159PT, SkBr3, MCF7, and MCF10A cells were treated with 20  $\mu$ M H<sub>2</sub>O<sub>2</sub> every two days for 14 days. Cytoplasmic and nuclear fractions were analyzed by Western blot for NRF2 expression. Experiments were performed in biological and technical triplicates. The protein level is shown as a relative value compared to the respective untreated control (marked as a dotted line), and results are presented as mean  $\pm$  SEM. Statistical analysis was performed using one-way ANOVA followed by Dunnett's multiple comparisons test. Significance is indicated as follows: \* p  $\leq$  0.05.

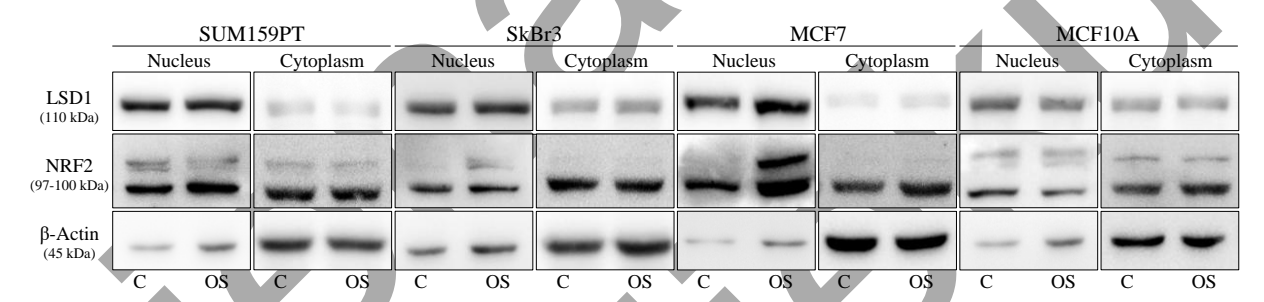


Figure 19. Representative immunoreactive bands for nuclear and cytoplasmic fractions in chronic oxidative stress

Representative immunoreactive bands showing LSD1, NRF2, and  $\beta$ -Actin protein expression in the nuclear and cytoplasmic fraction of SUM159PT, SkBr3, MCF7, and MCF10A cells in control (C) and oxidative stress (OS) conditions. LSD1 was used as a nuclear marker, while  $\beta$ -Actin served as a marker for the cytoplasmic fraction.

Representative immunoreactive bands for all analyzed whole-cell proteins under control and prolonged oxidative stress conditions are shown in Figure 20.

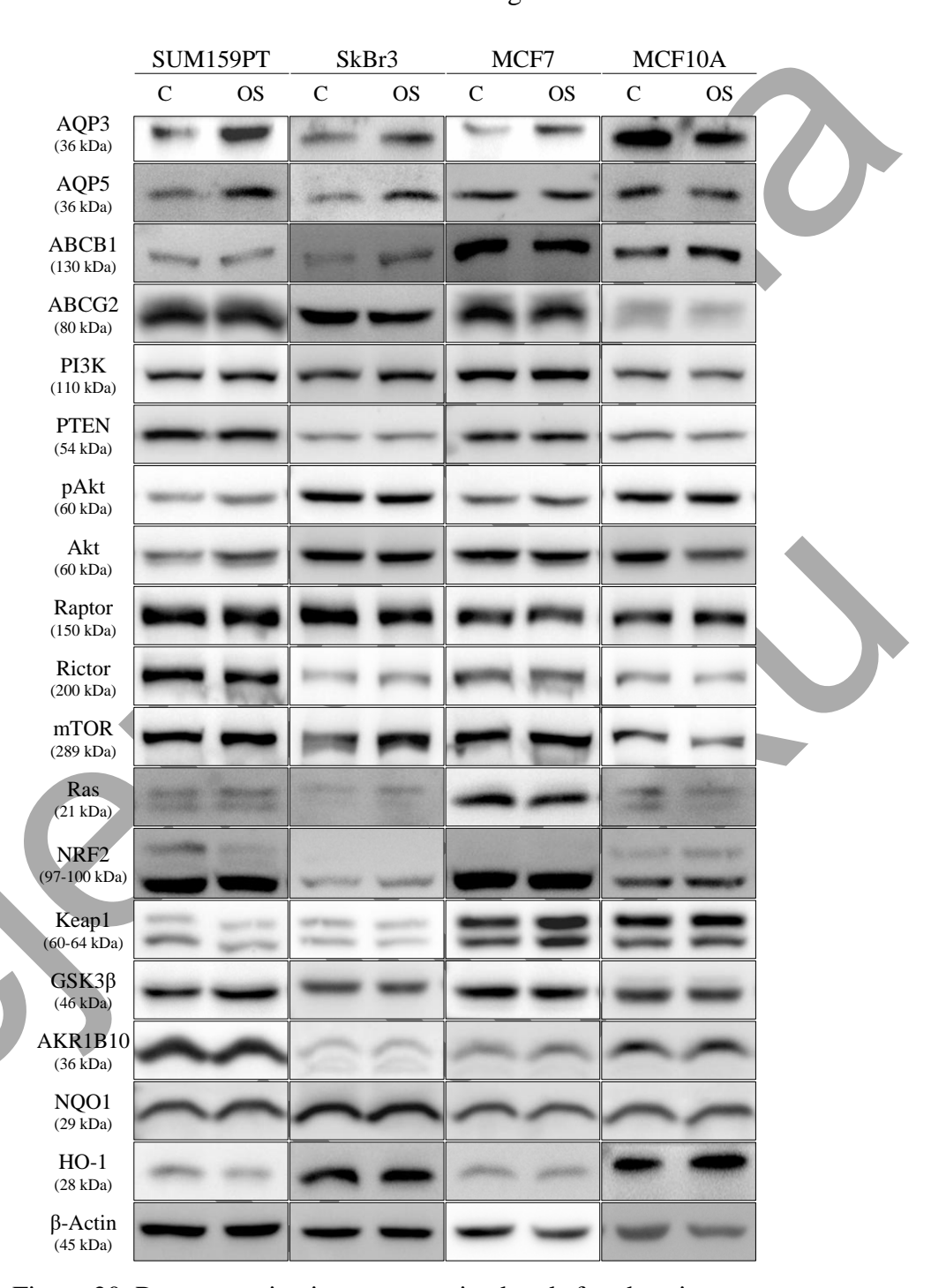


Figure 20. Representative immunoreactive bands for chronic stress

Representative immunoreactive bands showing AQP3, AQP5, ABCB1, ABCG2, PI3K, PTEN, pAkt, Akt, Raptor, Rictor, p-mTOR, Ras, NRF2, Keap1, GSK3 $\beta$ , AKR1B10, NQO1, HO-1, and  $\beta$ -Actin protein expression in SUM159PT, SkBr3, MCF7, and MCF10A cells in control (C) and oxidative stress (OS) conditions.

## 3.1.5. Gene Expression

To assess whether prolonged oxidative stress influenced aquaporin expression at the transcriptional level, peroxiporins AQP1, AQP3, AQP5, AQP9, and AQP11 mRNA levels were analyzed by RT-qPCR after 14 days of treatment with 20  $\mu$ M H<sub>2</sub>O<sub>2</sub>. In SUM159PT cells, expression of both AQP3 (p = 0.0300) and AQP5 (p = 0.0486) was significantly increased, along with an upregulation of AQP11 (p = 0.0410) (Figure 21a). In SkBr3 cells, AQP3 (p = 0.0061) and AQP5 (p = 0.0441) expression was also elevated (Figure 21b). In MCF7 cells, AQP3 increased (p = 0.0025), while AQP5 expression decreased (p = 0.0114) (Figure 21c). The non-tumorigenic MCF10A cells showed reduced AQP3 expression (p = 0.0131), whereas AQP5 (p  $\leq$  0.001), AQP1 (p = 0.0315), and AQP9 (p = 0.0127) were increased (Figure 21d).

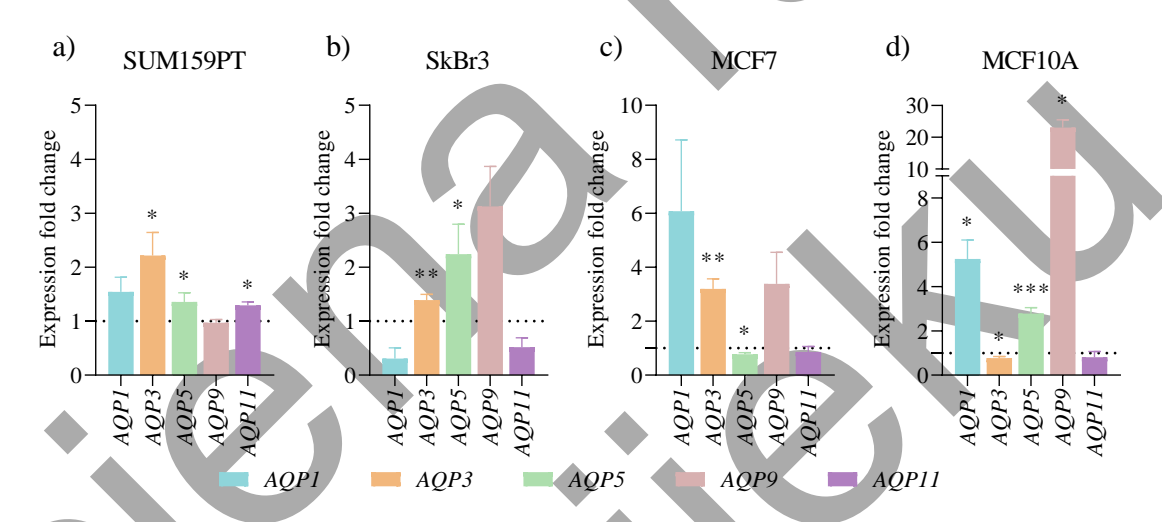


Figure 21. Effect of prolonged exposure to hydrogen peroxide on the aquaporin gene expression

SUM159PT (a), SkBr3 (b), MCF7 (c), and MCF10A (d) cells were treated with 20  $\mu$ M H<sub>2</sub>O<sub>2</sub> every two days for 14 days, after which the total RNA was isolated, transcribed into cDNA, and analyzed by RT-qPCR for AQP1, AQP3, AQP5, AQP9, and AQP11 gene expression. Experiments were performed in biological and technical triplicates. Gene expression was quantified by the 2^(- $\Delta\Delta$ Ct) method, relative to control (dotted line), and is presented as mean  $\pm$  SEM. Statistical analysis was performed using an unpaired two-tailed Student's t-test. Significance is indicated as follows: \* p  $\leq$  0.05, \*\* p  $\leq$  0.01, and \*\*\* p  $\leq$  0.001.

Finally, to determine if prolonged oxidative stress affected NRF2 at the transcriptional level, *NFE2L2* mRNA expression was analyzed by RT-qPCR following 14 days of treatment with 20  $\mu$ M H<sub>2</sub>O<sub>2</sub>. A significant decrease was observed only in SkBr3 cells (p  $\leq$  0.001), while no changes were detected in SUM159PT, MCF7, or MCF10A cells (Figure 22).

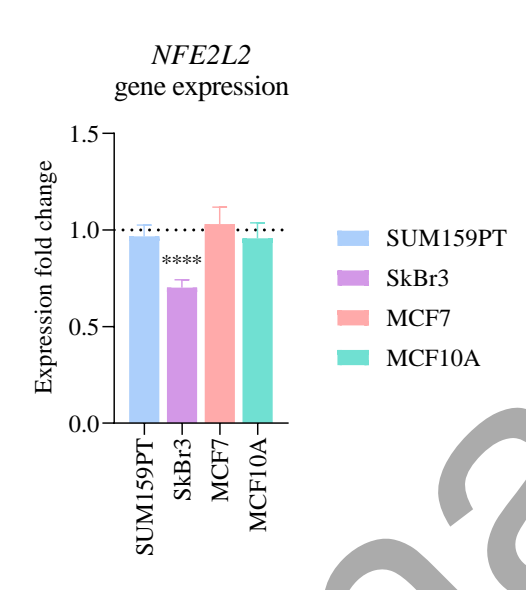


Figure 22. Effect of the prolonged exposure to hydrogen peroxide on *NFE2L2* gene expression

SUM159PT (a), SkBr3 (b), MCF7 (c), and MCF10A (d) cells were treated with 20  $\mu$ M H<sub>2</sub>O<sub>2</sub> every two days for 14 days, after which the total RNA was isolated, transcribed into cDNA, and analyzed by RT-qPCR for *NFE2L2* gene expression. Experiments were performed in biological and technical triplicates. Gene expression was quantified by the 2^(- $\Delta\Delta$ Ct) method, relative to control (dotted line), and is presented as mean  $\pm$  SEM. Statistical analysis was performed using an unpaired two-tailed Student's t-test. Significance is indicated as follows: \*\*\* p  $\leq$  0.001.

## 3.2. Effect of NRF2 Modulation

Since prolonged oxidative stress resulted in increased aquaporin expression along with enhanced NRF2 nuclear localization, indicating its activation, we examined whether NRF2 modulation influences aquaporin regulation.

### 3.2.1. Cell Viability

The effect of NRF2 pharmacological modulation was assessed after determining the non-toxic concentration using the cell viability assay. The NRF2 activator sulforaphane and the inhibitor ML385 were tested across concentrations ranging from 0 to 10  $\mu$ M for 24 h. In SUM159PT cells, sulforaphane significantly reduced viability at 7.5 and 10  $\mu$ M (both p  $\leq$  0.0001), while ML385 had no significant effect (Figure 23a). In SkBr3 cells, both sulforaphane and ML385 decreased cell viability at 5 (p = 0.0115, p = 0.0223), 7.5 (p  $\leq$  0.0001, p = 0.0209), and 10  $\mu$ M (p  $\leq$  0.0001, p = 0.0042) (Figure 23b). In MCF7 cells, sulforaphane significantly decreased viability at 7.5 and 10  $\mu$ M (both p  $\leq$  0.0001), while it increased viability at 1  $\mu$ M (p = 0.021)

(Figure 23c). In the non-tumorigenic MCF10A cells, sulforaphane reduced viability at 7.5 and  $10~\mu M$  (p = 0.0025, p  $\leq$  0.0001) (Figure 23d). Based on these results, 2.5  $\mu M$  sulforaphane was selected as the highest concentration that did not affect viability in any of the cell lines, while ML385 was used at 10  $\mu M$  to ensure sufficient NRF2 inhibition, despite its effect on viability in SkBr3 cells.

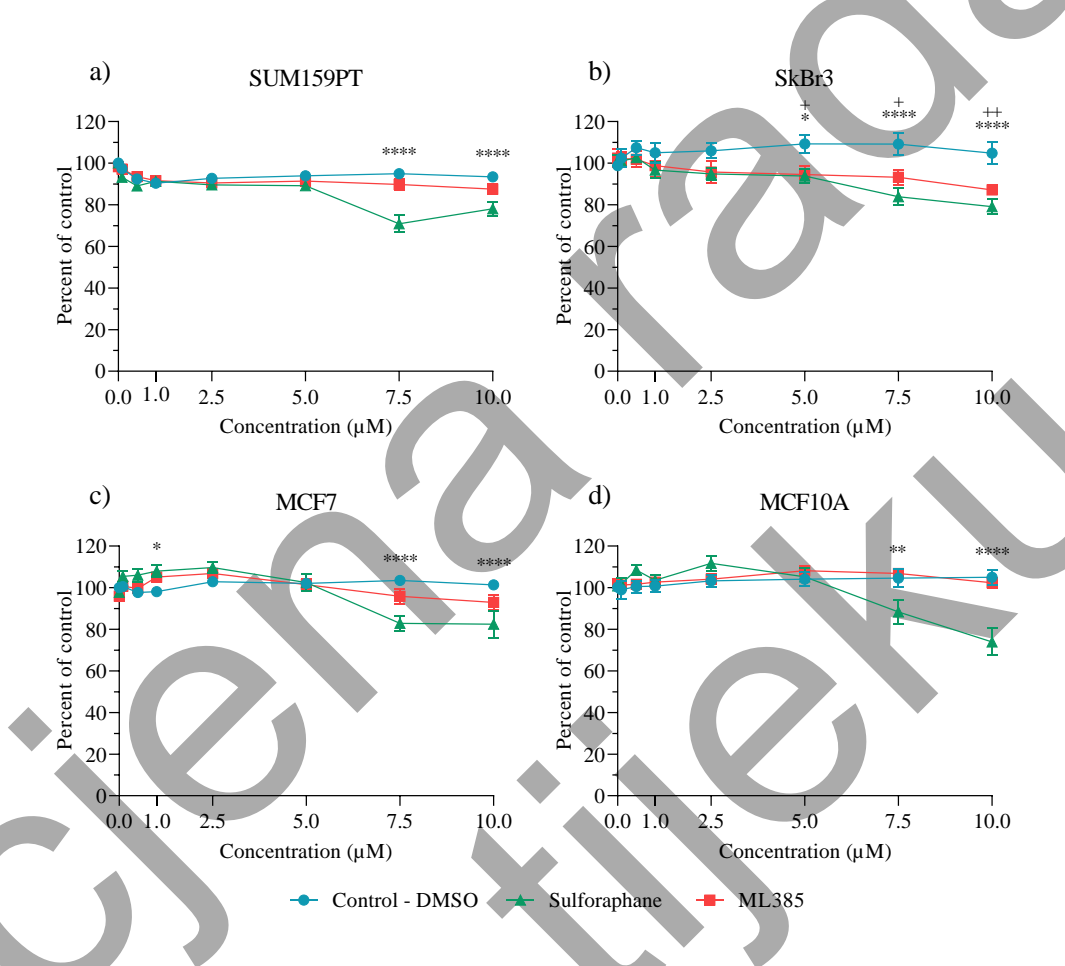


Figure 23. Effect of sulforaphane and ML385 on cell viability

SUM159PT (a), SkBr3 (b), MCF7 (c), and MCF10A (d) cells were treated with increasing concentrations (0-10  $\mu$ M) of sulforaphane or ML385 for 24 h, and cell viability was assessed by EZ4U assay 24 h post-treatment. Experiments were performed in biological and technical triplicates. Cell viability was calculated as the ratio of treated cells to untreated control cells and is expressed as a percentage of the control. The results are presented as mean  $\pm$  SEM. Statistical analysis was performed using two-way ANOVA followed by Tukey's multiple comparisons test. Significance is indicated as follows: \*/+ p  $\leq$  0.05, \*\*/++ p  $\leq$  0.01, \*\*\*\* p  $\leq$  0.0001. The asterisk (\*) indicates the p-value for the cells treated with sulforaphane, and the plus (+) indicates the p-value for the cells treated with ML385, compared to the control.

#### 3.2.2. Protein Expression and Localization

The success of NRF2 modulation was evaluated by measuring NRF2 protein levels, the expression of its regulator Keap1, and a downstream target HO-1 6 and 24 h post-treatment, and by confirming its nuclear translocation 2 h post-treatment. Once successful modulation was confirmed, AQP3 and AQP5 expression were analyzed.

In SUM159PT cells, sulforaphane increased NRF2 expression after 6 and 24 h (p = 0.0143, p = 0.0016), which was accompanied by an increase in Keap1 expression at 24 h (p  $\leq$  0.001) and HO-1 expression after 24 h (p  $\leq$  0.001), while ML385 did not significantly affect NRF2 expression or activity (Figure 24a). Since HO-1 is a downstream target of NRF2, its upregulation indicates NRF2 activity. This was further confirmed by increased NRF2 nuclear translocation observed 2 h after sulforaphane treatment (p  $\leq$  0.001) (Figure 24b). Following successful NRF2 activation, AQP3 and AQP5 protein expression were evaluated. AQP3 expression increased upon sulforaphane treatment after 6 and 24 h (p = 0.0243, p = 0.0235), while AQP5 expression remained unchanged (Figure 24c).

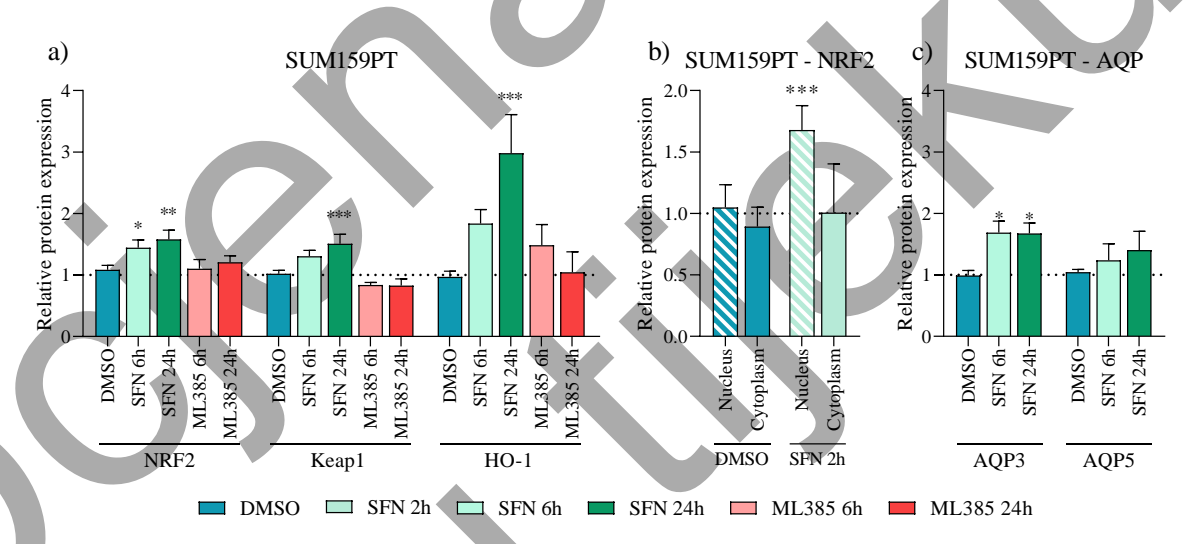


Figure 24. Effect of sulforaphane and ML385 on protein expression in SUM159PT cells

SUM159PT cells were treated with 2.5  $\mu$ M sulforaphane (SFN) or 10  $\mu$ M ML385 for 6 h and 24 h, and NRF2, Keap1, and HO-1 expression was analyzed (a). NRF2 nuclear translocation was assessed 2 h after treatment (b), and AQP3/AQP5 expression following successful NRF2 modulation (c). Experiments were performed in biological and technical triplicates. Protein levels are shown relative to the untreated control (indicated by a dotted line) and presented as mean  $\pm$  SEM. Statistical analysis was performed using one-way ANOVA (a, c) or two-way ANOVA (b) with Dunnett's multiple comparisons test. Significance is indicated as follows: \* p \le 0.05, \*\* p \le 0.01, \*\*\* p \le 0.001.

In the SkBr3 cell line, NRF2 protein expression did not change following sulforaphane or ML385 treatment, but an increase in Keap1 expression was observed 6 h after sulforaphane treatment (p = 0.0077). Even though NRF2 expression remained unchanged, HO-1 expression increased at both 6 and 24 h of sulforaphane treatment (p = 0.0191, p = 0.0021), indicating NRF2 activity (Figure 25a). However, unlike in SUM159PT, this upregulation of HO-1 was not accompanied by a significant increase in NRF2 nuclear translocation (Figure 25b). The effect on aquaporin expression was measured regardless, and although a trend toward higher AQP3 levels was observed, no significant changes were detected, with both AQP3 and AQP5 remaining unchanged (Figure 25c).

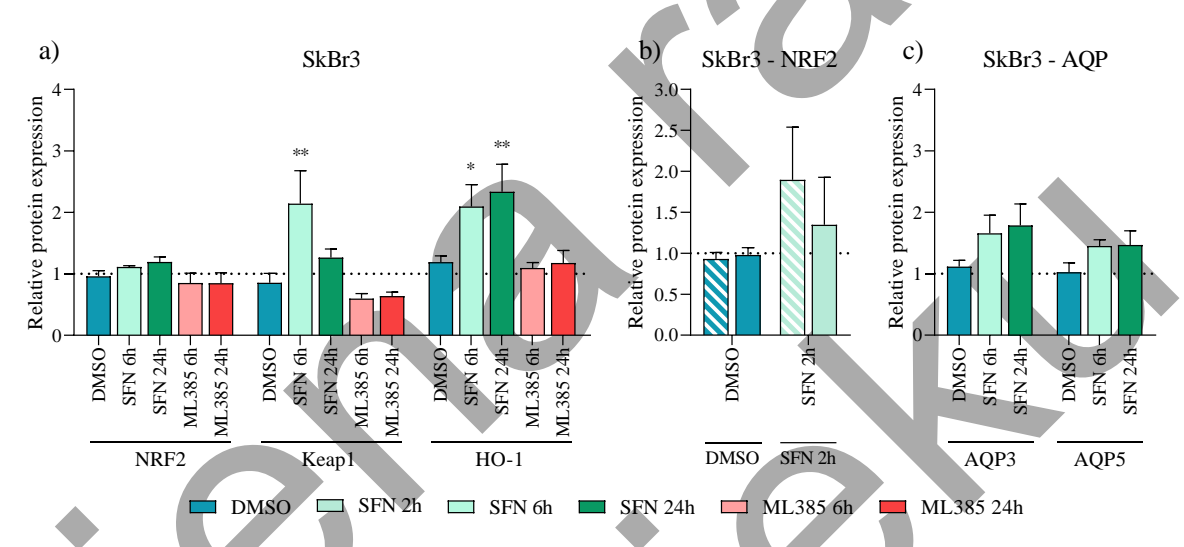


Figure 25. Effect of sulforaphane and ML385 on protein expression in SkBr3 cells

SkBr3 cells were treated with 2.5  $\mu$ M sulforaphane (SFN) or 10  $\mu$ M ML385 for 6 h and 24 h, and NRF2, Keap1, and HO-1 expression was analyzed (a). NRF2 nuclear translocation was assessed 2 h after treatment (b), and AQP3/AQP5 expression following successful NRF2 modulation (c). Experiments were performed in biological and technical triplicates. Protein levels are shown relative to the untreated control (indicated by a dotted line) and presented as mean  $\pm$  SEM. Statistical analysis was performed using one-way ANOVA (a, c) or two-way ANOVA (b) with Dunnett's multiple comparisons test. Significance is indicated as follows: \*p \le 0.05, \*\*p \le 0.01, \*\*\* p \le 0.001.

In the MCF7 cell line, NRF2 protein expression increased after sulforaphane treatment at both 6 and 24 h (p = 0.0018, p = 0.0442), while ML385 did not significantly affect NRF2 levels. HO-1 expression was upregulated after 6 and 24 h of sulforaphane treatment (p = 0.0358, p  $\leq$  0.001), indicating NRF2 activity (Figure 26a). However, as in SkBr3, this was not confirmed by a significant increase in NRF2 nuclear translocation (Figure 26b), and AQP3 and AQP5 expression remained unchanged (Figure 26c). Although ML385 treatment did not successfully inhibit NRF2 activity, it led to a reduction in Keap1 protein levels at both 6 and 24 h (p = 0.0049, p  $\leq$  0.001) (Figure 26a).

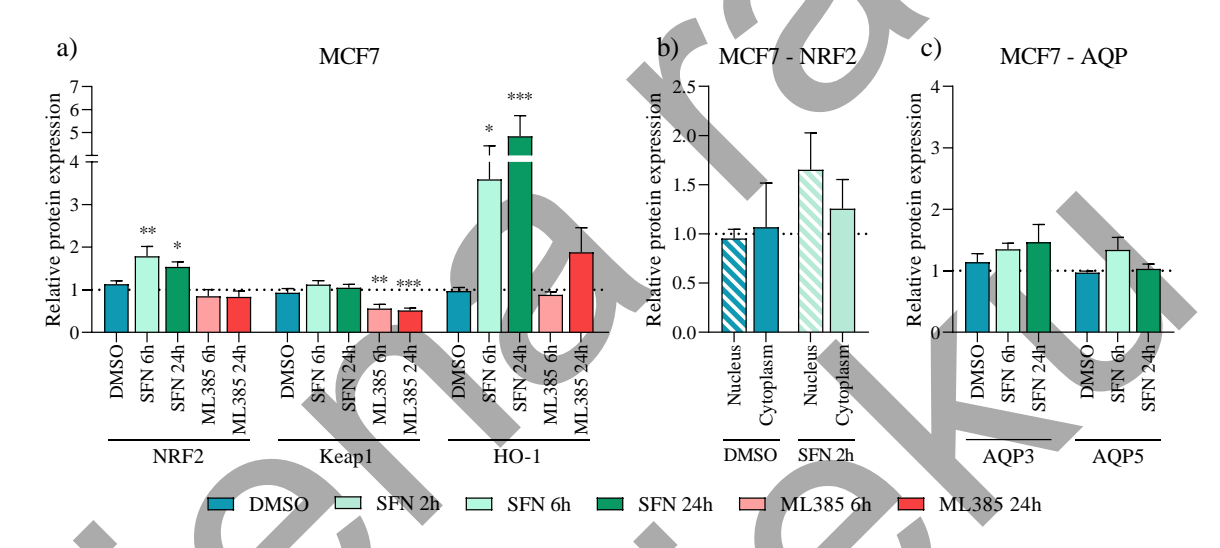


Figure 26. Effect of sulforaphane and ML385 on protein expression in MCF7 cells

MCF7 cells were treated with 2.5  $\mu$ M sulforaphane (SFN) or 10  $\mu$ M ML385 for 6 h and 24 h, and NRF2, Keap1, and HO-1 expression was analyzed (a). NRF2 nuclear translocation was assessed 2 h after treatment (b), and AQP3/AQP5 expression following successful NRF2 modulation (c). Experiments were performed in biological and technical triplicates. Protein levels are shown relative to the untreated control (indicated by a dotted line) and presented as mean  $\pm$  SEM. Statistical analysis was performed using one-way ANOVA (a, c) or two-way ANOVA (b) with Dunnett's multiple comparisons test. Significance is indicated as follows: \*p \le 0.05, \*\*p \le 0.01, \*\*\* p \le 0.001.

In the non-tumorigenic MCF10A cell line, NRF2 protein expression increased after 24 h of sulforaphane treatment (p = 0.011), accompanied by an upregulation of Keap1 (p = 0.0354) and HO-1 (p = 0.0244), indicating NRF2 activity (Figure 27a). However, nuclear translocation of NRF2 was not significantly altered following sulforaphane treatment (Figure 27b), and both AQP3 and AQP5 expression remained unchanged (Figure 27c).

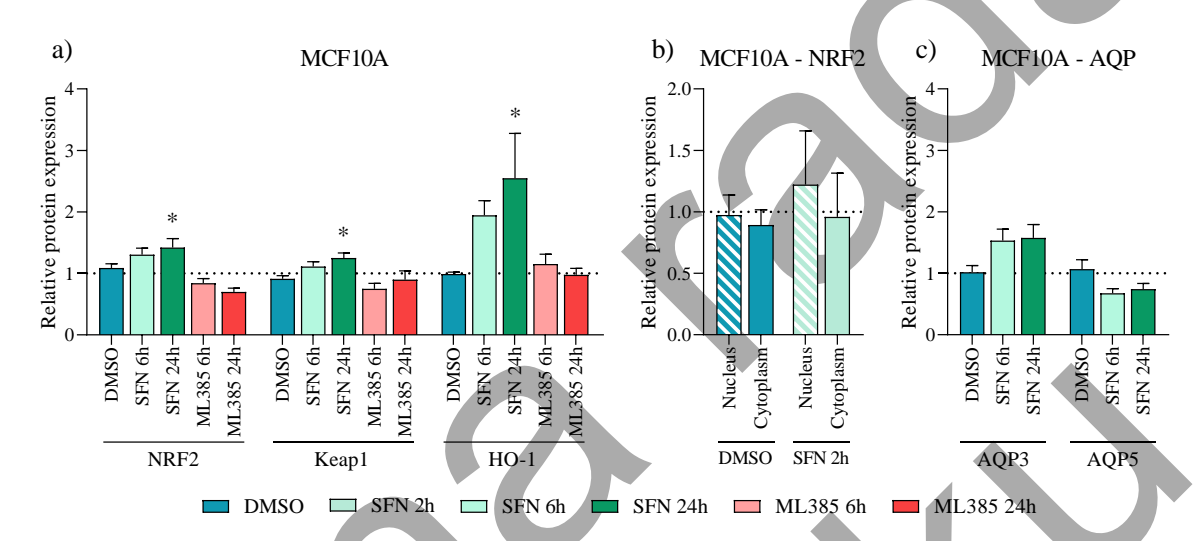


Figure 27. Effect of sulforaphane and ML385 on protein expression in MCF10A cells

MCF10A cells were treated with 2.5  $\mu$ M sulforaphane (SFN) or 10  $\mu$ M ML385 for 6 h and 24 h, and NRF2, Keap1, and HO-1 expression was analyzed (a). NRF2 nuclear translocation was assessed 2 h after treatment (b), and AQP3/AQP5 expression following successful NRF2 modulation (c). Experiments were performed in biological and technical triplicates. Protein levels are shown relative to the untreated control (indicated by a dotted line) and presented as mean  $\pm$  SEM. Statistical analysis was performed using one-way ANOVA (a, c) or two-way ANOVA (b) with Dunnett's multiple comparisons test. Significance is indicated as follows: \* p  $\leq$  0.05, \*\* p  $\leq$  0.01, \*\*\* p  $\leq$  0.001.

Sulforaphane treatment successfully activated NRF2 in all tested cell lines, but this did not lead to aquaporin upregulation in all of them. In contrast, ML385 did not achieve effective NRF2 inhibition.

Representative immunoreactive bands for total protein expression of NRF2, Keap1, HO-1, and  $\beta$ -Actin, which was used as a housekeeping protein, are shown in Figure 28.

Nuclear and cytoplasmic fractions of NRF2, with LSD1 and GAPDH serving as nuclear and cytoplasmic markers, respectively, are presented in Figure 29.

Representative bands for total protein expression of AQP3 and AQP5, together with  $\beta$ -Actin as a housekeeping protein, are shown in Figure 30.

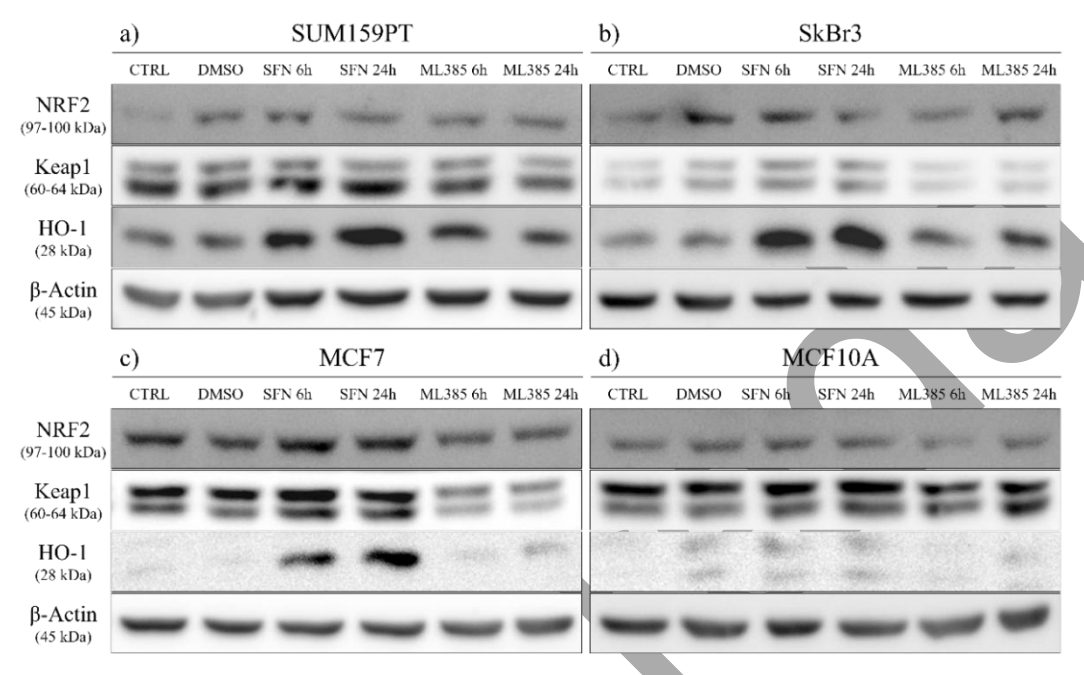


Figure 28. Representative immunoreactive bands after modulation of NRF2 activity

Representative immunoreactive bands showing NRF2, Keap1, HO-1, and  $\beta$ -Actin protein expression in SUM159PT (a), SkBr3 (b), MCF7 (c), and MCF10A (d) cells in control (CTRL), DMSO vehicle control, 2.5  $\mu$ M sulforaphane (SFN), or 10  $\mu$ M ML385 treatment for 6 h or 24 h.

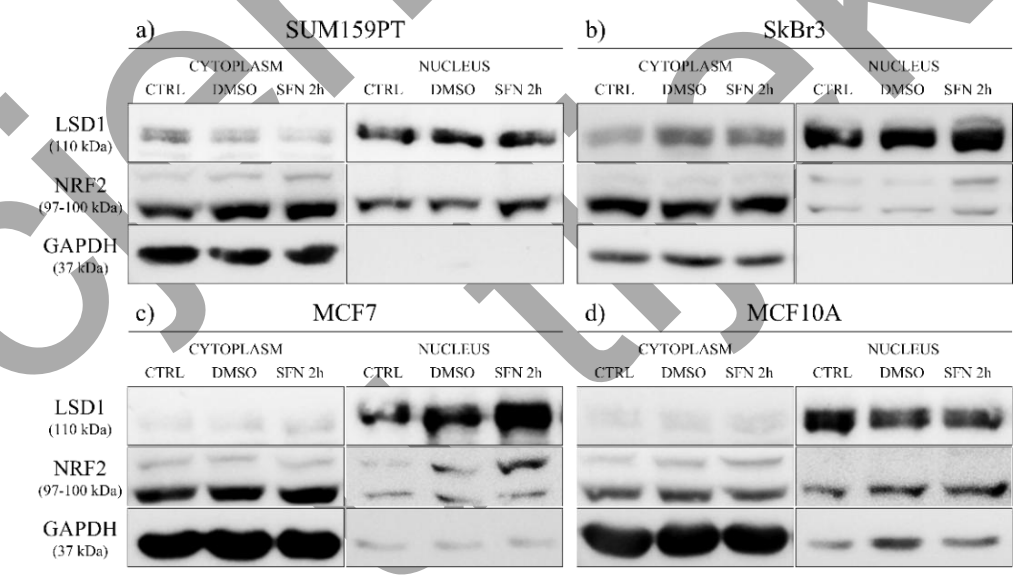


Figure 29. Representative immunoreactive bands of nuclear and cytoplasmic fractions after modulation of NRF2 activity

Representative immunoreactive bands showing LSD1, NRF2, and GAPDH protein expression in the nuclear and cytoplasmic fraction of SUM159PT (a), SkBr3 (b), MCF7 (c), and MCF10A (d) cells in control (CTRL), DMSO vehicle control, and  $2.5\,\mu\text{M}$  sulforaphane (SFN) treatment for 2 h. LSD1 was used as a nuclear marker, while GAPDH served as a marker for the cytoplasmic fraction.

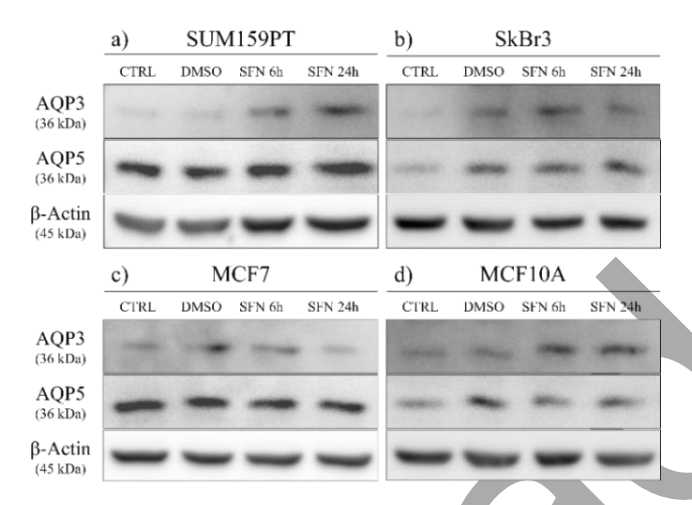


Figure 30. Representative immunoreactive bands of aquaporins after activation of NRF2

Representative immunoreactive bands showing AQP3, AQP5, and  $\beta$ -Actin protein expression in SUM159PT (a), SkBr3 (b), MCF7 (c), and MCF10A (d) cells in control (CTRL), DMSO vehicle control, 2.5  $\mu$ M sulforaphane (SFN) treatment for 6 h or 24 h.

Since pharmacological modulation of NRF2 activity achieved its successful activation but showed limitations in inhibition, we applied a genetic approach to further investigate its effect on aquaporin regulation. NRF2 was either silenced or stably overexpressed in breast cancer and non-tumorigenic breast epithelial cells. Stable overexpression was achieved through antibiotic selection and considered successful when non-transfected control cells did not survive the treatment, while transfected cells remained viable and were used for subsequent experiments. MCF10A cells, however, could not be successfully stably transfected and were excluded from this part of the analysis. To verify the efficiency of genetic modulation, NRF2 and its downstream target HO-1 were analyzed at the protein level. However, neither siRNA-mediated silencing nor stable overexpression resulted in consistent or significant changes in NRF2 or HO-1 expression across the tested cell lines, indicating that genetic modulation of NRF2 was not successful (Figure 31a, b). Representative immunoreactive bands for NRF2, HO-1, and  $\beta$ -Actin protein expression following NRF2 silencing and overexpression are shown in Figure 32. Since NRF2 modulation could not be reliably achieved at the genetic level, further analysis of aquaporins was not performed.

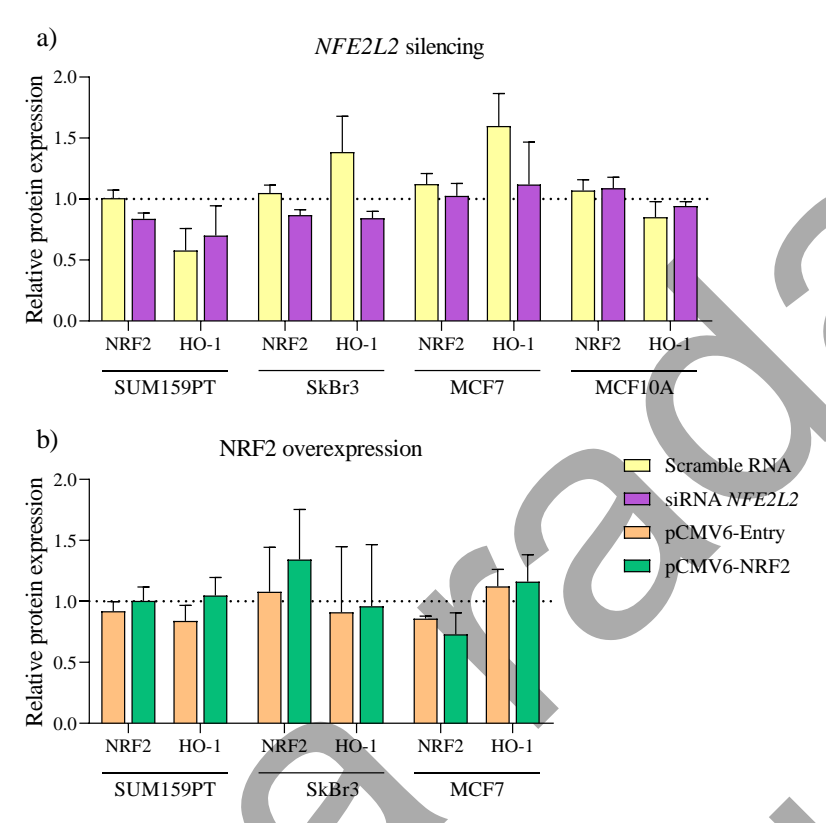


Figure 31. Effect of NRF2 silencing and overexpression on protein expression

SUM159PT, SkBr3, MCF7, and MCF10A cells were transiently transfected with *NFE2L2* siRNA (a), and stably with pCMV6-NRF2 (b), using scramble RNA and pCMV6-Entry as controls. Total proteins were analyzed for NRF2 and HO-1 expression. Experiments were performed in biological and technical triplicates. Protein levels are shown relative to the untreated control (indicated by a dotted line) and presented as mean  $\pm$  SEM. Statistical analysis was performed using two-way ANOVA with Dunnett's multiple comparisons test. A p-value  $\leq$  0.05 was considered statistically significant.

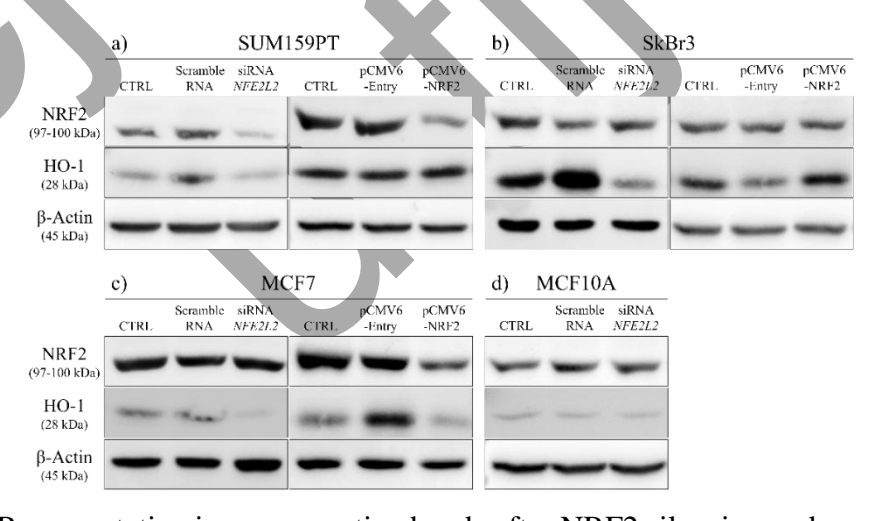


Figure 32. Representative immunoreactive bands after NRF2 silencing and overexpression

Representative immunoreactive bands showing NRF2, HO-1, and  $\beta$ -Actin protein expression in SUM159PT (a), SkBr3 (b), MCF7 (c), and MCF10A (d) cells in control (CTRL) condition, in cells transfected with scramble RNA or siRNA-*NFE2L2*, and with pCMV6-Entry or pCMV6-NRF2.

## 3.2.3. Gene Expression

Since sulforaphane treatment successfully activated NRF2, its effect on peroxiporin gene expression was evaluated. In SUM159PT cells, 24 h of sulforaphane treatment resulted in a significant decrease in AQP3, AQP5, and AQP11 expression (p = 0.0043, p = 0.313, p = 0.0155) (Figure 33a). In SkBr3 cells, sulforaphane treatment for 24 h significantly increased the expression of AQP1, AQP4, and AQP9 (p  $\leq$  0.001, p = 0.0017, p  $\leq$  0.0001), while a shorter exposure of 6 h increased only AQP9 expression (p = 0.016) (Figure 33b). In MCF7 cells, a decrease in AQP11 (p  $\leq$  0.001) expression was observed after 6 h of sulforaphane treatment (Figure 33c). In the non-tumorigenic MCF10A cells, sulforaphane treatment did not lead to significant changes in peroxiporin expression (Figure 33d).

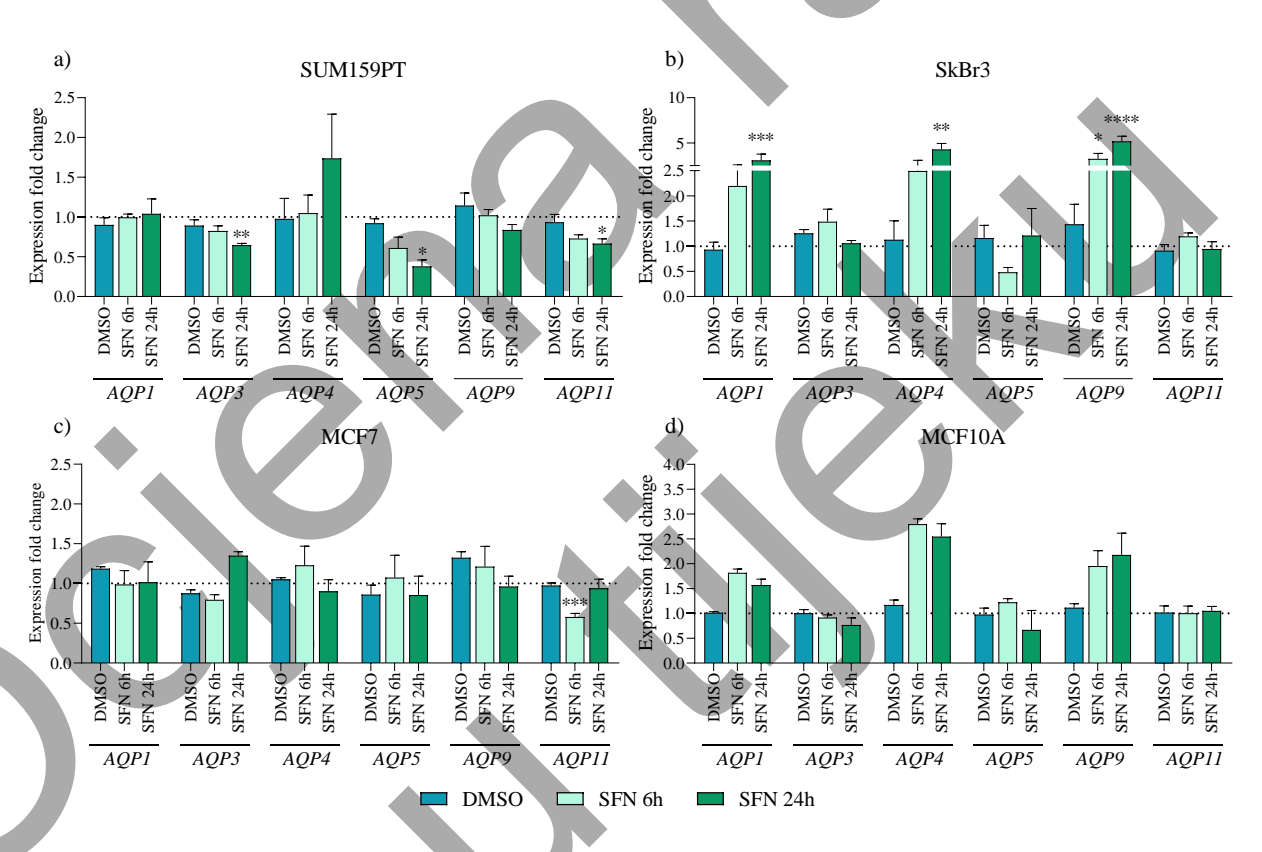


Figure 33. Effect of sulforaphane on peroxiporin gene expression

SUM159PT (a), SkBr3 (b), MCF7 (c), and MCF10A (d) cells were treated with 2.5  $\mu$ M sulforaphane for 6 h and 24 h, after which total RNA was isolated, reverse transcribed into cDNA, and analyzed by RT-qPCR to assess the expression of peroxiporin genes (*AQP1*, *AQP3*, *AQP4*, *AQP5*, *AQP9*, and *AQP11*). Experiments were conducted in biological and technical triplicates. Gene expression was quantified by the 2^(- $\Delta\Delta$ Ct) method, relative to control (dotted line), and is presented as mean  $\pm$  SEM. Statistical analysis was performed using two-way ANOVA with Dunnett's multiple comparisons test. Significance is indicated as follows: \*p  $\leq$  0.05, \*\* p  $\leq$  0.01, \*\*\* p  $\leq$  0.001 and \*\*\*\* p  $\leq$  0.0001.

## 3.2.4. Aquaporin Activity

Since sulforaphane treatment differently affected aquaporin protein and gene expression, its functional consequences on aquaporin activity were evaluated by measuring the rate of  $H_2O_2$  intake using the DCFH-DA fluorescent probe. After 24 h of sulforaphane treatment, SUM159PT and SkBr3 cells showed a significant increase in aquaporin-mediated  $H_2O_2$  transport ( $p \le 0.001$ ,  $p \le 0.0001$ ) (Figure 34). In contrast, no significant changes in aquaporin activity were observed in MCF7 cells or in the non-tumorigenic MCF10A cells.

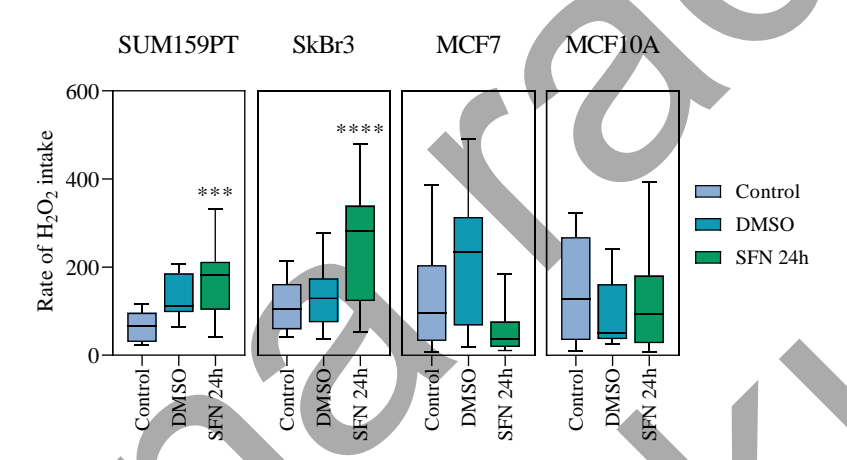


Figure 34. Effect of sulforaphane on aquaporin activity

SUM159PT, SkBr3, MCF7, and MCF10A cells were treated with 2.5  $\mu$ M sulforaphane for 24 h, after which the cells were loaded with 10  $\mu$ M DCFH-DA for 30 minutes. AQP activity was assessed by measuring the rate of  $H_2O_2$  intake after a 100  $\mu$ M  $H_2O_2$  challenge. Experiments were conducted in biological duplicates, and 10 cells were analyzed per experiment. Data is presented as mean  $\pm$  SEM. Statistical analysis was performed using one-way ANOVA with Dunnett's multiple comparisons test. Significance is indicated as follows: \*\*\* p  $\leq$  0.001 and \*\*\*\* p  $\leq$  0.0001

## 3.2.5. Predicted NRF2 binding in AQP3 and AQP5 regulatory regions

Besides the experimental approach, the potential connection between aquaporins and NRF2 was further assessed using *in silico* analysis. To investigate whether NRF2 may directly regulate AQP3 and AQP5, publicly available datasets were analyzed for predicted and experimentally validated NRF2 binding motifs within aquaporins' regulatory regions.

For *AQP3* (Figure 35), which is located on the short arm of chromosome 9 (9p13.3), GeneHancer identified several regulatory elements within ~10 kb of the locus. These included one high-confidence promoter (GH09J033442), one low-confidence promoter (GH09J033436), and several enhancers: high-confidence (GH09J033430, GH09J033434, GH09J033452), medium-confidence (GH09J033435, GH09J033438), and low-confidence (GH09J033437, GH09J033450). Evidence for NRF2 binding was found in multiple datasets. ENCODE4 ChIP-seq clusters showed binding signals in this region, which were also supported by ReMap ChIP-seq peaks. In addition, sequence-based predictions (JASPAR) highlighted several binding motifs, and FIMO scanning confirmed some of them within the regulatory elements. Among these, the enhancer GH09J033430 stood out because it was supported by both experimental and predicted data, making it the strongest candidate for NRF2 binding. The promoter GH09J033442 also showed some evidence, but less consistently.

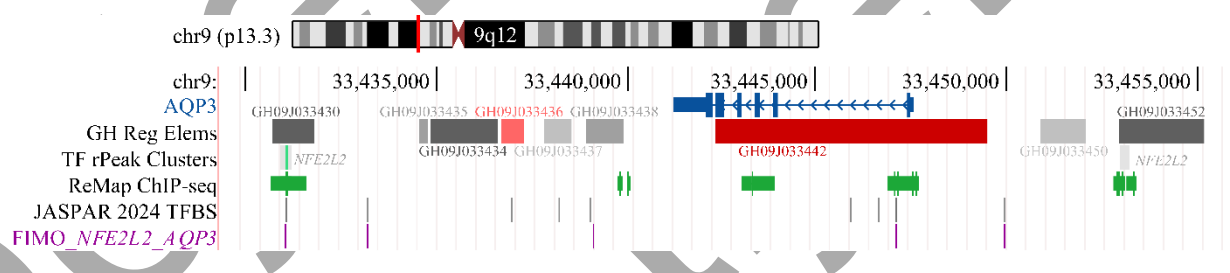


Figure 35. Predicted and experimental NRF2 binding motifs in AQP3 regulatory regions

The *AQP3* gene is shown on chromosome 9p13.3 (blue), transcribed from right to left. GeneHancer regulatory elements (GH Reg Elems) are displayed in a 10-20 kb window around the locus, with the high-confidence GH09J033442 (red), and low-confidence promoter GH09J033436 (pink), and several predicted enhancers: high-confidence GH09J033430, GH09J033434, and GH09J033452 (dark grey), medium-confidence GH09J033435, and GH09J033438 (medium grey), and low-confidence GH09J033437, and GH09J033450 (light grey). Evidence for transcription factor binding sites (TFBS) is shown in four independent tracks. The transcription factor representative peak (TF rPeak) clusters (grey boxes) represent ChIP-seq binding events for NRF2 (*NFE2L2*), identified across multiple experiments in the ENCODE4 project, with highlighted TF motif site (green). The ReMap ChIP-seq peaks (green boxes) display experimentally observed NRF2 binding sites from individual ChIP-seq datasets. The JASPAR 2024 TFBS predictions (black ticks) mark genomic positions that match the NRF2 consensus motif, and the FIMO track (purple ticks) shows predicted motif within GeneHancer-defined promoters and enhancers, based on direct sequence scanning using the JASPAR MA0150.2.

For AQP5 (Figure 36), located on the long arm of chromosome 12 (12q13.12), GeneHancer identified two medium-confidence promoters (GH12J049959, GH12J049966), one low-confidence promoter (GH12J049950), one high-confidence enhancer (GH12J049945), and one low-confidence enhancer (GH12J049952), also spanning ~10 kb around the locus. In this case, the enhancer GH12J049945 is the best candidate, supported by overlapping ENCODE4 clusters, ReMap peaks, and motif predictions from JASPAR and FIMO. The promoter GH12J049959 also appeared as a candidate, though the evidence came only from predictions and ReMap, without support from ENCODE4 clusters.

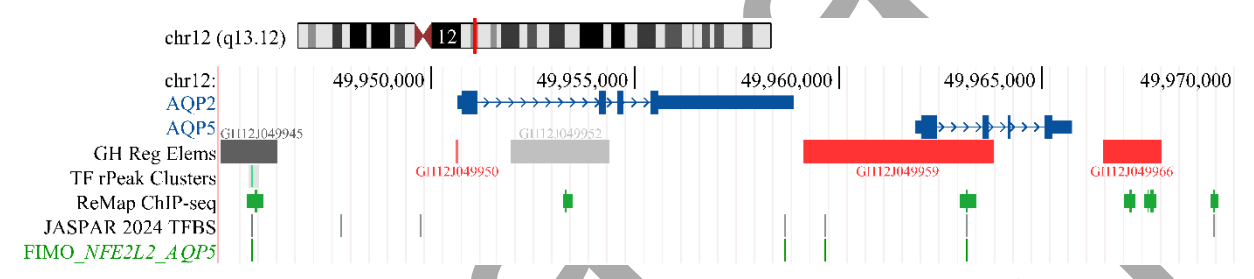


Figure 36. Predicted and experimental NRF2 binding motifs in AQP5 regulatory regions

The *AQP5* gene is shown on chromosome 12q13.12 (blue), transcribed from left to right. The neighboring *AQP2* gene is located upstream, and *AQP6* is downstream (not shown) within the same region. GeneHancer regulatory elements (GH Reg Elems) are displayed in a 10-20 kb window around the locus, with medium-confidence GH12J049959 and GH12J049966 (light red) and low-confidence promoter GH12J049950 (pink), high-confidence GH12J049945 (dark grey), and low-confidence enhancer GH12J049952 (light grey). Evidence for transcription factor binding sites (TFBS) is shown in four independent tracks. The transcription factor representative peak (TF rPeak) clusters (grey boxes) represent ChIP-seq binding events for NRF2 (*NFE2L2*), identified across multiple experiments in the ENCODE4 project, with highlighted TF motif site (green). The ReMap ChIP-seq peaks (green boxes) display experimentally observed NRF2 binding sites from individual ChIP-seq datasets. The JASPAR 2024 TFBS predictions (black ticks) mark genomic positions that match the NRF2 consensus motif, and the FIMO track (green ticks) shows predicted NRF2 motif within GeneHancer-defined promoters and enhancers, based on direct sequence scanning using the JASPAR MA0150.2.

Overall, the overlap of experimental datasets (ENCODE4 clusters, ReMap) with motif predictions (JASPAR, FIMO) suggests that NRF2 could directly bind to *AQP3* and *AQP5* regulatory regions. However, these predictions are based on publicly available datasets and require experimental validation in breast epithelial cells and related tumors.

Table 4 lists the predicted elements, positions, and motif sequences identified within AQP3 and AQP5 loci in the FIMO analysis.

Table 4. Predicted NRF2 binding motifs in AQP3 and AQP5 regulatory regions

Gene	GeneHancer ID	Element type	Start	End	p-value	q-value	Matched Sequence
	GH09J033430	Enhancer	33431065	33431079	1,49e-06	0,011	AGGGA <mark>TGAC</mark> TAA <mark>GC</mark> A
	GH09J033434	Enhancer	33433206	33433220	1,65e-05	0,138	CTGGG <mark>TGAC</mark> AGA <mark>GC</mark> A
	GH09J033435	Enhancer	33433206	33433220	1,65e-05	0,089	CTGGG <mark>TGAC</mark> AGA <mark>GC</mark> A
	GH09J033436	Promoter					
AQP3	GH09J033437	Enhancer	33439003	33439017	1,99e-05	0,128	AGGGGTGACACAGCT
	GH09J033438	Enhancer	33439003	33439017	1,99e-05	0,138	AGGGGTGACACAGCT
	GH09J033442	Promoter	33447149	33447163	2,07e-05	0,358	ACAAGTGACTCAGCC
	GH09J033450	Enhancer	33449941	33449955	7,99e-05	0,615	TGGAGTGAGTCATCA
	GH09J033452	Enhancer					
	GH12J049945	Enhancer	49945646	49945660	2,85e-05	0,244	ATTTGTGACTCAGCT
	GH12J049950	Promoter		<b>\</b>			
	GH12J049952	Enhancer					
AQP5			49959654	49959668	2,05e-05	0,129	GAGGA <mark>TGA</mark> GAAA <mark>GC</mark> A
	GH12J049959	Promoter	49958674	49958688	2,21e-05	0,129	CCAAA <mark>TGAC</mark> TTT <mark>GC</mark> A
			49963072	49963086	2,74e-05	0,129	AGCTG <mark>TGA</mark> GTCA <mark>GC</mark> C
	GH12J049966	Promoter					

FIMO (MEME Suite v5.5.8) was used to scan GeneHancer-defined promoters and enhancers from the UCSC Genome Browser for AQP3 and AQP5 with the JASPAR MA0150.2 NFE2L2 position weight matrix. GeneHancer IDs, element type, genomic coordinates (hg38), statistical significance, and matched sequences with marked antioxidant-responsive elements (red, 5'-TGACNNNGC-3') are shown. Reported hits met the  $p \le 0.0001$  threshold, and entries with no motif occurrences passing this threshold are blank.

#### 3.3. Cross-Regulation of Aquaporins

Since both prolonged oxidative stress and NRF2 modulation affected the expression of multiple aquaporins rather than a single isoform, the possibility of interdependence among aquaporins was considered. This raised the question of whether altering one aquaporin could influence the expression or activity of others, and whether such compensatory regulation might contribute to maintaining cellular homeostasis. To test this, both silencing and overexpression of AQP3 and AQP5 were performed using gene expression vectors, followed by antibiotic selection to establish stable cell lines. Attempts to establish stable silencing in MCF7 and SkBr3 cells were unsuccessful, and MCF10A cells could not be stably transfected at all. Therefore, subsequent analyses of aquaporin modulation were focused on SUM159PT cells, where both stable silencing and overexpression were achieved.

#### 3.3.1. Protein Expression

The efficiency of AQP3 and AQP5 modulation was evaluated at the protein level in SUM159PT cells. Stable knockdown of either AQP3 or AQP5 did not lead to a significant reduction in the targeted protein, indicating that silencing was not effective. In contrast, AQP5 levels were significantly increased in cells transfected with pCMV6-AQP5 ( $p \le 0.0001$ ), while AQP3 expression remained unchanged in pCMV6-AQP3-transfected cells (Figure 37).

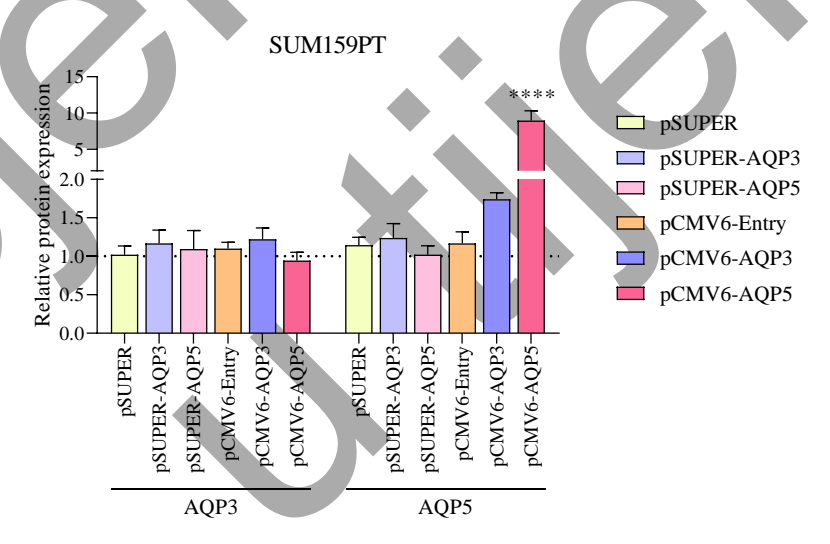


Figure 37. Effect of silencing or overexpression of AQP3 or AQP5 on protein expression in the SUM159PT cell line

SUM159PT cells were transfected with pSUPER-AQP3, pSUPER-AQP5, pCMV6-AQP3, or pCMV6-AQP5, with empty pSUPER and pCMV6-Entry as controls. Proteins were extracted and analyzed for AQP3, AQP5, and GAPDH expression. Experiments were performed in biological and technical triplicates. The protein level is expressed as a relative value compared to the control (indicated by a dotted line), and results are presented as the mean  $\pm$  SEM. Statistical analysis was performed using two-way ANOVA with Dunnett's multiple comparisons test. Significance is as follows: \*\*\*\* p  $\leq$  0.0001.

Representative immunoreactive bands for AQP3, AQP5, and GAPDH expression following silencing or overexpression are shown in Figure 38.

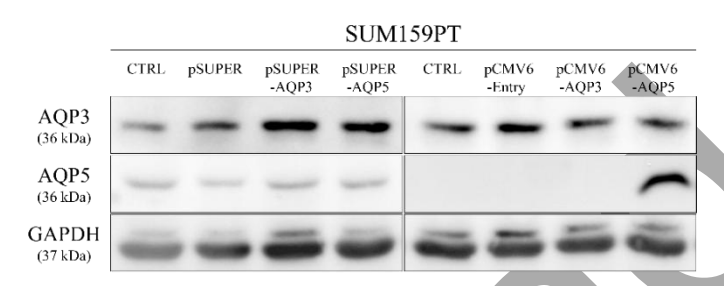


Figure 38. Representative immunoreactive bands of silencing or overexpression of AQP3 or AQP5 in the SUM159PT cell line

Representative immunoreactive bands showing AQP3, AQP5, and GAPDH protein expression in SUM159PT cells in the control (CTRL) condition, in cells stably transfected with pSUPER, pSUPER-AQP3, pSUPER-AQP5, pCMV6-Entry, pCMV6-AQP3, or pCMV6-AQP5.

## 3.3.2. Gene Expression

The efficiency of AQP3 and AQP5 modulation was evaluated at the mRNA level as well. AQP3 expression was significantly reduced following pSUPER-AQP3 transfection (p = 0.0109), indicating successful silencing, and was increased with pCMV6-AQP3 (p  $\leq$  0.0001), indicating successful overexpression (Figure 39c). Endogenous AQP3 mRNA, which could be distinguished from the plasmid-driven transcript in larger size, showed a decrease in the pCMV6-AQP3 group (p = 0.0079) (Figure 39d). AQP5 expression decreased following pSUPER-AQP5 transfection (p = 0.0231) and in pCMV6-AQP3 cells (p = 0.0382), while it was strongly upregulated after pCMV6-AQP5 (p  $\leq$  0.0001), confirming successful overexpression (Figure 39f).

Changes were observed in other AQP isoforms as well. AQP1 expression decreased in both pSUPER-AQP5 (p = 0.0055) and pCMV6-AQP3 cells (p = 0.0487) (Figure 39a). AQP4 was significantly reduced after pCMV6-AQP3 transfection (p = 0.0492) but increased in pCMV6-AQP5 cells (p = 0.0044) (Figure 39e). AQP9 expression was increased in both pSUPER-AQP3 (p = 0.0012) and pSUPER-AQP5 (p  $\leq$  0.001) groups but decreased in pCMV6-AQP3 cells (p = 0.0034) (Figure 39i). AQP10 expression was elevated in pCMV6-AQP5 cells (p  $\leq$  0.0001) (Figure 39j), while AQP11 was significantly increased in pCMV6-AQP3 cells (p = 0.0079) (Figure 39k). AQP2, AQP6, AQP7, and AQP12 showed no significant changes under any condition (Figure 39b, g, h, l), and AQP8 was not detected.

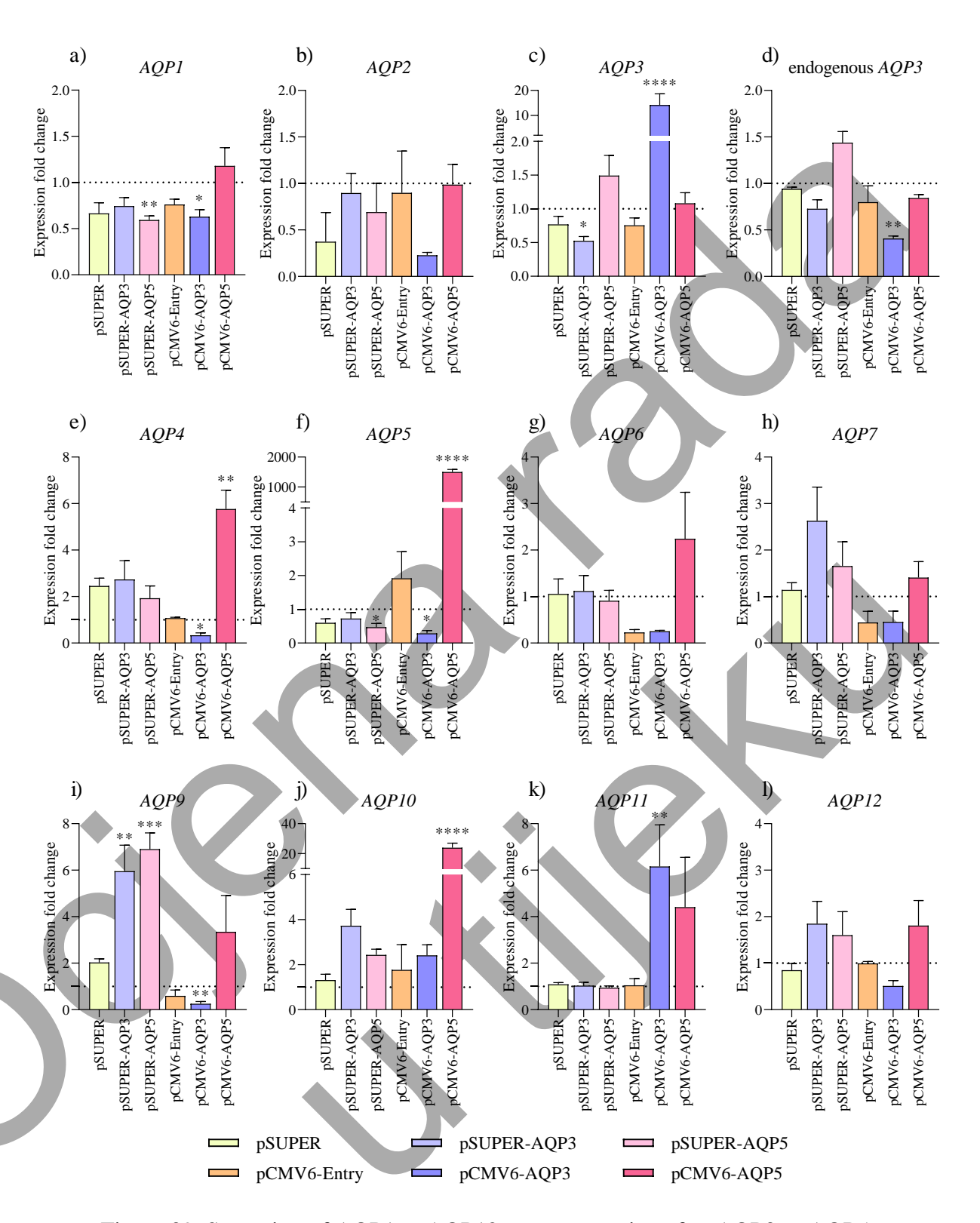


Figure 39. Screening of AQP1 to AQP12 gene expression after AQP3 or AQP5 silencing/overexpression in SUM159PT

SUM159PT cells were stably transfected with pSUPER-AQP3, pSUPER-AQP5, pCMV6-AQP3, or pCMV6-AQP5, with empty pSUPER and pCMV6-Entry as controls. Total RNA was isolated, reverse transcribed into cDNA, and analyzed by RT-qPCR to assess the expression of AQP genes (*AQP1*, *AQP2*, *AQP3*, endogenous *AQP3*, *AQP4*, *AQP5*, *AQP6*, *AQP7*, *AQP9*, *AQP10*, *AQP11*, and *AQP12*). Experiments were conducted in biological and technical triplicates. Gene expression was quantified by

the 2^(- $\Delta\Delta$ Ct) method, relative to control (dotted line), and is presented as mean  $\pm$  SEM. Statistical analysis was performed on  $\Delta$ Ct values using one-way ANOVA with Dunnett's multiple comparisons test. Significance is indicated as follows: \*p \le 0.05, \*\*p \le 0.01, \*\*\* p \le 0.001, and \*\*\*\* p \le 0.0001.

## 3.3.3. Aquaporin Activity

Since stable overexpression was successful only for AQP5 at the protein level, functional assays were performed to evaluate its impact on aquaporin activity. SUM159PT cells overexpressing AQP5 had a significantly higher rate of  $H_2O_2$  intake compared to control cells, as evidenced by the steeper slope in the DCFH-DA fluorescence trace (Figure 40a). Quantification confirmed that AQP5 overexpression led to a significant increase in aquaporinmediated  $H_2O_2$  transport (p = 0.018) (Figure 40b).

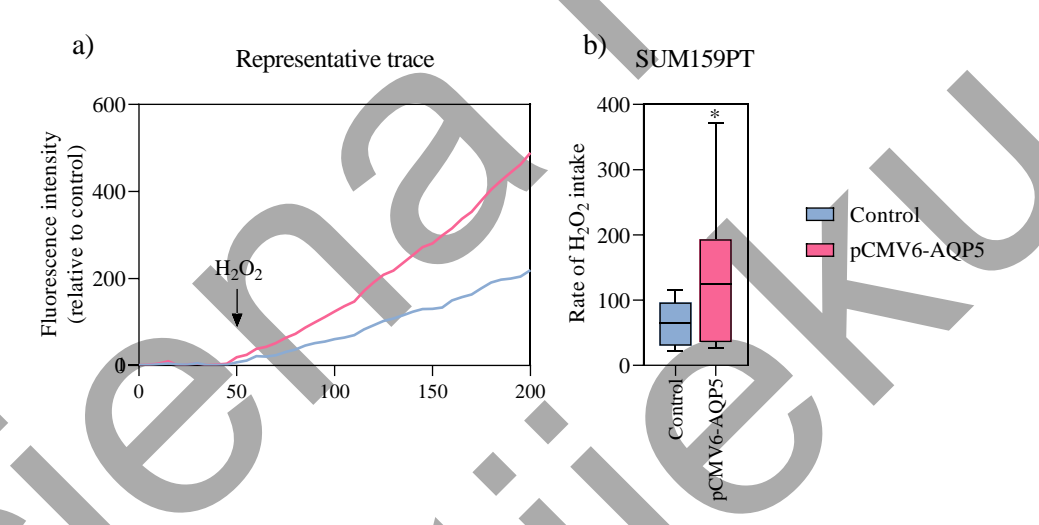


Figure 40. Effect of AQP5 overexpression on aquaporin activity

SUM159PT cells were stably transfected with pCMV6-AQP5 and were loaded with 10  $\mu$ M DCFH-DA for 30 minutes before measurement. Representative trace is shown on panel a), and AQP activity was assessed by measuring the rate of  $H_2O_2$  intake after a  $100\,\mu$ M  $H_2O_2$  challenge (b). Experiments were conducted in biological duplicates, analyzing 10 individual cells per replicate. Data is presented as mean  $\pm$  SEM. Statistical analysis was performed using one-way ANOVA with Dunnett's multiple comparisons test. Significance is indicated as follows: \*  $p \le 0.05$ .

#### 4. DISCUSSION

Breast cancer is a heterogeneous disease and remains a public-health challenge despite advances. The need for new diagnostic and prognostic biomarkers, as well as novel therapeutic targets, remains constant, and aquaporins have emerged as promising candidates. Dysregulated aquaporin expression has been reported in breast cancer and in other cancer types, where they are associated with tumor grade, nodal status, outcome, and chemoresistance. In breast cancer, AQP1, AQP3, and AQP5 are of particular interest as all are frequently described as overexpressed and linked to worse prognosis and therapy resistance. AQP3 is expressed in healthy mammary tissue and increases in cancer, whereas AQP5 expression is normally low but rises with cancer progression [176, 180]. Because of this, both have been suggested as prognostic markers for breast cancer, but are also being considered as contributors to cancer progression and potential therapeutic targets.

Aquaporins are transmembrane channels that facilitate the transport of water, glycerol, H<sub>2</sub>O<sub>2</sub>, and other small substrates across the membrane. This transport is passive and concentration-dependent, but is regulated at multiple levels, allowing cells to control substrate transport. By mediating H<sub>2</sub>O<sub>2</sub> transport, aquaporins contribute to the regulation of the cellular redox state and the activation of redox-dependent signaling pathways. It is known that chronic inflammation and persistent oxidative stress promote all stages of tumorigenesis, and cancer cells enhance their survival by modulating these processes [198]. Cancer cells also frequently have overexpressed aquaporins, which may support cancer progression through aquaporinmediated transport. By directing H<sub>2</sub>O<sub>2</sub> toward degradation, aquaporins may limit oxidative damage; in contrast, they may regulate the spatial distribution of H<sub>2</sub>O<sub>2</sub> and promote the activation of redox-sensitive pathways that enhance proliferation, survival, and migration. This raises the question of whether cancer cells adapt to high ROS conditions by increasing aquaporin expression. To investigate this, hormone-positive MCF7, HER2-positive SkBr3, and triple-negative SUM159PT breast cancer cell lines, along with the non-tumorigenic MCF10A cell line, were exposed to low-dose H<sub>2</sub>O<sub>2</sub>. After 14 days, cellular adaptation, aquaporin involvement, and differences in adaptation mechanisms between cancer and non-tumorigenic cells were evaluated. Concentrations of 10 and 20 µM H<sub>2</sub>O<sub>2</sub> were used to induce sublethal oxidative stress, as these mimic physiological conditions and do not damage redox-sensitive targets, but instead activate signaling pathways and promote adaptive responses. Prolonged exposure to H<sub>2</sub>O<sub>2</sub> induced cell-type-specific adaptive responses in breast cancer versus nontumorigenic breast epithelial cells, where all three cancer cell lines had an adaptive response,

either in the form of increased viability or proliferation upon acute H<sub>2</sub>O<sub>2</sub> challenge, whereas MCF10A cells behaved differently. In SUM159PT cells, prolonged exposure to 10 or 20 µM H<sub>2</sub>O<sub>2</sub> enhanced viability under acute challenge with 100 μM H<sub>2</sub>O<sub>2</sub>, while 20 μM pretreatment stimulated proliferation. A similar pattern was observed in MCF7 cells, where pretreatment improved survival at higher concentration challenges, and 20 µM pretreatment promoted proliferation at low concentrations. In SkBr3 cells, proliferation remained unaffected, but viability increased in 10 or 20 µM H<sub>2</sub>O<sub>2</sub> pretreated cells following low-dose H<sub>2</sub>O<sub>2</sub> exposure. In contrast, non-tumorigenic cells did not show protective adaptation in viability and were more sensitive to 75 µM challenge after 20 µM H<sub>2</sub>O<sub>2</sub> pretreatment. However, compared with cancer cells, MCF10A cells were overall less susceptible to H<sub>2</sub>O<sub>2</sub>, showing minimal cell death and a smaller reduction in proliferation. Consistent with the results of this study, MCF7 and MDA-MB-231 cells were more sensitive to H<sub>2</sub>O<sub>2</sub> exposure than MCF10A and exhibited both higher extracellular ROS production and antioxidant capacity [199]. On the other hand, MCF10A cells have been reported to be more sensitive to H<sub>2</sub>O<sub>2</sub> than breast cancer cell lines, undergoing cell death under conditions in which cancer cells remained resistant [200, 201]. These differences could be a result of variations in experimental design, including the concentrations and duration of H<sub>2</sub>O<sub>2</sub> treatment. Overall, results of prolonged exposure to low-dose H<sub>2</sub>O<sub>2</sub> demonstrate cancer cell adaptation, whereby adjusting to persistent oxidative stress, cancer cells not only become more resistant to H<sub>2</sub>O<sub>2</sub>-induced cell death but also use H<sub>2</sub>O<sub>2</sub> as a proliferative signal. Similar adaptive behavior has been reported previously, where chronic H<sub>2</sub>O<sub>2</sub>-induced oxidative stress in MCF7 breast cancer cells promoted growth, survival, tumorigenicity, metastatic potential, and cancer stem cell-like adaptation, and was proposed to contribute to resistance against ROSinducing chemotherapeutics [202]. Considering its effects on cancer cell adaptation in both viability and proliferation, 20 µM H<sub>2</sub>O<sub>2</sub> was selected for all subsequent experiments as a representative sublethal oxidative stress condition. To maintain low oxidative stress conditions that trigger adaptive responses, it was necessary to confirm that 20 µM H<sub>2</sub>O<sub>2</sub> did not cause damage. Fatty acid content was measured as an indicator of the available substrate for lipid peroxidation, and lipid hydroperoxides were assessed as markers of oxidative damage to lipids. There were no differences observed compared to control cells, indicating that 20 µM H<sub>2</sub>O<sub>2</sub> was sufficient to induce adaptive responses without causing oxidative damage. As cell migration is a key feature of cancer progression, which enables their invasion and metastasis, the next step was to analyze whether prolonged oxidative stress influenced migratory capacity. A woundhealing assay was performed over 48 h with the addition of mitomycin C to exclude proliferation. No changes in migration were detected after prolonged exposure to H<sub>2</sub>O<sub>2</sub> in any of the tested cell lines, but acute treatment resulted in enhanced wound closure in MCF7 and SkBr3 cells. Interestingly, SUM159PT and MCF10A cells closed the wound more rapidly than MCF7 and SkBr3. This is consistent with a previous report showing faster migration of MCF10A compared to cancer cell lines [203]. The lack of effect in SUM159PT and MCF10A may reflect their higher baseline migratory capacity, masking the influence of H<sub>2</sub>O<sub>2</sub> seen in MCF7 and SkBr3. Previously, ROS have been reported to stimulate migration through redoxsensitive pathways [204], and aquaporins are involved in this process through actin cytoskeleton reorganization initiated by estrogen-activated AQP3 [78]. Moreover, AQP3 has been shown to support migration via H<sub>2</sub>O<sub>2</sub>-dependent activation of the Akt signaling pathway [122]. This is supported by reduced migration and invasion of breast cancer cells following aquaporin silencing [122, 179]. In addition to their involvement in migration, aquaporins contribute to various processes, including cell proliferation, differentiation, angiogenesis, and tumorigenesis. To investigate whether they participate in cellular adaptation to oxidative stress, the protein and gene expression of these cells were analyzed after prolonged exposure to H<sub>2</sub>O<sub>2</sub>. AQP3 was consistently upregulated across all cancer cell lines, whereas it was significantly downregulated in the non-tumorigenic MCF10A cells. This suggests that AQP3 contributes to the adaptive response in cancer cells by facilitating H<sub>2</sub>O<sub>2</sub> transport and potentially enhancing redox-dependent signaling, while in non-tumorigenic cells, its expression may be suppressed to limit ROS entry. AQP5 expression was increased in SUM159PT and SkBr3, but unchanged in MCF7 and MCF10A. Considering that AQP5 has been associated with an increase in cancer aggressiveness, this result may reflect subtype-specific regulation in HER2-positive and triplenegative cell lines. These were partially confirmed at the transcriptional level. Both AQP3 and AQP5 mRNA were increased in SUM159PT and SkBr3 cells, while only AQP3 mRNA increased in MCF7 and decreased in MCF10A. While there were no differences on protein level, AQP5 gene expression decreased in MCF7 and increased in MCF10A cells, suggesting possible post-transcriptional regulation. Additionally, gene expression of other peroxiporins was analyzed, showing increased AQP11 mRNA in SUM159PT, and AQP1 and AQP9 mRNA in MCF10A. Changes in protein and gene expression observed in the non-tumorigenic cell line differ from those in cancer cells, possibly pointing to a shift in overall aquaporin function, although its role is unclear, and it remains unknown whether these changes translate to the protein level. Overall, these findings support aquaporin's role in cellular adaptation to oxidative stress, with cancer cells enhancing aquaporin expression under persistent ROS. Previous results already showed subtype-specific adaptation to acute 100 µM H<sub>2</sub>O<sub>2</sub> challenge, where SkBr3 and MCF7 both increased AQP3 mRNA expression in response to H<sub>2</sub>O<sub>2</sub>, while SUM159PT

decreased it [205]. The SkBr3 and MCF7 responses are in line with this study, but SUM159PT reacted differently, which may be explained by differences in the experimental setup. Compared to the acute high-dose setting, prolonged low ROS induced broader adaptation. AQP3 was upregulated in all cancer cell lines, while AQP5 increased in SUM159PT and SkBr3. In colorectal cancer cells, AQP3 and AQP5 mRNA expression increased in response to H<sub>2</sub>O<sub>2</sub>, suggesting they may act as an alternative to classical antioxidant defenses during oxidative stress [206]. Additionally, AQP5 has been reported to induce initial sensitivity under acute oxidative stress, but to promote improved survival and resistance during chronic stress [71]. These studies highlight the role of aquaporins in cellular response to oxidative stress, a mechanism that cancer cells exploit to sustain tumorigenesis and that may explain their frequent upregulation. In this way, aquaporins promote redox-sensitive oncogenic signaling. The most frequently activated signaling pathway in cancer, PI3K/Akt/mTOR, promotes cell survival, growth, and cell cycle progression, and its dysregulation through PI3K hyperactivity, PTEN loss, or Akt activation is often involved in tumorigenesis and therapy resistance [207]. Several studies have directly linked this pathway to aquaporins, and PI3K/Akt signaling has been shown to induce AQP3 expression in keratinocytes [208], while knockdown or siRNA-mediated suppression of AQP3 reduced Akt phosphorylation in multiple models [122, 209–212]. AQP3mediated H<sub>2</sub>O<sub>2</sub> was shown to modulate Akt signaling during migration in breast cancer cells [122], while in other models, AQP3 enhanced invasion and metastasis through the H<sub>2</sub>O<sub>2</sub>/Syk/PI3K/Akt axis during chronic inflammation [210], and regulated MMP expression through the PI3K/Akt signaling pathway [209]. In this study, prolonged exposure to low-dose H<sub>2</sub>O<sub>2</sub> did not alter PI3K, PTEN, or mTOR complex protein expression, nor Akt activity, suggesting that the observed AQP3 upregulation is not mediated by sustained PI3K/Akt/mTOR activation. The only detected change was increased Ras expression in SkBr3 cells, consistent with previous studies linking AQP5 to Ras activation and downstream EGFR/ERK or Rac1 signaling [213], and highlighting a possible HER2-specific adaptation. Absence of change in PI3K/Akt/mTOR signaling pathway suggests AQP3 upregulation in sustained low-grade stress is likely regulated in another way, although transient activation or responses to higher oxidative stress cannot be excluded. Therefore, additional research is needed to clarify which signaling pathways regulate aquaporin expression. Considering that aquaporins transport H<sub>2</sub>O<sub>2</sub>, a central signaling molecule in redox regulation, the involvement of NRF2, a major regulator of the antioxidant and cytoprotective response, was examined. Under basal conditions, NRF2 is continuously synthesized and rapidly degraded via the Keap1-CUL3-ubiquitin-proteasome pathway. In response to oxidative stress, Keap1 cysteine modifications impair NRF2

degradation, allowing newly synthesized NRF2 to accumulate, translocate to the nucleus, dimerize with small Maf proteins, and bind to AREs to activate the transcription of over 200 genes involved in redox balance, detoxification, and metabolism. In this way, NRF2 provides a controlled response to oxidative stress, ensuring protection is activated only when needed. However, cancer cells frequently exploit NRF2 hyperactivation to counteract elevated ROS and support survival, which makes this pathway relevant in the context of adaptation to oxidative stress. In this study, NRF2 protein expression did not change in SkBr3, MCF7, or MCF10A cells and was slightly reduced in SUM159PT. At the gene level, NFE2L2 decreased only in SkBr3, while the other lines showed no change. Keap1 expression was decreased in SUM159PT and SkBr3 but increased in MCF7, whereas GSK3\beta remained unaltered across all lines. Wellestablished NRF2 downstream targets HO-1 [30], NQO1 [29], and AKR1B10 [32], which are typically upregulated upon NRF2 activation, remained unaffected, suggesting no activation had occurred. However, analysis of nuclear and cytoplasmic fractions revealed increased NRF2 accumulation in the nucleus of all three cancer cell lines following prolonged H<sub>2</sub>O<sub>2</sub> exposure, indicating that NRF2 activation may have occurred. Consistently, previous studies have demonstrated H<sub>2</sub>O<sub>2</sub>-induced NRF2 nuclear translocation and its activation through different targets [214, 215]. Therefore, even without changes in total NRF2 protein or mRNA levels or induction of classical downstream targets, translocation to the nucleus could point to NRF2 activation. The changes in Keap1 expression in SUM159PT and SkBr3 possibly contribute to NRF2 activity, as reduced Keap1 levels would limit NRF2 degradation. In contrast, MCF7 cells had increased Keap1 expression, which would suppress NRF2, yet its nuclear localization was still elevated, suggesting that mechanisms other than Keap1 or GSK3β may regulate NRF2 in these conditions. Additionally, it is important to note that NRF2 activation is often cancerspecific, and in different models, cancer tissue showed higher NRF2 expression than adjacent healthy tissue [216–219]. Accordingly, in this study, NRF2 activation was not seen in the nontumorigenic MCF10A cells, which showed no changes in NRF2, Keap1, or nuclear localization, pointing to a cancer-specific response to prolonged oxidative stress. Since the classical NRF2 targets were unaffected, ABC transporters were analyzed as non-canonical NRF2 targets relevant for therapy resistance [220]. ABCB1 and ABCG2 are efflux pumps that reduce intracellular drug accumulation and contribute to multidrug resistance [221]. In breast cancer, their overexpression has been linked to poor therapeutic response and disease progression, as they limit the effectiveness of chemotherapeutic agents by actively exporting them from the cells. Although several studies link NRF2 activity and ABC transporters upregulation [220-223], in this study, both ABCB1 and ABCG2 expression were reduced in SkBr3 cells, while no changes were detected in SUM159PT, MCF7, or MCF10A cells, after prolonged oxidative stress. Overall, these results show that cancer cells adapt to prolonged low oxidative stress through coordinated changes in aquaporin expression and NRF2 activity. While AQP3 was consistently upregulated in cancer cells and AQP5 increased in specific subtypes, NRF2 nuclear localization also increased, despite no induction of its classical antioxidant targets. In contrast, non-tumorigenic MCF10A cells showed no NRF2 activation and downregulated AQP3, pointing to different strategies in adaptation to persistent ROS between cancer and non-tumorigenic cells. There is a potential connection between aquaporin responses to oxidative stress and their reported upregulation by chemotherapy. Understanding the mechanisms of this adaptation could clarify their role in therapy resistance and determine whether aquaporins, beyond their prognostic value, may also serve as indicators of therapy effectiveness or as targets to overcome resistance. Finally, as both aquaporins and NRF2 contribute to redox balance and therapy resistance, their interaction may represent a mechanism by which cancer cells adapt to oxidative stress and sustain tumorigenesis.

NRF2 acts as a cellular protector but also has a dual role, and in cancer, it is often persistently active, contributing to metabolic rewiring, adaptation to elevated oxidative stress, and therapy resistance. Both aquaporins and NRF2 can be upregulated and exploited in cancer, and in this study, both were found to increase with prolonged exposure to H<sub>2</sub>O<sub>2</sub>. This raised the question of whether NRF2 can affect aquaporin expression or activity. Although NRF2 regulates a wide array of genes, its ability to directly or indirectly regulate aquaporin expression remains unclear. To address this, NRF2 was pharmacologically activated with sulforaphane and inhibited with ML385, and genetically modulated through overexpression and siRNA-mediated silencing in breast cancer cell lines and in a non-tumorigenic breast epithelial cell line. Sulforaphane is a naturally occurring isothiocyanate known for its ability to activate NRF2 by covalently modifying reactive cysteine residues on its repressor Keap1, thereby disrupting NRF2 ubiquitination and proteasomal degradation [186]. As a result, NRF2 accumulates, translocates to the nucleus, and activates target genes. ML385 is a small-molecule inhibitor of NRF2 that blocks its heterodimerization with small Maf proteins and prevents binding to ARE sequences, thereby suppressing NRF2-driven transcription [224]. To determine the non-toxic concentration of NRF2 modulators, cell viability was assessed after 24-hour treatment with sulforaphane or ML385 across a 0-10 µM range. Both compounds showed dose-dependent effects. Sulforaphane significantly reduced viability in SUM159PT, MCF7, and MCF10A at 7.5 and 10 µM, while in SkBr3, the decrease was evident from 5 µM onward. ML385 had no effect in SUM159PT, MCF7, or MCF10A, but reduced viability in SkBr3 at 5-10 µM. Interestingly, 1 µM sulforaphane treatment resulted in increased viability of MCF7 cells, while higher concentrations were inhibitory. Previous studies reported similar cytotoxic effects of sulforaphane at higher concentrations in breast cancer cell lines [225], while ML385 decreased viability in a dose-dependent manner in head and neck squamous cell carcinoma [226]. Research on sulforaphane is extensive, and it shows that low micromolar concentrations (1-5 μM) primarily activate cytoprotective pathways such as NRF2, while higher doses shift its role toward anticancer activity by inducing apoptosis, cell cycle arrest, and inhibition of metastasis [227]. Sulforaphane has also been tested in clinical trials, which demonstrated that it is relatively safe and free of adverse effects at low doses and minimally harmful at higher doses [228-230]. Based on dose-response curves, 2.5 µM sulforaphane was selected for further experiments as the highest concentration that did not affect viability in any of the tested cell lines. For ML385, a 10 µM concentration was selected despite partial toxicity in SkBr3, as the reduction in viability was modest and no effect was observed in the other lines. Additionally, this concentration has previously been demonstrated to inhibit NRF2 [231]. Sulforaphane treatment successfully activated NRF2 in all tested cell lines, as evidenced by the induction of the downstream target HO-1 at 6 or 24 h after treatment, or both. NRF2 activation was also reflected at the protein level, in SUM159PT and MCF7 cells, NRF2 expression increased at both 6 and 24 h, while in MCF10A, the effect was apparent after 24 h, and in SkBr3, NRF2 expression remained unchanged. In SUM159PT cells, NRF2 activity was further supported by increased nuclear translocation detected two hours post-treatment, while in the other cell lines, only a trend toward increased nuclear localization was observed, without significant differences. However, NRF2 can also be activated without detectable changes in expression or nuclear translocation. For example, nuclear accumulation of NRF2 was not necessary for HO-1 induction, as Bach1 inactivation enabled already present nuclear NRF2 to induce HO-1 expression [232]. Nevertheless, independent of changes in NRF2 protein expression or translocation to the nucleus, HO-1 was upregulated in all cell lines, indicating that NRF2 activity was achieved. This is consistent with numerous previous studies demonstrating that sulforaphane promotes NRF2 nuclear translocation and activation of target genes such as HO-1, of which only a few are cited here as examples [233–235]. In addition to HO-1 induction, increased Keap1 expression was also observed following sulforaphane treatment in SUM159PT, SkBr3, and MCF10A, suggesting compensatory regulation of the NRF2-Keap1 axis. This is in line with previous reports showing that NRF2 can directly drive Keap1 expression at the transcriptional level as part of a negative feedback loop [236], as well as findings that tert-butylhydroquinone enhances NRF2 nuclear translocation and increases the expression of p62 and Keap1 [237]. On the other hand, ML385 treatment did not achieve effective NRF2 inhibition. Although ML385 reduced Keap1 protein levels in MCF7 cells at both 6 and 24 h, this did not translate into inhibition of NRF2 activity, as HO-1 remained unchanged. The reduction of Keap1 in this context may again point to a compensatory response. Similarly, in SUM159PT, SkBr3, and MCF10A cells, ML385 failed to downregulate NRF2 activity. Previous studies have shown that 10 µM ML385 effectively inhibited NRF2 signaling in head and neck squamous cell carcinoma cells, suppressing NRF2-ARE binding, nuclear localization, and target gene expression, including HO-1 [224, 238, 239]. In this study, ML385 did not exhibit the same effects, as NRF2 inhibition was not observed at the concentration used. Another study also reported that NRF2 levels remained unmodified by ML385, while increasing concentrations of ML385 reduced Keap1 protein levels [240]. This kind of compensatory regulation within the NRF2-Keap1 axis may have contributed to unsuccessful NRF2 inhibition in this study. In addition, there are cell-type-specific differences between breast cancer (and non-tumorigenic breast epithelial) models used in this study, and head and neck squamous cell carcinoma, where ML385 has effectively inhibited NRF2. Therefore, ML385 was not used in further experiments. In this study, genetic modulation of NRF2 was also attempted through overexpression and siRNA-mediated silencing in breast cancer and nontumorigenic breast epithelial cells. Stable overexpression was performed by antibiotic selection, and success was considered achieved when non-transfected control cells did not survive the treatment, while transfected cells remained viable and were used for subsequent experiments. However, stable transfection could not be established in MCF10A cells despite the use of multiple transfection reagents and protocols, and these were therefore excluded from further analysis. Confirmation of modulation efficacy was carried out by analyzing NRF2 and its downstream target HO-1 at the protein level. Neither siRNA-mediated silencing nor stable overexpression resulted in consistent or significant changes in NRF2 or HO-1 expression across the tested cell lines, indicating that genetic modulation of NRF2 was not achieved. Therefore, further evaluation of aquaporin expression under these conditions was not performed. Considering these limitations, subsequent analyses focused on the pharmacological modulation by sulforaphane, which consistently activated NRF2 and enabled evaluation of its impact on aquaporin expression, gene regulation, and functional activity. In SUM159PT cells, sulforaphane treatment led to a consistent upregulation of AQP3 at both 6 and 24 h, while AQP5 remained unchanged. In SkBr3 and MCF7 cells, neither AQP3 nor AQP5 showed significant changes despite NRF2 activation. In the non-tumorigenic MCF10A line, AQP3 and AQP5 were also unaffected by NRF2 activation. Although a slight trend toward increased AQP3 expression was observed across all cell lines, these differences did not reach statistical significance. Overall, these results indicate that NRF2 activation by sulforaphane was successful in all models, but its effect on aquaporin regulation is cell-type-specific, with a clear upregulation of AQP3 observed only in SUM159PT cells. To extend this analysis, peroxiporin gene expression was measured, but the results did not align with protein-level changes. In SUM159PT cells, AQP3 protein was consistently upregulated by sulforaphane, yet its mRNA expression was reduced after 24 h, along with decreased AQP5 and AQP11. In SkBr3 cells, sulforaphane increased AQP1, AQP4, and AQP9 mRNA expression, although corresponding protein levels were not assessed and thus remain uncertain. In MCF7 cells, a significant decrease in AQP11 mRNA was detected, while in MCF10A cells, no significant changes were observed. Furthermore, to test whether sulforaphane-induced NRF2 activation altered functional aquaporin activity, H<sub>2</sub>O<sub>2</sub> transport was measured. After 24 h of sulforaphane treatment, aquaporin-mediated H<sub>2</sub>O<sub>2</sub> intake was significantly increased in SUM159PT and SkBr3 cells, whereas no changes were detected in MCF7 or MCF10A cells. In SUM159PT, this increase in H<sub>2</sub>O<sub>2</sub> transport is consistent with the observed upregulation of AQP3 protein, supporting its role in facilitating H<sub>2</sub>O<sub>2</sub>. In SkBr3, the increase in H<sub>2</sub>O<sub>2</sub> transport may be linked to the increased mRNA expression of AQP1, AQP4, and AQP9, suggesting that sulforaphane might also activate these channels at the protein level, although this was not tested. In contrast, the absence of significant changes in aquaporin protein or gene expression in MCF7 and MCF10A cells possibly explains why H<sub>2</sub>O<sub>2</sub> transport remained unaffected in these models. These findings provide no evidence that sulforaphane-activated NRF2 transcriptionally targets a specific aquaporin isoform. Instead, its effect appears to be cell-type-specific or involves posttranscriptional or post-translational mechanisms. Moreover, the differential responses of distinct aquaporins across cell lines may point to a coordinated regulation of peroxiporin function, ensuring that overall transport capacity remains balanced and redox homeostasis is maintained. Several studies showed NRF2-aquaporin interplay, but it seems to be dependent on cell type and aquaporin isoform. For example, sulforaphane treatment was shown to increase AQP3 expression at both mRNA and protein levels in keratinocytes [241], and in a traumatic brain injury model, it elevated AQP4 expression in astrocytes [242]. However, silencing NRF2 in keratinocytes did not reduce AQP3 expression [243], suggesting that AQP3 upregulation in response to sulforaphane may not be directly mediated by NRF2. The same study also showed aquaporins influencing NRF2 activity, as AQP3 knockdown downregulated NRF2 and its target NQO1, whereas AQP3-overexpression enhanced their expression. Similarly, AQP5-transfected

MCF7 cells exhibited elevated NRF2 and AKR1B10 expression [244], suggesting that aquaporin gain-of-function enhances NRF2 signaling. On the other hand, impaired NRF2/HO-1 signaling, characterized by increased cytosolic but reduced nuclear NRF2, was associated with AQP1 downregulation in hypertensive injury [245]. While sulforaphane-driven NRF2 activation can elevate aquaporin expression, evidence also suggests that aquaporins themselves can modulate NRF2 signaling. However, it is unclear whether sulforaphane activation reflects direct transcriptional regulation by NRF2. To investigate this possibility, in silico analysis was performed to identify potential NRF2 binding motifs in the regulatory regions of AQP3 and AQP5. Multiple candidate sites were first identified using JASPAR sequence-based predictions in the UCSC genome browser, which scan for consensus motifs. Predicted motifs were crossreferenced with ENCODE4 and ReMap ChIP-seq datasets, and only a subset of predicted sites overlapped. To improve these predictions, FIMO was used, providing statistical estimates of the likelihood that predicted sites represent biologically relevant binding events. This highlighted the AQP3 enhancer GH09J033430 as a strong and statistically reliable NRF2 binding motif, supported by both motif predictions and experimental ChIP-seq evidence. The AQP3 promoter GH09J033442 showed weaker statistical support and limited experimental confirmation. For AQP5, the enhancer GH12J049945 emerged as the strongest candidate, while the promoter GH12J049959 lacked experimental validation. Considering the statistical confidence of predicted motifs, potential NRF2 regulation of AQP5 appears less confident than that of AQP3. In SUM159PT cells, where sulforaphane consistently increased AQP3 protein expression, the presence of an NRF2 binding site near the AQP3 locus may provide a mechanistic explanation, even though transcriptional changes did not align with protein expression. In both regulatory regions, the most promising sites were high-confidence enhancers, with consistent overlap between computational predictions and experimental datasets. Since enhancers are context-dependent and often require co-activators or permissive chromatin states, their activity could explain the cell-type-specific responses to sulforaphane observed in this study. It is also important to note that the ENCODE4 and ReMap datasets used in this analysis are derived from diverse cell types, not necessarily breast cancer or breast epithelial cells. Therefore, while the in silico predictions suggest that NRF2 may directly regulate AQP3 and AQP5, direct experimental validation in the relevant cellular models is required. In line with these results, analysis of the murine AQP3 promoter using Tfsitescan identified two NRF2/ARE consensus sites, and this was supported experimentally, as sulforaphane-activated NRF2 increased AQP3 gene and protein expression [241]. Beyond this single report for AQP3, the literature provides minimal evidence of NRF2 regulation of other aquaporins. Taken together, these results highlight that the NRF2-aquaporin association is highly context-dependent. Both were elevated after prolonged oxidative stress and showed complex, cell-type-specific changes during NRF2 activation with sulforaphane, while *in silico* predictions suggest possible NRF2 binding at aquaporin regulatory regions. This points to a potential association, but direct transcriptional control remains to be experimentally validated. Beyond transcription, post-transcriptional or post-translational mechanisms, as well as sulforaphane off-target effects, cannot be excluded. Importantly, in both prolonged oxidative stress and pharmacological NRF2 activation, aquaporin mRNA profiles shifted in a cell-type-specific manner. This suggests that instead of a single isoform being directly regulated, multiple aquaporins may contribute together to flux regulation and maintenance of redox balance.

Aquaporins are expressed in a tissue-specific manner and have different roles depending on their localization. Overall, they maintain cellular and tissue water homeostasis, participate in glycerol metabolism, and in the regulation of redox homeostasis. They are important in physiology and are often dysregulated in pathology, including cancer. Because of this, their expression and activity are tightly regulated by transcription, trafficking, and gating. These regulatory mechanisms enable on-demand transport and spatial control, which strongly influence redox-sensitive signaling. Furthermore, the 13 human isoforms differ in substrate specificity and intracellular location, and ensure isoform-specific functions. Considering all of this, the question arises whether cells can coordinate aquaporin abundance, localization, and gating to tune transport, suggesting that aquaporin-mediated transport is dynamically controlled rather than purely passive. Therefore, AQP3 and AQP5 overexpression and shRNA-mediated silencing were used to test whether altering one isoform changes the expression of others and to assess effects on overall function. For MCF10A, similar to the case of NRF2 overexpression discussed earlier, stable overexpression or silencing of AQP3 and AQP5 could not be achieved, as transfection was unsuccessful despite repeated attempts with different reagents and protocols. In MCF7 and SkBr3 cells, shRNA-mediated silencing failed as well, since the cells did not survive antibiotic selection, even after adjusting the puromycin concentration according to dose-response curves, lowering the dose, and modifying the protocol. SUM159PT cells were the only model in which both silencing and overexpression of AQP3 and AQP5 were successful, and were therefore used for all subsequent experiments. Stable modulation of AQP3 and AQP5 in SUM159PT cells showed different outcomes at the protein and gene levels. On the protein level, only AQP5 overexpression was successful, resulting in a significant increase, whereas AQP5 silencing did not reduce protein expression. Similarly, AQP3 overexpression or silencing did not cause changes in protein expression. At the gene level, modulation of both AQP3 and AQP5 was successful. Both increased after plasmid-driven overexpression and decreased following shRNA-mediated silencing. In the case of AQP3 overexpression, plasmidderived transcripts could be distinguished from endogenous mRNA, revealing a compensatory reduction in endogenous expression when plasmid mRNA was present. Because the plasmid transcript includes only coding sequences and lacks the regulatory 5' and 3' UTRs contained in the endogenous mRNA, it avoids normal post-transcriptional control and is expressed, prompting the cell to counteract by suppressing endogenous transcription. This mechanism likely explains why total AQP3 protein remained unchanged despite overexpression, suggesting that cells actively maintain AQP3 at a constant level to preserve transport capacity. For AQP5 overexpression, plasmid and endogenous transcripts could not be distinguished in this way, and therefore, only total expression was measured. Nevertheless, the strong increase in protein indicates that plasmid mRNA translated efficiently and overcame any compensatory suppression. The difference in modulation success may reflect baseline expression of these proteins. AQP3 is constitutively expressed in normal mammary epithelium and further increases in cancer, so in SUM159PT cells, its higher endogenous level may cause plasmiddriven AQP3 to be counterbalanced by suppression of the native transcript. AQP5, in contrast, is normally low and rises with progression, and in these cells, the endogenous protein was barely detectable on western blots compared to the strong signal after overexpression. This lower baseline makes AQP5 more permissive to overexpression, allowing plasmid-derived transcripts to translate efficiently into protein. In the case of AQP3 or AQP5 silencing, the absence of protein-level changes despite confirmed reductions in mRNA points to posttranscriptional or post-translational mechanisms that stabilize aquaporin proteins. This suggests that aquaporin levels are tightly regulated and that even when mRNA is reduced, protein expression is maintained to avoid changes in transport activity. In addition to changes in AQP3 and AQP5, modulation of one isoform influenced the expression of other aquaporins, indicating the presence of cross-regulation. AQP1 expression decreased after AQP5 silencing and also following AQP3 overexpression, while AQP4 decreased after AQP3 overexpression but increased following AQP5 overexpression, suggesting isoform-specific interactions rather than uniform regulation. AQP9 was induced after silencing of either AQP3 or AQP5, but was reduced when AQP3 was overexpressed, suggesting that glycerol-transporting isoforms may compensate for each other. Furthermore, AQP10 was increased in AQP5-overexpressing cells, while AQP11 was increased in AQP3-overexpressing cells. In contrast, AQP2, AQP6, AQP7, and AQP12 remained unchanged, and AQP8 was not detected. Overall, these findings suggest

that modulation of AQP3 and AQP5 not only affects their own expression but also triggers adjustments across other isoforms, potentially to preserve transport capacity. At the functional level, only AQP5 overexpression was tested, as it was the only condition that produced a significant protein increase. In SUM159PT cells overexpressing AQP5, significant enhancement of H<sub>2</sub>O<sub>2</sub> intake was observed, confirming its role as a peroxiporin and linking the observed molecular changes to functional consequences. The increase in AQP4 and AQP10 expression may have also contributed to the higher intake, but protein levels of these isoforms were not measured. Nevertheless, the effect of AQP5 overexpression highlights its contribution to redox regulation, where increased transport capacity could promote localized signaling and potentially enhance cancer cell adaptation to oxidative stress. aquaporins' compensatory mechanisms were already described in plants and human cells, suggesting that this is a general principle of aquaporin biology. They are also shown to be regulated at multiple levels. Regulation can occur between different variants of the same isoform, where their abundance shapes overall channel properties. In plants, aquaporins or plasma membrane intrinsic proteins (PIPs) form heterotetramers in which inactive maize PIP1 isoforms gain functionality through interactions with PIP2, showing that individual channel activity can be modified by the presence of adjacent isoforms [246]. Similar isoform-selective interactions were reported in cotton fibers, where different PIP2s regulate each other's activity to meet the demands of rapid tissue growth [247]. It has also been shown that interactions between plasma membrane aquaporins modulate their water channel activity [248]. Additionally, interactions within tetramers can further modify transport activity. In epithelial cells, the M1-AQP4 and M23-AQP4 form tetramers that assemble into large, stable structures that increase water permeability, and the relative abundance of the two isoforms regulates this organization [249]. Regulation may also take place between different isoforms, where changes in one affect the expression or function of another. Cooperative regulation extends to tissues such as the lens, with regulated spatial distribution patterns of AQP0 and AQP5, where AQP5 compensates for changes in the AQP0 functionality, ensuring stable water transport [250]. Furthermore, retinoic acid treatment shifts the balance between aquaglyceroporins in human keratinocytes, upregulating AQP3 while downregulating AQP9 [251], and pharmacological aquaporin inhibition in breast cancer models triggers compensatory expression of other isoforms [252]. In the fetal membranes and placenta, AQP1 knockdown reduced AQP9 but induced AQP8, highlighting that changes in one isoform may induce adjustments across others to maintain transport homeostasis [253]. Notably, AQP3 mRNA was also suppressed in AQP1-silenced cells, yet protein levels remained unchanged, showing that expression is regulated at several levels, including post-transcriptional, translational, and post-translational [253]. Overall, the results of this study, along with literature data, suggest that aquaporins act within a regulatory network, where changing one isoform can influence others at the transcriptional, translational, or functional level. Such regulation preserves transport capacity under both normal and pathological conditions.

Cancer-specific adaptation to prolonged low-dose oxidative stress induced coordinated changes in aquaporin expression and NRF2 activity, and modulation experiments together with *in silico* predictions partly supported a role of NRF2 in regulating aquaporin expression or function, although this appeared cell-type specific. What is clear is that aquaporins are tightly regulated, with compensatory changes across isoforms ensuring that overall transport remains balanced. In cancer, aquaporins strengthen redox signaling and, along with NRF2, enable cells to adapt to persistent oxidative stress. By upregulating certain aquaporins, cancer cells can fine-tune transport to support tumorigenesis while at the same time limiting damage from ROS-inducing therapies. This may explain their frequent association with poor prognosis and therapy resistance, and highlight them as potential therapeutic targets in addition to their proposed role as prognostic biomarkers.

### 5. CONCLUSIONS

- 1. Cancer-specific adaptations were observed after adaptation to prolonged low-dose H<sub>2</sub>O<sub>2</sub>. SUM159PT, SkBr3, and MCF7 cells adapted by increasing their viability and proliferation after exposure to prolonged low-dose H<sub>2</sub>O<sub>2</sub>, while MCF10A showed no difference. These changes were accompanied by increased AQP3 and AQP5 protein expression in SUM159PT and SkBr3, and AQP3 expression in MCF7, along with increased accumulation of NRF2 in the cancer cell nucleus. In contrast, MCF10A had no changes in aquaporin expression or NRF2 activity.
- 2. Genetic modulation of NRF2 did not produce a consistent change in NRF2 activity, and inhibition with ML385 was ineffective. Sulforaphane activated NRF2 in all tested cell lines. In SUM159PT, sulforaphane increased AQP3 expression and H<sub>2</sub>O<sub>2</sub> transport, while in SkBr3, it only increased H<sub>2</sub>O<sub>2</sub> transport. No effect was observed in MCF7 or MCF10A. *In silico* analysis identified NRF2 binding motifs near AQP3/AQP5 regulatory regions.
- 3. AQP3 overexpression/silencing and AQP5 silencing did not yield stable protein changes but did shift multiple other aquaporin isoforms, indicating compensatory regulation. Stable AQP5 overexpression increased H<sub>2</sub>O<sub>2</sub> transport in SUM159PT cells.

# 6. ACKNOWLEDGEMENTS

This study makes use of data generated by the ENCODE Consortium and the ENCODE production laboratories (Snyder Lab, Stanford). We acknowledge the ENCODE Consortium and the production laboratories that generated the data used in this study.



### 7. REFERENCES

- 1. Bray F, Laversanne M, Sung H, Ferlay J, Siegel RL, Soerjomataram I, Jemal A (2024) Global cancer statistics 2022: GLOBOCAN estimates of incidence and mortality worldwide for 36 cancers in 185 countries. CA Cancer J Clin 74:229–263
- 2. Tran KB, Lang JJ, Compton K, et al (2022) The global burden of cancer attributable to risk factors, 2010–19: a systematic analysis for the Global Burden of Disease Study 2019. The Lancet 400:563–591
- 3. Hanahan D (2022) Hallmarks of Cancer: New Dimensions. Cancer Discov 12:31–46
- 4. Hanahan D, Weinberg RA (2000) The Hallmarks of Cancer. Cell 100:57–70
- 5. Hanahan D, Weinberg RA (2011) Hallmarks of Cancer: The Next Generation. Cell 144:646–674
- 6. Harbeck N, Penault-Llorca F, Cortes J, Gnant M, Houssami N, Poortmans P, Ruddy K, Tsang J, Cardoso F (2019) Breast cancer. Nat Rev Dis Primers 5:1–31
- 7. Pearlman M, Jeudy M, Chelmow D (2017) Breast Cancer Risk Assessment and Screening in Average-Risk Women. Obstetrics and Gynecology 130:241–243
- 8. Brierley J, Gospodarowicz MD, Wittekind CT (2017) TNM Classification of Malignant Tumors International Union Against Cancer. Wiley pp57-62
- 9. Makki J (2015) Diversity of Breast Carcinoma: Histological Subtypes and Clinical Relevance. Clin Med Insights Pathol 8:23
- 10. Rosai J (2011) Rosai and Ackerman's Surgical Pathology, 10th ed. Elsevier, Philadelphia
- Orrantia-Borunda E, Anchondo-Nuñez P, Acuña-Aguilar LE, Gómez-Valles FO, Ramírez-Valdespino CA (2022) Breast Cancer. Breast Cancer. https://doi.org/10.36255/EXON-PUBLICATIONS-BREAST-CANCER-SUBTYPES
- Ward ZJ, Atun R, Hricak H, Asante K, McGinty G, Sutton EJ, Norton L, Scott AM, Shulman LN (2021) The impact of scaling up access to treatment and imaging modalities on global disparities in breast cancer survival: a simulation-based analysis. Lancet Oncol 22:1301–1311
- 13. Sies H (2019) Oxidative Stress: Eustress and Distress in Redox Homeostasis. Stress: Physiology, Biochemistry, and Pathology Handbook of Stress Series, Volume 3 153–163
- 14. De Almeida AJPO, De Oliveira JCPL, Da Silva Pontes LV, De Souza Júnior JF, Gonçalves TAF, Dantas SH, De Almeida Feitosa MS, Silva AO, De Medeiros IA (2022) ROS: Basic Concepts, Sources, Cellular Signaling, and its Implications in Aging Pathways. Oxid Med Cell Longev 2022:1225578
- 15. Herb M, Schramm M (2021) Functions of ROS in Macrophages and Antimicrobial Immunity. Antioxidants 10:313

- 16. Murphy MP (2009) How mitochondria produce reactive oxygen species. Biochemical Journal 417:1–13
- 17. Lambeth JD (2004) NOX enzymes and the biology of reactive oxygen. Nat Rev Immunol 4:181–189
- 18. Schieber M, Chandel NS (2014) ROS Function in Redox Signaling and Oxidative Stress. Current Biology 24:R453–R462
- 19. Rhee SG (2006) H2O2, a necessary evil for cell signaling. Science (1979) 312:1882–1883
- 20. Veal EA, Day AM, Morgan BA (2007) Hydrogen Peroxide Sensing and Signaling. Mol Cell 26:1–14
- 21. Sies H, Jones DP (2020) Reactive oxygen species (ROS) as pleiotropic physiological signalling agents. Nature Reviews Molecular Cell Biology 2020 21:7 21:363–383
- 22. Roscoe JM, Sevier CS (2020) Pathways for sensing and responding to hydrogen peroxide at the endoplasmic reticulum. Cells 9:1–21
- 23. Pizzino G, Irrera N, Cucinotta M, Pallio G, Mannino F, Arcoraci V, Squadrito F, Altavilla D, Bitto A (2017) Oxidative Stress: Harms and Benefits for Human Health. Oxid Med Cell Longev 2017:8416763
- 24. Rojo de la Vega M, Chapman E, Zhang DD (2018) NRF2 and the Hallmarks of Cancer. Cancer Cell 34:21–43
- 25. Mitsuishi Y, Motohashi H, Yamamoto M (2012) The Keap1-Nrf2 system in cancers: stress response and anabolic metabolism. Front Oncol. https://doi.org/10.3389/FONC.2012.00200
- 26. Itoh K, Wakabayashi N, Katoh Y, Ishii T, Igarashi K, Engel JD, Yamamoto M (1999) Keap1 represses nuclear activation of antioxidant responsive elements by Nrf2 through binding to the amino-terminal Neh2 domain. Genes Dev 13:76–86
- 27. Itoh K, Wakabayashi N, Katoh Y, Ishii T, O'Connor T, Yamamoto M (2003) Keap1 regulates both cytoplasmic-nuclear shuttling and degradation of Nrf2 in response to electrophiles. Genes to Cells 8:379–391
- 28. Tonelli C, Chio IIC, Tuveson DA (2018) Transcriptional Regulation by Nrf2. Antioxid Redox Signal 29:1727
- 29. Itoh K, Chiba T, Takahashi S, et al (1997) An Nrf2/small Maf heterodimer mediates the induction of phase II detoxifying enzyme genes through antioxidant response elements. Biochem Biophys Res Commun 236:313–322
- 30. Alam J, Stewart D, Touchard C, Boinapally S, Choi AMK, Cook JL (1999) Nrf2, a Cap'n'Collar transcription factor, regulates induction of the heme oxygenase-1 gene. Journal of Biological Chemistry 274:26071–26078
- 31. Rushmore TH, Morton MR, Pickett CB (1991) The antioxidant responsive element. Activation by oxidative stress and identification of the DNA consensus sequence required for functional activity. Journal of Biological Chemistry 266:11632–11639

- 32. Nishinaka T, Miura T, Okumura M, Nakao F, Nakamura H, Terada T (2011) Regulation of aldo–keto reductase AKR1B10 gene expression: Involvement of transcription factor Nrf2. Chem Biol Interact 191:185–191
- 33. Rada P, Rojo AI, Chowdhry S, McMahon M, Hayes JD, Cuadrado A (2011) SCF/β-TrCP Promotes Glycogen Synthase Kinase 3-Dependent Degradation of the Nrf2 Transcription Factor in a Keap1-Independent Manner. Mol Cell Biol 31:1121–1133
- 34. Dhakshinamoorthy S, Jain AK, Bloom DA, Jaiswal AK (2005) Bach1 competes with Nrf2 leading to negative regulation of the antioxidant response element (ARE)-mediated NAD(P)H:quinone oxidoreductase 1 gene expression and induction in response to antioxidants. Journal of Biological Chemistry 280:16891–16900
- 35. Kageyama S, Gudmundsson SR, Sou YS, et al (2021) p62/SQSTM1-droplet serves as a platform for autophagosome formation and anti-oxidative stress response. Nat Commun 12:1–16
- 36. Cuadrado A, Rojo AI, Wells G, et al (2019) Therapeutic targeting of the NRF2 and KEAP1 partnership in chronic diseases. Nat Rev Drug Discov 18:295–317
- 37. Szatrowski2 TP, Nathan CF Production of Large Amounts of Hydrogen Peroxide by Human Tumor Cells1.
- 38. Liou GY, Storz P (2010) Reactive oxygen species in cancer. Free Radic Res 44:479-496
- 39. Cairns RA, Harris IS, Mak TW (2011) Regulation of cancer cell metabolism. Nat Rev Cancer 11:85–95
- 40. Storz P (2005) Reactive oxygen species in tumor progression. Frontiers in Bioscience 10:1881–1896
- 41. Gupta SC, Hevia D, Patchva S, Park B, Koh W, Aggarwal BB (2012) Upsides and Downsides of Reactive Oxygen Species for Cancer: The Roles of Reactive Oxygen Species in Tumorigenesis, Prevention, and Therapy. Antioxid Redox Signal 16:1295
- 42. Cichon MA, Radisky DC (2014) ROS-induced epithelial-mesenchymal transition in mammary epithelial cells is mediated by NF-κB-dependent activation of Snail. Oncotarget 5:2827
- 43. Liu B, Chen Y, St. Clair DK (2008) ROS and p53: A versatile partnership. Free Radic Biol Med 44:1529–1535
- 44. Chen X, Song M, Zhang B, Zhang Y (2016) Reactive Oxygen Species Regulate T Cell Immune Response in the Tumor Microenvironment. Oxid Med Cell Longev 2016:1580967
- 45. Sepich-Poore GD, Zitvogel L, Straussman R, Hasty J, Wargo JA, Knight R (2021) The microbiome and human cancer. Science (1979). https://doi.org/10.1126/SCIENCE.ABC4552/ASSET/9A5424A1-02C6-41DE-A7CC-F4A5C993F947/ASSETS/GRAPHIC/371\_ABC4552\_F6.JPEG

- 46. Yaswen P, MacKenzie KL, Keith WN, et al (2015) Therapeutic targeting of replicative immortality. Semin Cancer Biol 35:S104–S128
- 47. Takasugi M, Yoshida Y, Hara E, Ohtani N (2023) The role of cellular senescence and SASP in tumour microenvironment. FEBS J 290:1348–1361
- 48. Tudek B, Winczura A, Janik J, Siomek A, Foksinski M, Oliński R (2010) Involvement of oxidatively damaged DNA and repair in cancer development and aging. Am J Transl Res 2:254
- 49. Milkovic L, Gasparovic AC, Zarkovic N (2015) Overview on major lipid peroxidation bioactive factor 4-hydroxynonenal as pluripotent growth-regulating factor. Free Radic Res 49:850–860
- 50. Baird L, Yamamoto M (2020) The Molecular Mechanisms Regulating the KEAP1-NRF2 Pathway. Mol Cell Biol 40:e00099-20
- 51. Wang X, Campos CR, Peart JC, Smith LK, Boni JL, Cannon RE, Miller DS (2014) Nrf2 upregulates ATP binding cassette transporter expression and activity at the bloodbrain and blood-spinal cord barriers. Journal of Neuroscience 34:8585–8593
- 52. Wu S, Lu H, Bai Y (2019) Nrf2 in cancers: A double-edged sword. Cancer Med 8:2252–2267
- 53. Brandl N, Seitz R, Sendtner N, Müller M, Gülow K (2025) Living on the Edge: ROS Homeostasis in Cancer Cells and Its Potential as a Therapeutic Target. Antioxidants 14:1002
- 54. Denker BM, Smith BL, Kuhajda FP, Agres P (1988) Identification, Purification, and Partial Characterization of a Novel Mr 28,000 Integral Membrane Protein from Erythrocytes and Renal Tubules\*. J Biol Chem 263:15634–15642
- 55. Agre P (2005) Aquaporin water channels. Biosci Rep 24:127–163
- 56. Brown D (2017) The Discovery of Water Channels (Aquaporins). Ann Nutr Metab 70:37–42
- 57. Chaumont F, Barrieu F, Wojcik E, Chrispeels MJ, Jung R (2001) Aquaporins Constitute a Large and Highly Divergent Protein Family in Maize. Plant Physiol 125:1206
- 58. Jung+ JS, Preston+ GM, Smith+ BL, Gugginoll WB, Agres P (1994) Molecular Structure of the Water Channel through Aquaporin CHIP. J Biol Chem 269:14648–14654
- 59. Verkman AS, Mitra AK (2000) Structure and function of aquaporin water channels. Am J Physiol Renal Physiol 278:13–28
- 60. Murata K, Mitsuoka K, Hirai T, Walz T, Agrek P, Bernard Heymann J, Engel A, Fujiyoshi Y, Mu ME (2000) Structural determinants of water permeation through aquaporin-1. Nature 407:
- 61. Hub JS, De Groot BL (2008) Mechanism of selectivity in aquaporins and aquaglyceroporins. Proc Natl Acad Sci U S A 105:1198–1203

- 62. Ozu M, Galizia L, Acuña C, Amodeo G (2018) Aquaporins: More Than Functional Monomers in a Tetrameric Arrangement. Cells 7:209
- 63. Ishibashi K (2006) Aquaporin subfamily with unusual NPA boxes. Biochimica et Biophysica Acta (BBA) Biomembranes 1758:989–993
- 64. Anthony TL, Brooks HL, Boassa D, Leonov S, Yanochko GM, Regan JW, Yool AJ (2000) Cloned Human Aquaporin-1 Is a Cyclic GMP-Gated Ion Channel. Mol Pharmacol 57:576–588
- 65. Uehleln N, Lovisolo C, Siefritz F, Kaldenhoff R (2003) The tobacco aquaporin NtAQP1 is a membrane CO2 pore with physiological functions. Nature 425:734–737
- 66. Herrera M, Hong NJ, Garvin JL (2006) Aquaporin-1 transports NO across cell membranes. Hypertension 48:157–164
- 67. Liu Z, Shen J, Carbrey JM, Mukhopadhyay R, Agre P, Rosen BP (2002) Arsenite transport by mammalian aquaglyceroporins AQP7 and AQP9. Proc Natl Acad Sci U S A 99:6053–6058
- 68. Bienert GP, Møller ALB, Kristiansen KA, Schulz A, Møller IM, Schjoerring JK, Jahn TP (2007) Specific aquaporins facilitate the diffusion of hydrogen peroxide across membranes. Journal of Biological Chemistry 282:1183–1192
- 69. Almasalmeh A, Krenc D, Wu B, Beitz E (2014) Structural determinants of the hydrogen peroxide permeability of aquaporins. FEBS Journal 281:647–656
- 70. Miller EW, Dickinson BC, Chang CJ (2010) Aquaporin-3 mediates hydrogen peroxide uptake to regulate downstream intracellular signaling. Proc Natl Acad Sci U S A 107:15681–15686
- 71. Rodrigues C, Mósca AF, Martins AP, Nobre T, Prista C, Antunes F, Gasparovic AC, Soveral G (2016) Rat Aquaporin-5 Is pH-Gated Induced by Phosphorylation and Is Implicated in Oxidative Stress. International Journal of Molecular Sciences 2016, Vol 17, Page 2090 17:2090
- 72. Rodrigues C, Pimpão C, Mósca AF, Coxixo AS, Lopes D, Da Silva IV, Pedersen PA, Antunes F, Soveral G (2019) Human aquaporin-5 facilitates hydrogen peroxide permeation affecting adaption to oxidative stress and cancer cell migration. Cancers (Basel) 11:932
- 73. Pellavio G, Martinotti S, Patrone M, Ranzato E, Laforenza U (2022) Aquaporin-6 May Increase the Resistance to Oxidative Stress of Malignant Pleural Mesothelioma Cells. Cells. https://doi.org/10.3390/CELLS11121892,
- 74. Watanabe S, Moniaga CS, Nielsen S, Hara-Chikuma M (2016) Aquaporin-9 facilitates membrane transport of hydrogen peroxide in mammalian cells. Biochem Biophys Res Commun 471:191–197
- 75. Bestetti S, Galli M, Sorrentino I, Pinton P, Rimessi A, Sitia R, Medraño-Fernandez I (2020) Human aquaporin-11 guarantees efficient transport of H2O2 across the endoplasmic reticulum membrane. Redox Biol. https://doi.org/10.1016/j.redox.2019.101326

- 76. Jung HJ, Kwon TH (2016) Molecular mechanisms regulating aquaporin-2 in kidney collecting duct. Am J Physiol Renal Physiol 311:F1318–F1328
- 77. Jablonski EM, McConnell NA, Hughes FM, Huet-Hudson YM (2003) Estrogen Regulation of Aquaporins in the Mouse Uterus: Potential Roles in Uterine Water Movement. Biol Reprod 69:1481–1487
- 78. Huang YT, Zhou J, Shi S, Xu HY, Qu F, Zhang D, Chen YD, Yang J, Huang HF, Sheng JZ (2015) Identification of Estrogen Response Element in Aquaporin-3 Gene that Mediates Estrogen-induced Cell Migration and Invasion in Estrogen Receptor-positive Breast Cancer. Scientific Reports 2015 5:1 5:1–13
- 79. Fan Y, Song TR, Wei Q, et al (2020) Modulatory effect of aquaporin 5 on estrogen-induced epithelial-mesenchymal transition in prostate epithelial cells. Chin Med J (Engl) 134:448
- 80. dos Passos Junior RR, de Freitas RA, Reppetti J, Medina Y, Dela Justina V, Bach CW, Bomfim GF, Lima VV, Damiano AE, Giachini FR (2021) High Levels of Tumor Necrosis Factor-Alpha Reduce Placental Aquaporin 3 Expression and Impair in vitro Trophoblastic Cell Migration. Front Physiol. https://doi.org/10.3389/FPHYS.2021.696495,
- 81. Li A, Lu D, Zhang Y, Li J, Fang Y, Li F, Sun J (2013) Critical role of aquaporin-3 in epidermal growth factor-induced migration of colorectal carcinoma cells and its clinical significance. Oncol Rep 29:535–540
- 82. Yuan JL, Dong JX, Li W, Zu YM, Guo YJ, Zhang Y, Chen Y (2025) Association between aquaporin 3 and transforming growth factor-beta 1 levels in decidual tissue and serum of patients with missed abortion. Front Med (Lausanne) 12:1540257
- 83. Procino G, Carmosino M, Marin O, et al (2003) Ser-256 phosphorylation dynamics of aquaporin 2 during maturation from the endoplasmic reticulum to the vesicular compartment in renal cells. FASEB Journal 17:1–24
- 84. McCoy ES, Haas BR, Sontheimer H (2009) Water Permeability Through Aquaporin-4 is regulated by Protein Kinase C and becomes Rate-Limiting for Glioma Invasion. Neuroscience 168:971
- 85. Ishikawa Y, Cho G, Yuan Z, Inoue N, Nakae Y (2006) Aquaporin-5 water channel in lipid rafts of rat parotid glands. Biochimica et Biophysica Acta (BBA) Biomembranes 1758:1053–1060
- 86. Zelenina M, Bondar AA, Zelenin S, Aperia A (2003) Nickel and extracellular acidification inhibit the water permeability of human aquaporin-3 in lung epithelial cells. Journal of Biological Chemistry 278:30037–30043
- 87. Mósca AF, de Almeida A, Wragg D, Martins AP, Sabir F, Leoni S, Moura TF, Prista C, Casini A, Soveral G (2018) Molecular Basis of Aquaporin-7 Permeability Regulation by pH. Cells 7:207

- 88. Gotfryd K, Mósca AF, Missel JW, et al (2018) Human adipose glycerol flux is regulated by a pH gate in AQP10. Nat Commun. https://doi.org/10.1038/S41467-018-07176-Z,
- 89. Kreida S, Roche JV, Missel JW, Al-Jubair T, Hagströmer CJ, Wittenbecher V, Linse S, Gourdon P, Törnroth-Horsefield S (2024) The role of phosphorylation in calmodulin-mediated gating of human AQP0. Biochemical Journal 481:17–32
- 90. Chepelinsky AB (2009) Structural Function of MIP/Aquaporin 0 in the Eye Lens; Genetic Defects Lead to Congenital Inherited Cataracts. Handb Exp Pharmacol 190:265–297
- 91. Varadaraj K, Kumari SS, Patil R, Wax MB, Mathias RT (2008) Functional characterization of a human aquaporin 0 mutation that leads to a congenital dominant lens cataract. Exp Eye Res 87:9
- 92. Gerometta R, Candia OA (2016) A decrease in the permeability of aquaporin zero as a possible cause for presbyopia. Med Hypotheses 86:132–134
- 93. Schey KL, Gletten RB, O'Neale CVT, Wang Z, Petrova RS, Donaldson PJ (2022) Lens Aquaporins in Health and Disease: Location is Everything! Front Physiol 13:882550
- 94. Oshio K, Watanabe H, Song Y, Verkman AS, Manley GT (2005) Reduced cerebrospinal fluid production and intracranial pressure in mice lacking choroid plexus water channel Aquaporin-1. The FASEB Journal 19:76–78
- 95. Hua Y, Ying X, Qian Y, Liu H, Lan Y, Xie A, Zhu X (2019) Physiological and pathological impact of AQP1 knockout in mice. Biosci Rep 39:BSR20182303
- 96. Ma T, Yang B, Gillespie A, Carlson EJ, Epstein CJ, Verkman AS (1998) Severely impaired urinary concentrating ability in transgenic mice lacking aquaporin-1 water channels. Journal of Biological Chemistry 273:4296–4299
- 97. Saadoun S, Papadopoulos MC, Davies DC, Bell BA, Krishna S (2002) Increased aquaporin I water channel expression in human brain tumours. Br J Cancer 87:621–623
- 98. Chen Y, Tachibana O, Oda M, Xu R, Hamada JI, Yamashita J, Hashimoto N, Takahashi JA (2006) Increased expression of aquaporin 1 in human hemangioblastomas and its correlation with cyst formation. J Neurooncol 80:219–225
- 99. Vacca A, Frigeri A, Ribatti D, Nicchia GP, Nico B, Ria R, Svelto M, Dammacco F (2001) Microvessel overexpression of aquaporin 1 parallels bone marrow angiogenesis in patients with active multiple myeloma. Br J Haematol 113:415–421
- 100. Moon C, Soria JC, Jang SJ, Lee J, Hoque MO, Sibony M, Trink B, Chang YS, Sidransky D, Mao L (2003) Involvement of aquaporins in colorectal carcinogenesis. Oncogene 22:6699–6703
- 101. Pan H, Sun CC, Zhou CY, Huang HF (2008) Expression of aquaporin-1 in normal, hyperplasic, and carcinomatous endometria. International Journal of Gynecology and Obstetrics 101:239–244

- 102. Yang JH, Shi YF, Chen XD, Qi WJ (2006) The influence of aquaporin-1 and microvessel density on ovarian carcinogenesis and ascites formation. International Journal of Gynecological Cancer 16:400–405
- 103. Hoque MO, Soria JC, Woo J, et al (2006) Aquaporin 1 is overexpressed in lung cancer and stimulates NIH-3T3 cell proliferation and anchorage-independent growth.

  American Journal of Pathology 168:1345–1353
- 104. Otterbach F, Callies R, Kimmig R, Schmid KW, Bánkfalvi A (2008) Aquaporin-1-expression bei invasiven mammakarzinomen. Pathologe 29:357–362
- 105. Kang BW, Kim JG, Lee SJ, Chae YS, Jeong JY, Yoon GS, Park SY, Kim HJ, Park JS, Choi GS (2015) Expression of aquaporin-1, aquaporin-3, and aquaporin-5 correlates with nodal metastasis in colon cancer. Oncology (Switzerland) 88:369–376
- 106. MacHida Y, Ueda Y, Shimasaki M, Sato K, Sagawa M, Katsuda S, Sakuma T (2011) Relationship of aquaporin 1, 3, and 5 expression in lung cancer cells to cellular differentiation, invasive growth, and metastasis potential. Hum Pathol 42:669–678
- 107. Otterbach F, Callies R, Adamzik M, Kimmig R, Siffert W, Schmid KW, Bankfalvi A (2010) Aquaporin 1 (AQP1) expression is a novel characteristic feature of a particularly aggressive subgroup of basal-like breast carcinomas. Breast Cancer Res Treat 120:67–76
- 108. Sato K, Miyamoto M, Takano M, Furuya K, Tsuda H (2020) Different Prognostic Implications of Aquaporin-1 and Aquaporin-5 Expression among Different Histological Types of Ovarian Carcinoma. Pathology and Oncology Research 26:263– 271
- 109. Yoshida T, Hojo S, Sekine S, Sawada S, Okumura T, Nagata T, Shimada Y, Tsukada K (2013) Expression of aquaporin-1 is a poor prognostic factor for stage II and III colon cancer. Mol Clin Oncol 1:953–958
- 110. Deen PMT, Verdijk MAJ, Knoers NVAM, Wieringa B, Monnens LAH, van Os CH, van Oost BA (1994) Requirement of Human Renal Water Channel Aquaporin-2 for Vasopressin-dependent Concentration of Urine. Science (1979) 264:92–95
- 111. Wang Y, Yin JY, Li XP, Chen J, Qian CY, Zheng Y, Fu YL, Chen ZY, Zhou HH, Liu ZQ (2014) The association of transporter genes polymorphisms and lung cancer chemotherapy response. PLoS One. https://doi.org/10.1371/JOURNAL.PONE.0091967,
- 112. Zou LB, Zhang RJ, Tan YJ, et al (2011) Identification of estrogen response element in the aquaporin-2 gene that mediates estrogen-induced cell migration and invasion in human endometrial carcinoma. Journal of Clinical Endocrinology and Metabolism. https://doi.org/10.1210/JC.2011-0426,
- 113. Ma T, Song Y, Yang B, Gillespie A, Carlson EJ, Epstein CJ, Verkman AS (2000) Nephrogenic diabetes insipidus in mice lacking aquaporin-3 water channels. Proc Natl Acad Sci U S A 97:4386–4391

- 114. Huynh N V., Rehage C, Nguyen P-H, Hyndman KA (2024) Can Acetylation of Lysine 282 of Aquaporin 3 Improve Urinary Concentration in Mice with Lithium-Induced Nephrogenic Diabetes Insipidus? Journal of the American Society of Nephrology. https://doi.org/10.1681/ASN.2024CSRH8Q8K
- 115. Hara M, Ma T, Verkman AS (2002) Selectively reduced glycerol in skin of aquaporin-3-deficient mice may account for impaired skin hydration, elasticity, and barrier recovery. Journal of Biological Chemistry 277:46616–46621
- 116. Niu D, Kondo T, Nakazawa T, Yamane T, Mochizuki K, Kawasaki T, Matsuzaki T, Takata K, Katoh R (2012) Expression of Aquaporin3 in human neoplastic tissues. Histopathology 61:543–551
- 117. Hara-Chikuma M, Verkman AS (2008) Prevention of Skin Tumorigenesis and Impairment of Epidermal Cell Proliferation by Targeted Aquaporin-3 Gene Disruption. Mol Cell Biol 28:326–332
- 118. Liu YL, Matsuzaki T, Nakazawa T, et al (2007) Expression of aquaporin 3 (AQP3) in normal and neoplastic lung tissues. Hum Pathol 38:171–178
- 119. Li A, Lu D, Zhang Y, Li J, Fang Y, Li F, Sun J (2013) Critical role of aquaporin-3 in epidermal growth factor-induced migration of colorectal carcinoma cells and its clinical significance. Oncol Rep 29:535–540
- 120. Ismail M, Bokaee S, Davies J, Harrington KJ, Pandha H (2009) Inhibition of the aquaporin 3 water channel increases the sensitivity of prostate cancer cells to cryotherapy. Br J Cancer 100:1889–1895
- 121. Li A, Lu D, Zhang Y, Li J, Fang Y, Li F, Sun J (2013) Critical role of aquaporin-3 in epidermal growth factor-induced migration of colorectal carcinoma cells and its clinical significance. Oncol Rep 29:535–540
- 122. Satooka H, Hara-Chikuma M (2016) Aquaporin-3 Controls Breast Cancer Cell Migration by Regulating Hydrogen Peroxide Transport and Its Downstream Cell Signaling. Mol Cell Biol 36:1206–1218
- 123. Direito I, Paulino J, Vigia E, Brito MA, Soveral G (2017) Differential expression of aquaporin-3 and aquaporin-5 in pancreatic ductal adenocarcinoma. J Surg Oncol 115:980–996
- 124. Rubenwolf PC, Otto W, Denzinger S, Hofstädter F, Wieland W, Georgopoulos NT (2014) Expression of aquaporin water channels in human urothelial carcinoma: Correlation of AQP3 expression with tumour grade and stage. World J Urol 32:991–997
- 125. Verkman AS, Ratelade J, Rossi A, Zhang H, Tradtrantip L (2011) Aquaporin-4: Orthogonal array assembly, CNS functions, and role in neuromyelitis optica. Acta Pharmacol Sin 32:702–710
- 126. Lennon VA, Kryzer TJ, Pittock SJ, Verkman AS, Hinson SR (2005) IgG marker of optic-spinal multiple sclerosis binds to the aquaporin-4 water channel. Journal of Experimental Medicine 202:473–477

- 127. Saadoun S, Papadopoulos MC, Davies DC, Krishna S, Bell BA (2002) Aquaporin-4 expression is increased in oedematous human brain tumours. J Neurol Neurosurg Psychiatry 72:262–265
- 128. Ding T, Ma Y, Li W, Liu X, Ying G, Fu L, Gu F (2011) Role of aquaporin-4 in the regulation of migration and invasion of human glioma cells. Int J Oncol 38:1521–1531
- 129. Mcferrin MB, Sontheimer H (2006) A role for ion channels in glioma cell invasion. Neuron Glia Biol 2:39–49
- 130. Soelberg K, Larsen SR, Moerch MT, et al (2016) Aquaporin-4 IgG autoimmune syndrome and immunoreactivity associated with thyroid cancer. Neurol Neuroimmunol Neuroinflamm 3:e252
- 131. Yamamoto A, Shimizu H, Takiguchi K, et al (2024) The Expression and Role of Aquaporin 4 in Colon Cancer. Anticancer Res 44:567–573
- 132. Fu L, Zhao Z, Zhao S, Zhang M, Teng X, Wang L, Yang T (2024) The involvement of aquaporin 5 in the inflammatory response of primary Sjogren's syndrome dry eye: potential therapeutic targets exploration. Front Med (Lausanne) 11:1439888
- 133. Song Y, Sonawane N, Verkman AS (2002) Localization of aquaporin-5 in sweat glands and functional analysis using knockout mice. Journal of Physiology 541:561–568
- 134. Ma T, Song Y, Gillespie A, Carlson EJ, Epstein CJ, Verkman AS (1999) Defective secretion of saliva in transgenic mice lacking aquaporin-5 water channels. Journal of Biological Chemistry 274:20071–20074
- 135. Sasaki Y, Tsubota K, Kawedia JD, Menon AG, Yasui M (2007) The Difference of Aquaporin 5 Distribution in Acinar and Ductal Cells in Lacrimal and Parotid Glands. Curr Eye Res 32:923–929
- 136. Yang JH, Shi YF, Cheng Q, Deng L (2006) Expression and localization of aquaporin-5 in the epithelial ovarian tumors. Gynecol Oncol 100:294–299
- 137. Sung KK, Young KC, Woo J, Myoung SK, Jong CP, Lee J, Soria JC, Se JJ, Sidransky D, Moon C (2008) Role of human aquaporin 5 in colorectal carcinogenesis. American Journal of Pathology 173:518–525
- 138. Chae YK, Woo J, Kim MJ, et al (2008) Expression of aquaporin 5 (AQP5) promotes tumor invasion in human non small cell lung cancer. PLoS One. https://doi.org/10.1371/JOURNAL.PONE.0002162,
- 139. Zhang Z, Chen Z, Song Y, Zhang P, Hu J, Bai C (2010) Expression of aquaporin 5 increases proliferation and metastasis potential of lung cancer. Journal of Pathology 221:210–220
- 140. Jung HJ, Park JY, Jeon HS, Kwon TH (2011) Aquaporin-5: A marker protein for proliferation and migration of human breast cancer cells. PLoS One. https://doi.org/10.1371/JOURNAL.PONE.0028492,

- Jung HJ, Park JY, Jeon HS, Kwon TH (2011) Aquaporin-5: a marker protein for proliferation and migration of human breast cancer cells. PLoS One. https://doi.org/10.1371/JOURNAL.PONE.0028492,
- 142. Zhang T, Zhao C, Chen D, Zhou Z (2012) Overexpression of AQP5 in cervical cancer: Correlation with clinicopathological features and prognosis. Medical Oncology 29:1998–2004
- 143. Huang YH, Zhou XY, Wang HM, Xu H, Chen J, Lv NH (2013) Aquaporin 5 promotes the proliferation and migration of human gastric carcinoma cells. Tumor Biology 34:1743–1751
- 144. Yasul M, Hazama A, Kwon TH, Nielsen S, Guggino WB, Agre P (1999) Rapid gating and artion permeability of an intracellular aquaporin. Nature 402:184–187
- 145. Ma J, Zhou C, Yang J, Ding X, Zhu Y, Chen X (2016) Expression of AQP6 and AQP8 in epithelial ovarian tumor. J Mol Histol 47:129–134
- 146. Lebeck J (2014) Metabolic impact of the glycerol channels AQP7 and AQP9 in adipose tissue and liver. J Mol Endocrinol 52:R165–R178
- 147. Sohara E, Rai T, Miyazaki JI, Verkman AS, Sasaki S, Uchida S (2005) Defective water and glycerol transport in the proximal tubules of AQP7 knockout mice. Am J Physiol Renal Physiol 289:1195–1200
- 148. Dai C, Charlestin V, Wang M, et al (2020) Aquaporin-7 regulates the response to cellular stress in breast cancer. Cancer Res 80:4071–4086
- 149. Burghardt B, Nielsen S, Steward MC (2006) The role of aquaporin water channels in fluid secretion by the exocrine pancreas. Journal of Membrane Biology 210:143–53
- 150. Calamita G, Mazzone A, Bizzoca A, Cavalier A, Cassano G, Thomas D, Svelto M (2001) Expression and immunolocalization of the aquaporin-8 water channel in rat gastrointestinal tract. Eur J Cell Biol 80:711–719
- 151. Saparov SM, Liu K, Agre P, Pohl P (2006) Fast and Selective Ammonia Transport by Aquaporin-8. J Biol Chem 282:5296
- 152. Vieceli Dalla Sega F, Prata C, Zambonin L, Angeloni C, Rizzo B, Hrelia S, Fiorentini D (2017) Intracellular cysteine oxidation is modulated by aquaporin-8-mediated hydrogen peroxide channeling in leukaemia cells. BioFactors 43:232–242
- 153. Vieceli Dalla Sega F, Zambonin L, Fiorentini D, Rizzo B, Caliceti C, Landi L, Hrelia S, Prata C (2014) Specific aquaporins facilitate Nox-produced hydrogen peroxide transport through plasma membrane in leukaemia cells. Biochim Biophys Acta Mol Cell Res 1843:806–814
- 154. Rojek AM, Skowronski MT, Füchtbauer EM, Füchtbauer AC, Fenton RA, Agre P, Frøkiær J, Nielsen S (2007) Defective glycerol metabolism in aquaporin 9 (AQP9) knockout mice. Proc Natl Acad Sci U S A 104:3609–3614

- 155. Chen Q, Zhu L, Zheng B, Wang J, Song X, Zheng W, Wang L, Yang D, Wang J (2016) Effect of AQP9 Expression in Androgen-Independent Prostate Cancer Cell PC3. International Journal of Molecular Sciences 2016, Vol 17, Page 738 17:738
- 156. Öberg F, Sjöhamn J, Fischer G, Moberg A, Pedersen A, Neutze R, Hedfalk K (2011) Glycosylation Increases the Thermostability of Human Aquaporin 10 Protein. Journal of Biological Chemistry 286:31915–31923
- 157. Laforenza U, Scaffino MF, Gastaldi G (2013) Aquaporin-10 Represents an Alternative Pathway for Glycerol Efflux from Human Adipocytes. PLoS One 8:e54474
- 158. Zhu L, Ma N, Wang B, Wang L, Zhou C, Yan Y, He J, Ren Y (2019) Significant prognostic values of aquaporin mRNA expression in breast cancer. Cancer Manag Res 11:1503
- 159. Okada S, Misaka T, Tanaka Y, Matsumoto I, Ishibashi K, Sasaki S, Abe K (2008) Aquaporin-11 knockout mice and polycystic kidney disease animals share a common mechanism of cyst formation. The FASEB Journal 22:3672–3684
- 160. Morishita Y, Matsuzaki T, Hara-chikuma M, et al (2005) Disruption of Aquaporin-11 Produces Polycystic Kidneys following Vacuolization of the Proximal Tubule. Mol Cell Biol 25:7770
- 161. Inoue Y, Sohara E, Kobayashi K, et al (2014) Aberrant glycosylation and localization of polycystin-1 cause polycystic kidney in an AQP11 knockout model. Journal of the American Society of Nephrology 25:2789–2799
- 162. Price ME, Fishler KP, Muff-Luett M, Mauch TJ, Brunelli L, Euteneuer JC (2023) Variants in AQP11 may result in autosomal recessive bilateral cystic renal dysgenesis. Am J Med Genet A 191:612–616
- 163. Itoh T, Rai T, Kuwahara M, Ko SBH, Uchida S, Sasaki S, Ishibashi K (2005) Identification of a novel aquaporin, AQP12, expressed in pancreatic acinar cells. Biochem Biophys Res Commun 330:832–838
- 164. Wang J, Feng L, Zhu Z, Zheng M, Wang D, Chen Z, Sun H (2015) Aquaporins as diagnostic and therapeutic targets in cancer: How far we are? J Transl Med. https://doi.org/10.1186/S12967-015-0439-7,
- 165. Papadopoulos MC, Saadoun S (2015) Key roles of aquaporins in tumor biology. Biochim Biophys Acta Biomembr 1848:2576–2583
- 166. Chow PH, Bowen J, Yool AJ (2020) Combined systematic review and transcriptomic analyses of mammalian aquaporin classes 1 to 10 as biomarkers and prognostic indicators in diverse cancers. Cancers (Basel) 12:1–31
- 167. Lee SJ, Kang BW, Kim JG, et al (2017) AQP5 Variants Affect Tumoral Expression of AQP5 and Survival in Patients with Early Breast Cancer. Oncology 92:153–160
- 168. Lee SJ, Chae YS, Kim JG, Kim WW, Jung JH, Park HY, Jeong JY, Park JY, Jung HJ, Kwon TH (2014) AQP5 expression predicts survival in patients with early breast cancer. Ann Surg Oncol 21:375–383

- 169. Zhu Z, Jiao L, Li T, Wang H, Wei W, Qian H (2018) Expression of AQP3 and AQP5 as a prognostic marker in triple-negative breast cancer. Oncol Lett 16:2661–2667
- 170. Kang S, Chae YS, Lee SJ, et al (2015) Aquaporin 3 Expression Predicts Survival in Patients with HER2-positive Early Breast Cancer. Anticancer Res 35:2775–82
- 171. Qin F, Zhang H, Shao Y, Liu X, Yang L, Huang Y, Fu L, Gu F, Ma Y (2016) Expression of aquaporin1, a water channel protein, in cytoplasm is negatively correlated with prognosis of breast cancer patients. Oncotarget 7:8143
- 172. Yin Z, Chen W, Yin J, Sun J, Xie Q, Wu M, Zeng F, Ren H (2021) RIPK1 is a negative mediator in Aquaporin 1-driven triple-negative breast carcinoma progression and metastasis. NPJ Breast Cancer 7:1–11
- 173. Guo Z, Zhang H, Liu X, Zhao Y, Chen Y, Jin J, Guo C, Zhang M, Gu F, Ma Y (2023) Water channel protein AQP1 in cytoplasm is a critical factor in breast cancer local invasion. Journal of Experimental and Clinical Cancer Research 42:1–25
- 174. Esteva-Font C, Jin BJ, Verkman AS (2014) Aquaporin-1 gene deletion reduces breast tumor growth and lung metastasis in tumor-producing MMTV-PyVT mice. FASEB J 28:1446–1453
- 175. Chong W, Zhang H, Guo Z, et al (2020) Aquaporin 1 promotes sensitivity of anthracycline chemotherapy in breast cancer by inhibiting β-catenin degradation to enhance TopoIIα activity. Cell Death Differ 28:382–400
- 176. Mobasheri A, Barrett-Jolley R (2014) Aquaporin Water Channels in the Mammary Gland: From Physiology to Pathophysiology and Neoplasia. J Mammary Gland Biol Neoplasia 19:91–102
- 177. Mlinarić M, Lučić I, Milković L, da Silva I V., Tartaro Bujak I, Musani V, Soveral G, Čipak Gašparović A (2023) AQP3-Dependent PI3K/Akt Modulation in Breast Cancer Cells. Int J Mol Sci 24:8133
- 178. Hara-Chikuma M, Watanabe S, Satooka H (2016) Involvement of aquaporin-3 in epidermal growth factor receptor signaling via hydrogen peroxide transport in cancer cells. Biochem Biophys Res Commun 471:603–609
- 179. Arif M, Kitchen P, Conner MT, et al (2018) Downregulation of aquaporin 3 inhibits cellular proliferation, migration and invasion in the MDA-MB-231 breast cancer cell line. Oncol Lett 16:713–720
- 180. Bystrup M, Login FH, Edamana S, Borgquist S, Tramm T, Kwon TH, Nejsum LN (2022) Aquaporin-5 in breast cancer. APMIS 130:253–260
- 181. Jang SJ, Moon C (2023) Aquaporin 5 (AQP5) expression in breast cancer and its clinicopathological characteristics. PLoS One. https://doi.org/10.1371/JOURNAL.PONE.0270752
- Jung HJ, Park JY, Jeon HS, Kwon TH (2011) Aquaporin-5: A marker protein for proliferation and migration of human breast cancer cells. PLoS One. https://doi.org/10.1371/JOURNAL.PONE.0028492,

- 183. Zhu Z, Li T, Wang H, Jiao L (2024) AQP5 promotes epithelial-mesenchymal transition and tumor growth through activating the Wnt/β-catenin pathway in triple-negative breast cancer. Mutat Res 29:111868
- 184. Li X, Pei B, Wang H, Tang C, Zhu W, Jin F (2018) Effect of AQP-5 silencing by siRNA interference on chemosensitivity of breast cancer cells. Onco Targets Ther 11:3359–3368
- 185. Li Y-B, Sun S-R, Han X-H (2016) Down-regulation of AQP4 Inhibits Proliferation, Migration and Invasion of Human Breast Cancer Cells. Folia Biol (Praha) 62:131–137
- 186. Dinkova-Kostova AT, Fahey JW, Kostov R V., Kensler TW (2017) KEAP1 and done? Targeting the NRF2 pathway with sulforaphane. Trends Food Sci Technol 69:257
- 187. De Ieso ML, Pei JV (2018) An accurate and cost-effective alternative method for measuring cell migration with the circular wound closure assay. Biosci Rep 38:20180698
- 188. Folch J, Lees M, Sloane Stanley GH (1957) A simple method for the isolation and purification of total lipides from animal tissues. Journal of Biological Chemistry 226:497–509
- 189. Mihaljević B, Katušin-Ražem B, Ražem D (1996) The reevaluation of the ferric thiocyanate assay for lipid hydroperoxides with special considerations of the mechanistic aspects of the response. Free Radic Biol Med 21:53–63
- 190. Bradford MM (1976) A rapid and sensitive method for the quantitation of microgram quantities of protein utilizing the principle of protein-dye binding. Anal Biochem 72:248–254
- 191. Livak KJ, Schmittgen TD (2001) Analysis of relative gene expression data using real-time quantitative PCR and the 2-ΔΔCT method. Methods 25:402–408
- 192. Perez G, Barber GP, Benet-Pages A, et al (2025) The UCSC Genome Browser database: 2025 update. Nucleic Acids Res 53:D1243–D1249
- 193. Fishilevich S, Nudel R, Rappaport N, et al (2017) GeneHancer: genome-wide integration of enhancers and target genes in GeneCards. Database 2017:1–17
- 194. Abascal F, Acosta R, Addleman NJ, et al (2022) Author Correction: Expanded encyclopaedias of DNA elements in the human and mouse genomes. Nature 605:E3–E3
- 195. Hammal F, De Langen P, Bergon A, Lopez F, Ballester B (2022) ReMap 2022: a database of Human, Mouse, Drosophila and Arabidopsis regulatory regions from an integrative analysis of DNA-binding sequencing experiments. Nucleic Acids Res 50:D316–D325
- 196. Rauluseviciute I, Riudavets-Puig R, Blanc-Mathieu R, et al (2024) JASPAR 2024: 20th anniversary of the open-access database of transcription factor binding profiles. Nucleic Acids Res 52:D174–D182

- 197. Grant CE, Bailey TL, Noble WS (2011) FIMO: scanning for occurrences of a given motif. Bioinformatics 27:1017–1018
- 198. Neganova M, Liu J, Aleksandrova Y, Klochkov S, Fan R (2021) Therapeutic Influence on Important Targets Associated with Chronic Inflammation and Oxidative Stress in Cancer Treatment. Cancers (Basel). https://doi.org/10.3390/CANCERS13236062
- 199. Hecht F, Cazarin JM, Lima CE, Faria CC, Leitão AA da C, Ferreira ACF, Carvalho DP, Fortunato RS (2016) Redox homeostasis of breast cancer lineages contributes to differential cell death response to exogenous hydrogen peroxide. Life Sci 158:7–13
- 200. JY B, SJ A, W H, DY N (2007) Peroxiredoxin I and II inhibit H2O2-induced cell death in MCF-7 cell lines. J Cell Biochem. https://doi.org/10.1002/JCB.21155
- 201. Stemberger MB, Ju JA, Thompson KN, et al (2023) Hydrogen Peroxide Induces α-Tubulin Detyrosination and Acetylation and Impacts Breast Cancer Metastatic Phenotypes. Cells 12:1266
- 202. Mahalingaiah PKS, Singh KP (2014) Chronic Oxidative Stress Increases Growth and Tumorigenic Potential of MCF-7 Breast Cancer Cells. PLoS One 9:e87371
- 203. Kwon S, Yang W, Moon D, Kim KS (2020) Biomarkers to quantify cell migration characteristics. Cancer Cell Int 20:217
- 204. Hurd TR, DeGennaro M, Lehmann R (2012) Redox regulation of cell migration and adhesion. Trends Cell Biol 22:107
- 205. Rodrigues C, Milkovic L, Bujak IT, Tomljanovic M, Soveral G, Cipak Gasparovic A (2019) Lipid Profile and Aquaporin Expression under Oxidative Stress in Breast Cancer Cells of Different Malignancies. Oxid Med Cell Longev. https://doi.org/10.1155/2019/2061830
- 206. Gašparović AČ, Milković L, Rodrigues C, Mlinarić M, Soveral G (2021) Peroxiporins Are Induced upon Oxidative Stress Insult and Are Associated with Oxidative Stress Resistance in Colon Cancer Cell Lines. Antioxidants 10:1856
- 207. Glaviano A, Foo ASC, Lam HY, et al (2023) PI3K/AKT/mTOR signaling transduction pathway and targeted therapies in cancer. Mol Cancer 22:1–37
- 208. Park SG, Jo IJ, Park SA, Park MC, Mun YJ (2022) Poria cocos Extract from Mushrooms Stimulates Aquaporin-3 via the PI3K/Akt/mTOR Signaling Pathway. Clin Cosmet Investig Dermatol 15:1919–1931
- 209. Xu H, Xu Y, Zhang W, Shen L, Yang L, Xu Z (2011) Aquaporin-3 positively regulates matrix metalloproteinases via PI3K/AKT signal pathway in human gastric carcinoma SGC7901 cells. Journal of Experimental and Clinical Cancer Research 30:1–6
- 210. Wang Q, Lin B, Wei H, Wang X, Nie X, Shi Y (2024) AQP3 Promotes the Invasion and Metastasis in Cervical Cancer by Regulating NOX4-derived H2O2 Activation of Syk/PI3K/Akt Signaling Axis. J Cancer 15:1124

- 211. Liang Y, Chen P, Wang S, et al (2024) SCFFBXW5-mediated degradation of AQP3 suppresses autophagic cell death through the PDPK1-AKT-MTOR axis in hepatocellular carcinoma cells. Autophagy 20:1984–1999
- 212. Tarawneh N, Hamadneh L, Alshaer W, Al Bawab AQ, Bustanji Y, Abdalla S (2024) Downregulation of aquaporins and PI3K/AKT and upregulation of PTEN expression induced by the flavone scutellarein in human colon cancer cell lines. Heliyon 10:e39402
- 213. Woo J, Lee J, Kim MS, Jang SJ, Sidransky D, Moon C (2008) The effect of aquaporin 5 overexpression on the Ras signaling pathway. Biochem Biophys Res Commun 367:291–298
- 214. Covas G, Marinho HS, Cyrne L, Antunes F (2013) Activation of Nrf2 by H2O2: De novo synthesis versus nuclear translocation. Methods Enzymol 528:157–171
- 215. Fourquet S, Guerois R, Biard D, Toledano MB (2010) Activation of NRF2 by Nitrosative Agents and H2O2 Involves KEAP1 Disulfide Formation. J Biol Chem 285:8463
- 216. Onodera Y, Motohashi H, Takagi K, et al (2014) NRF2 immunolocalization in human breast cancer patients as a prognostic factor. Endocr Relat Cancer 21:241–252
- 217. Tao S, Wang S, Moghaddam SJ, Ooi A, Chapman E, Wong PK, Zhang DD (2014) Oncogenic KRAS confers chemoresistance by upregulating NRF2. Cancer Res 74:7430
- 218. Li QK, Singh A, Biswal S, Askin F, Gabrielson E (2011) KEAP1 gene mutations and NRF2 activation are common in pulmonary papillary adenocarcinoma. J Hum Genet 56:230–234
- 219. Li C, Wu H, Wang S, Zhu J (2016) Expression and correlation of NRF2, KEAP1, NQO-1 and HO-1 in advanced squamous cell carcinoma of the larynx and their association with clinicopathologic features. Mol Med Rep 14:5171–5179
- 220. Ji L, Li H, Gao P, Shang G, Zhang DD, Zhang N, Jiang T (2013) Nrf2 pathway regulates multidrug-resistance-associated protein 1 in small cell lung cancer. PLoS One. https://doi.org/10.1371/JOURNAL.PONE.0063404
- 221. Ji X, Lu Y, Tian H, Meng X, Wei M, Cho WC (2019) Chemoresistance mechanisms of breast cancer and their countermeasures. Biomedicine & Pharmacotherapy 114:108800
- 222. Jeddi F, Soozangar N, Sadeghi MR, Somi MH, Shirmohamadi M, Eftekhar-Sadat AT, Samadi N (2018) Nrf2 overexpression is associated with P-glycoprotein upregulation in gastric cancer. Biomedicine & Pharmacotherapy 97:286–292
- 223. Singh A, Wu H, Zhang P, Happel C, Ma J, Biswal S (2010) Expression of ABCG2 (BCRP) is regulated by Nrf2 in cancer cells that confers side population and chemoresistance phenotype. Mol Cancer Ther 9:2365–2376
- 224. Singh A, Venkannagari S, Oh KH, et al (2016) Small Molecule Inhibitor of NRF2 Selectively Intervenes Therapeutic Resistance in KEAP1-Deficient NSCLC Tumors. ACS Chem Biol 11:3214–3225

- 225. Pawlik A, Wiczk A, Kaczyńska A, Antosiewicz J, Herman-Antosiewicz A (2013) Sulforaphane inhibits growth of phenotypically different breast cancer cells. Eur J Nutr 52:1949
- 226. Jeong EJ, Choi JJ, Lee SY, Kim YS (2024) The Effects of ML385 on Head and Neck Squamous Cell Carcinoma: Implications for NRF2 Inhibition as a Therapeutic Strategy. Int J Mol Sci 25:7011
- 227. Kaiser AE, Baniasadi M, Giansiracusa D, Giansiracusa M, Garcia M, Fryda Z, Wong TL, Bishayee A (2021) Sulforaphane: A Broccoli Bioactive Phytocompound with Cancer Preventive Potential. Cancers (Basel) 13:4796
- 228. Yagishita Y, Fahey JW, Dinkova-Kostova AT, Kensler TW (2019) Broccoli or Sulforaphane: Is It the Source or Dose That Matters? Molecules. https://doi.org/10.3390/MOLECULES24193593
- 229. Tahata S, Singh S V., Lin Y, et al (2018) Evaluation of Biodistribution of Sulforaphane after Administration of Oral Broccoli Sprout Extract in Melanoma Patients with Multiple Atypical Nevi. Cancer Prev Res (Phila) 11:429–437
- 230. Alumkal JJ, Slottke R, Schwartzman J, et al (2015) A phase II study of sulforaphanerich broccoli sprout extracts in men with recurrent prostate cancer. Invest New Drugs 33:480–489
- 231. Yuan J, Huang W, Lin M, Sun S, Zhong F, Ye L, Yin H, Ou X, Zeng Z (2025) ML385 increases ferroptosis via inhibiting Nrf2/HO-1 pathway to enhances the sensitivity of MCF-7 TAMR to tamoxifen. Naunyn Schmiedebergs Arch Pharmacol 1–13
- 232. Reichard JF, Motz GT, Puga A (2007) Heme oxygenase-1 induction by NRF2 requires inactivation of the transcriptional repressor BACH1. Nucleic Acids Res 35:7074–7086
- 233. Lee YJ, Lee SH (2011) Sulforaphane Induces Antioxidative and Antiproliferative Responses by Generating Reactive Oxygen Species in Human Bronchial Epithelial BEAS-2B Cells. J Korean Med Sci 26:1474–1482
- 234. Calcabrini C, Maffei F, Turrini E, Fimognari C (2020) Sulforaphane Potentiates Anticancer Effects of Doxorubicin and Cisplatin and Mitigates Their Toxic Effects. Front Pharmacol 11:567
- 235. Kubo E, Chhunchha B, Singh P, Sasaki H, Singh DP (2017) Sulforaphane reactivates cellular antioxidant defense by inducing Nrf2/ARE/Prdx6 activity during aging and oxidative stress. Sci Rep 7:1–17
- 236. Tian Y, Liu Q, Yu S, Chu Q, Chen Y, Wu K, Wang L (2020) NRF2-Driven KEAP1 transcription in human lung cancer. Molecular Cancer Research 18:1465–1476
- 237. Wei R, Enaka M, Muragaki Y (2019) Activation of KEAP1/NRF2/P62 signaling alleviates high phosphate-induced calcification of vascular smooth muscle cells by suppressing reactive oxygen species production. Sci Rep 9:1–13
- 238. Jeong EJ, Choi JJ, Lee SY, Kim YS (2024) The Effects of ML385 on Head and Neck Squamous Cell Carcinoma: Implications for NRF2 Inhibition as a Therapeutic Strategy. Int J Mol Sci 25:7011

- 239. Ji L, Moghal N, Zou X, Fang Y, Hu S, Wang Y, Tsao MS (2022) The NRF2 antagonist ML385 inhibits PI3K-mTOR signaling and growth of lung squamous cell carcinoma cells. Cancer Med 12:5688
- 240. Juszczak M, Tokarz P, Woźniak K (2024) Potential of NRF2 Inhibitors—Retinoic Acid, K67, and ML-385—In Overcoming Doxorubicin Resistance in Promyelocytic Leukemia Cells. International Journal of Molecular Sciences 2024, Vol 25, Page 10257 25:10257
- 241. Helwa I, Choudhary V, Chen X, Kaddour-Djebbar I, Bollag WB (2017) Anti-psoriatic drug monomethylfumarate increases nuclear factor erythroid 2-related factor 2 levels and induces aquaporin-3 mRNA and protein expression. Journal of Pharmacology and Experimental Therapeutics 362:243–253
- 242. Zhao J, Moore AN, Clifton GL, Dash PK (2005) Sulforaphane enhances aquaporin-4 expression and decreases cerebral edema following traumatic brain injury. J Neurosci Res 82:499–506
- 243. Kim NH, Kim HJ, Lee AY (2023) Aquaporin-3 Downregulation in Vitiligo Keratinocytes Increases Oxidative Stress of Melanocytes. Biomol Ther (Seoul) 31:648–654
- 244. Lučić I, Mlinarić M, Čipak Gašparović A, Milković L (2025) The Influence of AQP5 on the Response to Hydrogen Peroxide in Breast Cancer Cell Lines. Int J Mol Sci 26:3243
- 245. Chang SY, Lo CS, Zhao XP, Liao MC, Chenier I, Bouley R, Ingelfinger JR, Chan JSD, Zhang SL (2016) Overexpression of angiotensinogen downregulates aquaporin 1 expression via modulation of Nrf2-HO-1 pathway in renal proximal tubular cells of transgenic mice. J Renin Angiotensin Aldosterone Syst. https://doi.org/10.1177/1470320316668737
- 246. Vajpai M, Mukherjee M, Sankararamakrishnan R (2018) Cooperativity in Plant Plasma Membrane Intrinsic Proteins (PIPs): Mechanism of Increased Water Transport in Maize PIP1 Channels in Hetero-tetramers. Sci Rep 8:1–17
- 247. Li D Di, Ruan XM, Zhang J, Wu YJ, Wang XL, Li XB (2013) Cotton plasma membrane intrinsic protein 2s (PIP2s) selectively interact to regulate their water channel activities and are required for fibre development. New Phytol 199:695–707
- 248. Fetter K, Van Wilder V, Moshelion M, Chaumont F (2004) Interactions between plasma membrane aquaporins modulate their water channel activity. Plant Cell 16:215– 228
- 249. Silberstein C, Bouley R, Huang V, Fang P, Pastor-Soler N, Brown D, Van Hoek AN (2004) Membrane organization and function of M1 and M23 isoforms of aquaporin-4 in epithelial cells. Am J Physiol Renal Physiol 287:501–511
- 250. Petrova RS, Schey KL, Donaldson PJ, Grey AC (2015) Spatial distributions of AQP5 and AQP0 in embryonic and postnatal mouse lens development. Exp Eye Res 132:124

- 251. Sugiyama Y, Yamazaki K, Kusaka-Kikushima A, Nakahigashi K, Hagiwara H, Miyachi Y (2014) Analysis of aquaporin 9 expression in human epidermis and cultured keratinocytes. FEBS Open Bio 4:611
- 252. Charlestin V, Tan E, Arias-Matus CE, et al (2024) Evaluation of the Mammalian Aquaporin Inhibitors Auphen and Z433927330 in Treating Breast Cancer. Cancers (Basel) 16:2714
- 253. Luo H, Liu Y, Song Y, Hua Y, Zhu X (2020) Aquaporin 1 affects pregnancy outcome and regulates aquaporin 8 and 9 expressions in the placenta. Cell Tissue Res 381:543–554



### 8. SUMMARY

Breast cancer is one of the most frequently diagnosed cancers and a leading cause of mortality in women, and despite advances in diagnosis and treatment, it remains a major health challenge. Cancer, including breast cancer, arises as a consequence of loss of control over proliferation, differentiation, and cell death. Cancer cells adapt through changes in signaling pathways and metabolism, and by reshaping the microenvironment. Because of these numerous changes, the cancer cells are heterogeneous both within a single tumor and between different tumors, which further highlights the biological diversity of the disease. Oxidative stress participates in all stages of cancer initiation and progression and can cause oxidative damage to DNA, proteins, and lipids, but it can also participate in cell signaling. The outcome depends on the amount of reactive oxygen species (ROS) and on the cell's antioxidant capacity. Hydrogen peroxide (H<sub>2</sub>O<sub>2</sub>) is of particular interest because, even under physiological conditions, it serves as an important second messenger involved in many redox-dependent signaling pathways, whereas its excessive accumulation leads to damage. To limit such effects, the cell activates an antioxidant system regulated by the transcription factor NRF2, which coordinates antioxidant and detoxification responses. In cancer cells, ROS levels are often elevated, which suggests damage and cell death. However, the antioxidant capacity is also elevated in cancer, including increased NRF2 activity, thereby preventing such damage. Aquaporins are membrane proteins originally described as water channels, but later shown to conduct other small molecules such as glycerol and H<sub>2</sub>O<sub>2</sub>. In this way, they participate in the regulation of water homeostasis, cellular metabolism, and cellular redox status. Under physiological conditions, aquaporins are tightly regulated at the transcriptional and post-transcriptional levels, by trafficking and gating. Their expression is also tissue-specific and organ-dependent. However, in cancer, some aquaporins are often overexpressed and have been discussed as potential prognostic markers. In breast cancer, AQP3 and AQP5 are most frequently overexpressed. Although they are overexpressed in cancer cells, their role, especially in adaptation to oxidative stress and potential influence on therapeutic outcome, remains unclear.

The role of AQP3 and AQP5 in the cellular response to low, physiological oxidative stress, which is a characteristic of cancer cells, was examined in three breast cancer cell lines, hormone receptor-positive MCF7, HER2-positive SkBr3, and triple-negative SUM159PT, and in the non-tumorigenic breast epithelial cell line MCF10A. Oxidative stress was induced by 14-day exposure to low  $\rm H_2O_2$  concentrations (10 and 20  $\mu$ M), after which adaptation was assessed. Prolonged exposure to  $\rm H_2O_2$  led to adaptation of cancer cells, confirmed by improved viability

and/or accelerated proliferation at increasing H<sub>2</sub>O<sub>2</sub> concentrations. Increased AQP3 expression was measured in all three cancer cell lines, and increased AQP5 was measured in SUM159PT and SkBr3. At the same time, enhanced translocation of NRF2 to the nucleus was observed in cancer cell lines, indicating its activation. The non-tumorigenic cell line did not show an increase in viability or proliferation, nor an increase in aquaporin expression or NRF2 activation, confirming a distinct response of cancer cells. Considering the change in aquaporin expression and NRF2 activity, the potential influence of NRF2 on aquaporin expression and/or function was investigated. Pharmacological activation of NRF2 with sulforaphane increased AQP3 expression and H<sub>2</sub>O<sub>2</sub> transport into cells in SUM159PT, whereas in SkBr3, it only accelerated H<sub>2</sub>O<sub>2</sub> transport. No effects were observed in MCF7 and MCF10A. In silico prediction of NRF2 binding sites in the regulatory regions of AQP3 and AQP5 further supported the possible direct regulation, although additional studies are required for confirmation. During analysis of aquaporin genes after prolonged oxidative stress and after NRF2 modulation, changes were observed in multiple aquaporin isoforms, prompting the question of compensatory regulation of aquaporin isoforms. Therefore, AQP3 and AQP5 were overexpressed or stably silenced to assess the effect on other isoforms and on overall function. During these modulations, changes in the expression of individual aquaporins were recorded regardless, indicating interdependence of isoforms in maintaining transport. The only modulation stably confirmed at the protein level was AQP5 overexpression, which resulted in increased H<sub>2</sub>O<sub>2</sub> intake.

The association of elevated aquaporin expression and cancer aggressiveness, and the differences between cancer cells and non-tumorigenic cells, were confirmed and are in line with the literature. Furthermore, the NRF2 effect on aquaporin expression and function was supported, with the note that this effect is cell-type-specific and context-dependent. Strong regulation of aquaporins was also demonstrated, whereby the expression of different isoforms adjusts to preserve overall transport. The role of aquaporins in cancer is therefore likely linked to the regulation of oxidative stress, which may explain their increased expression in breast cancer. Overall, these results indicate aquaporins as potential therapeutic targets, not merely prognostic biomarkers.

## 9. SAŽETAK

Tumor dojke jedan je od najčešće dijagnosticiranih zloćudnih tumora i vodećih uzroka smrtnosti u žena te, unatoč napretku u dijagnostici i liječenju, i dalje predstavlja velik zdravstveni problem. Tumor, uključujući i karcinom dojke, nastaje kao posljedica gubitka kontrole stanice nad proliferacijom, diferencijacijom i staničnom smrću. Tumorske se stanice pritom prilagođavaju novim uvjetima promjenama u signalnim putevima i metabolizmu te preoblikovanjem mikrookoliša. Upravo zbog svih promjena, populacija tumorskih stanica heterogena je i unutar pojedinog tumora i između različitih tumora, što dodatno naglašava biološku raznolikost bolesti. Oksidacijski stres sudjeluje u svim fazama inicijacije i progresije tumora te može uzrokovati oksidacijska oštećenja DNA, proteina i lipida, ali i sudjelovati u staničnoj signalizaciji. Ishod ovisi o količini reaktivnih kisikovih vrsta (ROS) kao i o antioksidacijskom kapacitetu stanice. Vodikov peroksid (H<sub>2</sub>O<sub>2</sub>) posebno je zanimljiv jer i u fiziološkim uvjetima služi kao važan sekundarni glasnik uključen u brojne redoks-ovisne signalne putove, dok njegovo pretjerano nakupljanje dovodi do oštećenja. Radi ograničavanja takvih učinaka, stanica aktivira antioksidacijski sustav kojim upravlja transkripcijski čimbenik NRF2, odgovoran za koordinaciju antioksidacijskog i detoksikacijskog odgovora. U tumorskim stanicama razine ROS-a su često povišene, što bi upućivalo na veće oštećenje i staničnu smrt, no istovremeno stanice povisuju i antioksidacijski kapacitet, uključujući pojačanu aktivnost NRF2, čime izbjegavaju oštećenja. Akvaporini su membranski proteini prvotno opisani kao kanali za vodu, ali naknadno je pokazano da provode i druge male molekule, poput glicerola i H<sub>2</sub>O<sub>2</sub>. Na taj način sudjeluju u regulaciji homeostaze vode, staničnog metabolizma i redoksstatusa u stanici. U fiziološkim uvjetima akvaporini su regulirani na transkripcijskoj i posttranskripcijskoj razini, lokalizacijom u stanici i otvaranjem/zatvaranjem kanala. Također, njihova je ekspresija tkivno specifična i ovisna o organu. Međutim, u tumoru su akvaporini često prekomjerno eksprimirani te se spominju i kao potencijalni prognostički markeri. Primjerice, u karcinomu dojke najčešće se ističu AQP3 i AQP5. Iako znamo da su prekomjerno eksprimirani u tumorskim stanicama, i dalje nije poznata njihova uloga, posebice u kontekstu prilagodbe na oksidacijski stres te potencijalni utjecaj na terapijski ishod.

U tri tumorske stanične linije raka dojke, hormonski pozitivnoj MCF7, HER2-pozitivnoj SkBr3 i trostruko negativnoj SUM159PT, te u ne-tumorigenoj staničnoj liniji epitela dojke MCF10A, ispitana je uloga AQP3 i AQP5 u staničnom odgovoru na blagi, fiziološki oksidacijski stres karakterističan za tumorske stanice. Oksidacijski stres induciran je 14-dnevnim izlaganjem niskim koncentracijama H<sub>2</sub>O<sub>2</sub> (10 i 20 μM), nakon čega je procijenjena

adaptacija. Produljena izloženost H<sub>2</sub>O<sub>2</sub> dovela je do adaptacije tumorskih stanica, potvrđene boljim preživljenjem i/ili ubrzanom proliferacijom pri rastućim koncentracijama H<sub>2</sub>O<sub>2</sub>. Zabilježena je povišena ekspresija AQP3 u sve tri tumorske linije te povišenje AQP5 u SUM159PT i SkBr3. U tumorskim linijama istovremeno je uočena i pojačana translokacija NRF2 u jezgru, što upućuje na njegovu aktivaciju. Ne-tumorogena linija na nije imala porast u vijabilnosti i proliferaciji, niti porast ekspresije akvaporina ili aktivacije NRF2, što potvrđuje različit odgovor tumorskih stanica. S obzirom na istovremenu promjenu ekspresije akvaporina i aktivnosti NRF2, ispitano je utječe li NRF2 na ekspresiju i/ili funkciju akvaporina. Farmakološkom aktivacijom NRF2 sulforafanom pokazano je da u SUM159PT dolazi do porasta ekspresije AQP3 i bržeg ulaska H<sub>2</sub>O<sub>2</sub> u stanice, dok je u SkBr3 zabilježeno ubrzanje ulaska H<sub>2</sub>O<sub>2</sub> bez značajne promjene razine akvaporina, dok u MCF7 i MCF10A učinci nisu uočeni. In silico predviđanjem mjesta vezanja NRF2 (ARE motivi) u regulatornim regijama AQP3 i AQP5 dodatno je potvrđena pretpostavka o mogućoj izravnoj regulaciji, iako su za konačnu potvrdu potrebna dodatna istraživanja. Tijekom analize gena za akvaporine nakon produljenog oksidacijskog stresa i nakon modulacije NRF2 uočene su promjene više izoformi, što je potaknulo pitanje međusobne kompenzacije unutar mreže akvaporina. Zbog toga su AQP3 i AQP5 prekomjerno eksprimirani ili stabilno utišani kako bi se procijenio učinak na ostale izoforme i sveukupnu funkciju. Tijekom modulacija zabilježene su promjene u ekspresiji pojedinih akvaporina neovisno o tome je li ciljna promjena na proteinskoj razini bila potpuna, što upućuje na međusobnu ovisnost izoformi u održavanju transporta. Jedina stabilno potvrđena modulacija na proteinskoj razini bila je prekomjerna ekspresija AQP5, koja je rezultirala povećanim ulaskom H<sub>2</sub>O<sub>2</sub> u stanice.

U skladu s literaturom potvrđena je povezanost povišene ekspresije akvaporina s agresivnošću tumora te razlika između tumorskih i ne-tumorskih stanica. Nadalje, potvrđena je pretpostavka o učinku NRF2 na ekspresiju i/ili funkciju akvaporina, uz napomenu da je taj učinak ovisan o staničnom tipu i kontekstu. Zabilježena je i čvrsta regulacija akvaporina, pri čemu se ekspresija različitih izoformi prilagođava kako bi se očuvao sveukupni transport. Uloga akvaporina u tumoru vjerojatno je povezana s regulacijom oksidacijskog stresa, što može objasniti njihovu povišenu ekspresiju. Sveukupno, ovi rezultati ukazuju na akvaporine kao potencijalne terapijske mete, a ne samo prognostičke biomarkere.

### 10. CV

Name: Monika Mlinarić

E-mail: Monika.Mlinaric@irb.hr

Date and place of birth: 24.09.1996, Gospić, Croatia

### Work:

Laboratory for Membrane Transport and Signaling, Division of Molecular Medicine,
 Ruder Bošković Institute, Zagreb, Croatia (2021-Present)

### **Education:**

- Interdisciplinary doctoral studies of Molecular Biosciences, Department of Biology, Josip Juraj Strossmayer University of Osijek, Osijek, Croatia (2022-present)
- Master's in Experimental Biology, Department of Biology, Faculty of Science, University of Zagreb, Zagreb, Croatia (2018-2021)
- Bachelor's in Biology, Department of Biology, Department of Biology, Faculty of Science, University of Zagreb, Zagreb, Croatia (2015-2018)

## **Training schools and courses:**

- FEBS 2024 Advanced Course: Redox biochemistry: cellular responses and disease relevance, Spetses, Greece (30.9.-6.10.2024)
- Writing Successful Fellowship Applications, Fellowsherpa, Split, Croatia (10-11.9.2024)
- EMBO Workshop on Communicating Research: Paper Writing and Short Presentations, Split, Croatia (12.9.2024)
- BenBedPhar Training School 2024: Physiological oxygen levels to investigate NRF2 regulated redox signaling in cell biology to improve clinical translation; London, UK (5.-8.3.2024)
- IG17104 Training school: Rational drug discovery based on computational modelling, high-throughput virtual screening, imagebased screening technologies, lead optimisation, structure relationship activities (SAR) analysis; Lisbon, Portugal (10-12.7.2023)
- Introduction to Molecular Modeling, CACR (12/2021); Zagreb, Croatia (2-6.12.2021)
- Training course for people working with experimental animals and animals for the production of biological preparations Category A, Zagreb, Croatia (10/2018 01/2019)

## **Research experience:**

- Research Institute for Medicines, Faculty of Pharmacy, University of Lisbon, Lisbon, Portugal (6-26.3.2022; 10.10.-8.11.2024)
- Department of Clinical and Movement Neurosciences, UCL Institute of Neurology, London, UK (5-18.3.2023)
- Institute for Vascular Biology and Thrombosis Research, Medical University of Vienna, Vienna, Austria (1.7.-31.8.2018)

### **Grants and scholarships:**

- IRB financial support, financed by the European Union NextGeneration EU (MZ2-24, 2024)
- COST ITC Conference Grant (CA20121, 2024)
- SFRR-E European travel grant (2024)
- COST Short-Term Scientific Mission Grant (CA20121, 2023)
- COST Short-Term Scientific Mission Grant (CA17104, 2022)
- CEEPUS CIII-Free Mover, The Austrian Agency for International Cooperation in Education & Research (2019)
- STEM scholarship, Ministry of Science and Education of the Republic of Croatia (2017)

## Awards:

- Annual award of the Society to young scientists and artists for 2024
- Annual award of the Ruđer Bošković Institute for the best scientific papers in 2023: Mlinarić M, Lučić I, Milković L, da Silva I V., Tartaro Bujak I, Musani V, Soveral G, Čipak Gašparović A (2023) AQP3-Dependent PI3K/Akt Modulation in Breast Cancer Cells. Int J Mol Sci. https://doi.org/10.3390/IJMS24098133

### **Conferences:**

### Oral:

- 2025 biennial meeting of the Society for Free Radical Research International (SFRRI)
  hosted by the Society for Free Radical Research Europe "The New Era of Redox
  Biology: from Basic Biochemistry to Redox Omics", Galway, Ireland (3-6.6.2025)
- BenBedPhar Training School 2024: Physiological oxygen levels to investigate NRF2 regulated redox signaling in cell biology to improve clinical translation, London, UK (5.-8.3.2024)
- 2nd Scientific meeting of the COST action CA20121 "Scientific meeting and industry showcase: translating NRF2 research from bed to bench" Madrid, Spain (19.-21.5.2022)

### Poster:

- FEBS 2024 Advanced Course: Redox biochemistry: cellular responses and disease relevance, Spetses, Greece (30.9.-6.10.2024)
- 2024 annual meeting of the Society for Free Radical Research Europe (SFRRE) "From Molecules to Tissues: Redox Biology in Action"; Istanbul, Turkey (5.-7.6.2024)
- 5th Scientific meeting of the COST action CA20121 "Translating NRF2 research into clinical practice", Graz, Austria (12.-13.10.2023)
- 4th Scientific meeting of the COST action CA20121 "From Physiology to Pathology"; Zagreb, Hrvatska (20.-21.4.2023)
- 2023 annual meeting of the Society for Free Radical Research Europe (SFRRE) "Redox Biology in Translation", Vienna, Austria (6.-9.6.2023)
- Sixth Meeting of the Croatian Association for Cancer Research with international participation "Targeting Cancer", Zagreb, Croatia (10.-12.11.2022)
- 3rd Scientific meeting of the COST action CA20121 "Research and therapeutic tools in the field of NRF2 medicine"; Bucharest, Romania (13.-14.10.2022)
- Fifth Congress of the Serbian Association for Cancer Research with international participation "Translational potential of cancer research in Serbia; online (3.12.2021)

### 11. PUBLICATIONS:

- Lučić I, Mlinarić M, Čipak Gašparović A, Milković L (2025) The Influence of AQP5 on the Response to Hydrogen Peroxide in Breast Cancer Cell Lines. Int J Mol Sci. https://doi.org/10.3390/IJMS26073243
- Mlinarić M, Lučić I, Tomljanović M, Tartaro Bujak I, Milković L, Čipak Gašparović A
   (2024) AQP3 and AQP5 Modulation in Response to Prolonged Oxidative Stress in Breast
   Cancer Cell Lines. Antioxidants (Basel). https://doi.org/10.3390/ANTIOX13060626
- da Silva I V., Mlinarić M, Lourenço AR, Pérez-Garcia O, Čipak Gašparović A, Soveral G (2024) Peroxiporins and Oxidative Stress: Promising Targets to Tackle Inflammation and Cancer. Int J Mol Sci. https://doi.org/10.3390/IJMS25158381
- Bijelić A, Silovski T, Mlinarić M, Čipak Gašparović A (2024) Peroxiporins in Triple-Negative Breast Cancer: Biomarker Potential and Therapeutic Perspectives. Int J Mol Sci. https://doi.org/10.3390/IJMS25126658
- Mlinarić M, Lučić I, Milković L, da Silva I V., Tartaro Bujak I, Musani V, Soveral G,
   Čipak Gašparović A (2023) AQP3-Dependent PI3K/Akt Modulation in Breast Cancer
   Cells. Int J Mol Sci. https://doi.org/10.3390/IJMS24098133
- Lučić I, Kurtović M, Mlinarić M, Piteša N, Čipak Gašparović A, Sabol M, Milković L
   (2023) Deciphering Common Traits of Breast and Ovarian Cancer Stem Cells and
   Possible Therapeutic Approaches. Int J Mol Sci. https://doi.org/10.3390/IJMS241310683
- Milković L, Mlinarić M, Lučić I, Čipak Gašparović A (2023) The Involvement of Peroxiporins and Antioxidant Transcription Factors in Breast Cancer Therapy Resistance. Cancers (Basel), https://doi.org/10.3390/CANCERS15245747
- Gašparović AČ, Milković L, Rodrigues C, Mlinarić M, Soveral G (2021) Peroxiporins Are Induced upon Oxidative Stress Insult and Are Associated with Oxidative Stress Resistance in Colon Cancer Cell Lines. Antioxidants (Basel). https://doi.org/10.3390/ANTIOX10111856